



FINAL REPORT

EXPERIMENTAL STUDY OF THE BEHAVIOR OF REINFORCED MASONRY WALL AND HOLLOW BRICK INFILLED CONCRETE FRAME UNDER CYCLIC LOADING



Department of Civil Engineering

Bangladesh University of Engineering and Technology (BUET)

Dhaka- 1000, Bangladesh

June 2023





EXPERIMENTAL STUDY OF THE BEHAVIOR OF REINFORCED MASONRY WALL AND HOLLOW BRICK INFILLED CONCRETE FRAME UNDER CYCLIC LOADING

Principal Investigator

Dr. Raquib Ahsan

Professor

Department of Civil Engineering, BUET



Department of Civil Engineering
Bangladesh University of Engineering and Technology

April 2023

ACKNOWLEDGEMENT

This research was conducted as per the terms of the "Letter of Collaboration" signed between GPH Ispat and the Department of Civil Engineering, BUET on 3rd December 2018.

I express my gratitude to Eco Ceramics and GPH Ispat for their material and financial support without which the research could not have been possible.

I would also like to thanks to the Department of Civil Engineering for providing space within the department to conduct this research. I would like to acknowledge the constant support of the technical staff of the "Concrete & Materials Lab" and the "Strength of The Materials Lab" during the experiment.

ABSTRACT

Bangladesh is situated in a tectonically active region, making it susceptible to earthquakes. Unreinforced masonry structure (URM) is one of Bangladesh's most common structural typologies. Unreinforced masonry load-bearing walls are the main load-resisting elements of URM structures that are often designed to resist only gravity loads. Weakness in resisting lateral forces and the limited ductility capacity of these masonry structures make them more vulnerable to earthquakes. Integrating grouted reinforcement into masonry structures can be a viable solution. In this study, the behavior of reinforced masonry (RM) made of indigenous materials has been observed under cyclic loading to determine whether it can overcome the shortcomings of URM.

An experimental laboratory investigation has been carried out to study the in-plane cyclic behavior of reinforced masonry structures, along with a comparative study of load-carrying capacity, stiffness, ductility, and energy dissipation between unreinforced masonry structures and reinforced masonry structures. In this research, six half-scale reinforced masonry walls have been constructed with three different cement to the sand ratio (1:2, 1:4, and 1:6) and two different grades of steel (420 DWR and 500 CWR). Six half-scale unreinforced reinforced walls have been constructed with corresponding mortar types and two brick types (solid and hollow). Afterward, all the walls were subjected to lateral cyclic loading applied by a hydraulic jack. This experiment revealed that perforated clay brick are effective to increase the ductility and energy absorption capacity of the specimen. Perforated bricks masonry exhibited 9% - 11% more displacement before failure and dissipated 3% - 10% more cumulative energy than wall having solid bricks. On the other hand, reinforced masonry walls had 3.4 to 6.7 times higher ultimate load-carrying capacity and 1.5 - 2.3 times higher energy absorption capacity than unreinforced masonry walls. On the other hand, For higher mortar strength, RM walls shows 20% - 38% more ultimate load carrying capacity and dissipates 43% more energy than infilled walls.

TABLE OF CONTENTS

ACKNOWLEDGEMENT	ii
ABSTRACT	iii
TABLE OF CONTENTS	iv
LIST OF TABLES	vii
LIST OF FIGURES	viii
CHAPTER 1	1
INTRODUCTION	1
1.1 Background	1
1.2 Objectives of the Study	2
1.3 Methodology	2
1.4 Scope of the Investigation	2
1.5 Outline of the Study	3
CHAPTER 2	4
LITERATURE REVIEW	4
2.1 Introduction	4
2.2 Unreinforced Masonry	4
2.3 Reinforced masonry	5
2.3.1 Factors Affecting Reinforced Masonry walls	8
2.4 Masonry Infilled RC Frame	11
2.4.1 Different Failure Modes of Masonry Infilled RC Frame Structures	13
2.5 Standards and Codes	14
2.5.1 Reinforcement Detailing of Reinforced Masonry Wall	15
CHAPTER 3	17
EXPERIMENTAL STUDY	17

3.1 Introduction	17
3.2 Material Properties	17
3.2.1 Cement	17
3.2.2 Fine Aggregate	18
3.2.3 Coarse Aggregate	18
3.2.4 Reinforcement	18
3.2.5 Clay Brick	18
3.2.6 Mortar	19
3.2.7 Prism Test	21
3.2.8 Grout	22
3.2.9 Concrete	22
3.3 Details of Specimens	22
3.3.1 Reinforced Masonry walls	23
3.3.2 Unreinforced Masonry	24
3.3.3 Infilled Frame	26
3.4 Preparation of Specimens	29
3.4.1 Reinforced Masonry wall Preparation	29
3.4.2 Unreinforced Masonry wall Preparation	34
3.4.3 Masonry Infilled Frame Wall Preparation	35
3.5 Experimental Setup	39
3.5.1 Hydraulic Jack	40
3.6 Test Procedure	43
CHAPTER 4	44
RESULTS AND DISCUSSIONS	44
4.1 Introduction	44
4.2 Damage Assessment and Failure Mode of the Specimens	44
4.2.1 Failure Analysis of SURM4	44

4.2.2 Failure Analysis of HURM4	47
4.2.3 Failure Analysis of RM4-420	49
4.2.4 Failure Analysis of SB	52
4.3 Summary of The Experimental Results of The Specimens	55
4.4 Comparative Study	58
4.4.1 Comparison between Solid Brick Masonry and Hollow brick Masonry	58
4.4.2 Comparison between Unreinforced Masonry and Reinforced Masonry	62
4.4.3 Comparison between Reinforced Masonry and Infilled Frame	65
4.5 Cost Analysis	67
CHAPTER 5	68
CONCLUSIONS	68
B 5.1 General	68
5.2 Conclusions from the Experiments	68
REFERENCES	70
Appendix-A	74
Appendix-B	75
Appendix-C	77
Appendix-D	79
Appendix-E	81
Appendix-F	83
Appendix-G	84
Appendix-H	87
Appendix-I	94
Appendix-I	101

LIST OF TABLES

Table 3.1- Properties of cement	. 17
Table 3.2- Tension test results of reinforcement	18
Table 3.3- Properties of clay brick	.19
Table 3.4- Compressive strength of brick prism	.21
Table 3.5- Details of the reinforced masonry walls	.23
Table 3.6- Details of the unreinforced masonry walls	.25
Table 3.7- Details of the masonry infilled frame walls	27
Table 4.1- Summary of The Experimental Results of unreinforced masonry walls	.55
Table 4.2- Summary of The Experimental Results of Reinforced masonry walls	56
Table 4.3- Summary of The Experimental Results of infilled frame walls	. 57
Table A.1- Yield strength and ultimate strength of reinforcement	.74
Table B.1- Compressive strength of solid clay brick	.75
Table B.2- Compressive strength of perforated clay brick	. 75
Table C.1- Water absorption capacity of solid clay brick	77
Table C.2- Water absorption capacity of perforated clay brick	.77
Table D.1- Compressive strength of mortar cube	.79
Table E.1- Compressive strength of solid and perforated brick prism for three mortar type.	.81
Table F.1- Compressive strength of concrete cylinder	83

LIST OF FIGURES

Figure 2.1- The failure modes of masonry wall (Wilson and Varkey, 2019)	5
Figure 2.2- Role of reinforcement in RM (Letelier et al., 2019)	6
Figure 2.3- Joint Reinforcement Applications in Masonry (Fodi, 2011)	. 7
Figure 2.4- Placing of reinforcement in masonry	7
Figure 2.5- a) Reinforced cavity wall, b) Reinforced solid masonry, c) Reinforced hollow us	nit
masonry, d) Reinforced grouted masonry, e) Reinforced pocket type wall. (Fodi, 2011)	8
Figure 2.6- ASTM specification for Grout	9
Figure 2.7- Direction of diagonal cracks in masonry shears walls (Sivaraja, 2012)	10
Figure 2.8- Equivalent truss mechanisms for infill frame (Polyakov, 1960)	11
Figure 2.9- Modeling of seismic behavior before and after detachment of masonry infill	12
(Tomazevic, 1999)	12
Figure 2.10- Change in the lateral load transfer mechanism owing to the inclusion of	13
masonry infill walls (Murty and Jain, 2000).	13
Figure 2.11- Failure mechanisms of infilled frames (Mehrabi et al., 1994).	13
Figure 2.12- Reinforcement detailing for reinforced masonry wall	16
Figure 3.1- (a) Front / back elevation, (b) plan view, (c) side elevation of a full scale solid	
clay brick (Every unit is in mm).	19
Figure 3.2- (a) Front / back elevation, (b) plan view, (c) side elevation of a full scale	19
perforated clay brick (Every unit is in mm).	19
Figure 3.3- Compressive strength of mortar cube for mix ratio 1:2.	20
Figure 3.4- Compressive strength of mortar cube for mix ratio 1:4.	20
Figure 3.5- Compressive strength of mortar cube for mix ratio 1:6.	21
Figure 3.6- Compressive strength of concrete cylinder.	22
Figure 3.7- Schematic drawing of Reinforced Masonry wall (Every unit is in mm)	24
Figure 3.8- Schematic drawing of perforated unreinforced Masonry wall (Every unit is in	
mm)	25
Figure 3.9- Schematic drawing of solid unreinforced Masonry wall (Every unit is in mm)	26
Figure 3.10- Schematic drawing of infilled frame without lintel (Every unit is in mm)	27
Figure 3.11- Schematic drawing of infilled frame with lintel (Every unit is in mm)	28
Figure 3.12- Schematic drawing of reinforced infilled frame (Every unit is in mm)	28
Figure 3.13- Reinforcement Preparation for base of RM walls.	29

Figure 3.14- Vertical Reinforcement Preparation for base of RM	30
Figure 3.15- Formwork Preparation of RM walls	31
Figure 3.16- Measuring slump and concrete casting of RM walls.	31
Figure 3.17- Base of RM walls after 28days of casting.	32
Figure 3.18- Eight half-scale bricks produced from a single full-scale brick	32
Figure 3.19- Masonry work of RM walls.	33
Figure 3.20- Reinforced Masonry Wall after whitewash.	34
Figure 3.21- Base Construction for URM.	34
Figure 3.22- URM wall construction	35
Figure 3.23- URM wall after whitewash.	35
Figure 3.24- (a) lintel, (b) beam-column joint, (c) stirrups / ties, (d) column-base joint,	36
(e) a full reinforced structure.	36
Figure 3.25- Shuttering work.	36
Figure 3.26- Measuring slump and concrete casting.	37
Figure 3.27- (a) curing, (b) a concrete frame after 28 days of casting.	37
Figure 3.28- Masonry work for Infilled Frame.	38
Figure 3.29- Infilled Frame after whitewash.	38
Figure 3.30- Schematic diagram of the experimental setup for masonry wall	39
Figure 3.31- Schematic diagram of the experimental setup for infilled frame wall	39
Figure 3.32- (a) Hydraulic Jack 1, (b) hydraulic jack 2 for infilled frame	40
Figure 3.33- Hydraulic Jack for masonry wall (a) Horizontal Loading (b) Gravity Loading	g. 41
Figure 3.34-Anchor bolt and steel plate	41
Figure 3.35- Full experimental setup of infilled frame wall	42
Figure 3.36- Full experimental setup of masonry wall	42
Figure 3.37- Applied loading pattern of Masonry wall during testing.	43
Figure 3.38- Applied loading pattern of Infilled Frame Wall during testing.	43
Figure 4.1- SURM4 at complete failure.	45
Figure 4.2- Cracks at final state of SURM4 (Sliding).	45
Figure 4.3- Hysteretic load-displacement curve for SURM4.	46
Figure 4.4- Stiffness degradation curve for SURM4.	46
Figure 4.5- HURM4 at complete failure.	47
Figure 4.6- Cracks at final state of SURM4 (Rocking).	48
Figure 4.7- Hysteretic load-displacement curve for HURM4.	48
Figure 4.8- Stiffness degradation curve for HURM4.	49

Figure 4.9- RM4-420 after the completion of cycle 7.	50
Figure 4.10- RM4-420 at complete failure.	51
Figure 4.11- Hysteretic load-displacement curve for RM2-420.	51
Figure 4.12- Stiffness degradation curve for RM4-420.	52
Figure 4.13- SB at complete failure (at cycle 4).	53
Figure 4.14- Hysteretic load-displacement curve for SB.	54
Figure 4.15- Stiffness degradation curve for SB.	54
Figure 4.16- Stiffness degradation of SURM2 & HURM2	59
Figure 4.17- Stiffness degradation of SURM4 & HURM4.	59
Figure 4.18- Stiffness degradation of SURM6 & HURM6.	59
Figure 4.19- Stiffness degradation of SB & PB.	60
Figure 4.20- Stiffness degradation of SBL & PBL.	60
Figure 4.21- Cumulative energy dissipation of HURM2 & SURM2.	60
Figure 4.23- Cumulative energy dissipation of HURM4 & SURM4.	61
Figure 4.24- Cumulative energy dissipation of HURM6 & SURM6.	61
Figure 4.25- Cumulative energy dissipation of SB & PB.	61
Figure 4.26- Cumulative energy dissipation of SBL & PBL.	62
Figure 4.27- First cracking load of URM & RM walls.	63
Figure 4.28- Ultimate load carrying capacity of URM & RM walls.	63
Figure 4.29- Maximum displacement of URM & RM walls.	63
Figure 4.30- Stiffness at maximum displacement of URM & RM walls	64
Figure 4.31- Cumulative energy dissipation of URM & RM walls.	64
Figure 4.32- Ultimate load carrying capacity of URM & RM infilled frame walls	64
Figure 4.33- Stiffness at maximum displacement of URM & RM infilled frame walls	65
Figure 4.34- Cumulative energy dissipation of URM & RM infilled frame walls	65
Figure 4.35- Ultimate load carrying capacity of RM walls & infilled frame walls	66
Figure 4.36- Maximum displacement of RM walls & infilled frame walls	66
Figure 4.37- Cumulative energy dissipation of RM walls & infilled frame walls	66
Figure A.1- Testing of rebar.	74
Figure B.1- (a) Capping of solid and parforated brick before testing,	76
(b) Compressive strength testing of brick.	76
Figure C.1- Weighting of (a) solid clay brick and (b) perforated clay brick during	78
absorption capacity testing.	78
Figure D.1- Prepared mortar cubes mortar testing.	80

Figure E.1- Testing of prepared prisms.	82
Figure F.1- (a) Prepared concrete cylinders (b) cylinder testing	83
Figure G.1- Calibration curve of hydraulic jack 1	84
Figure G.2- Calibration curve of hydraulic jack 2.	85
Figure G.3- Calibration curve of hydraulic jack 3.	86
Figure H.1- SURM2 at complete failure.	87
Figure H.2- SURM6 at complete failure.	87
Figure H.3- HURM2 at complete failure.	88
Figure H.4- HURM6 at complete failure.	88
Figure H.5- RM2-420 at complete failure.	89
Figure H.6- RM2-500 at complete failure.	89
Figure H.7- RM4-500 at complete failure.	90
Figure H.8- RM6-420 at complete failure.	90
Figure H.9- RM6-500 at complete failure.	91
Figure H.10- RIF at complete failure.	91
Figure H.11- PB at complete failure.	92
Figure H.12- SBL at complete failure.	92
Figure H.13- PBL at complete failure.	93
Figure I.1- Hysteretic load-displacement curve for SURM2.	94
Figure I.2- Hysteretic load-displacement curve for SURM6.	94
Figure I.3- Hysteretic load-displacement curve for HURM2	95
Figure I.4- Hysteretic load-displacement curve for HURM6	95
Figure I.5- Hysteretic load-displacement curve for RM4-420.	96
Figure I.6- Hysteretic load-displacement curve for RM6-420.	96
Figure I.7- Hysteretic load-displacement curve for RM2-500.	97
Figure I.8- Hysteretic load-displacement curve for RM4-500.	97
Figure I.9- Hysteretic load-displacement curve for RM6-500.	98
Figure I.10- Hysteretic load-displacement curve for SBL.	98
Figure I.11- Hysteretic load-displacement curve for PB.	99
Figure I.12- Hysteretic load-displacement curve for PBL.	99
Figure I.13- Hysteretic load-displacement curve for RIF.	100
Figure J.1- Stiffness degradation curve for SURM2.	101
Figure J.2- Stiffness degradation curve for SURM6.	101
Figure J.3- Stiffness degradation curve for HURM2.	101

Figure J.4- Stiffness degradation curve for HURM6.	102
Figure J.5- Stiffness degradation curve for RM2-420.	102
Figure J.6- Stiffness degradation curve for RM6-420.	102
Figure J.7- Stiffness degradation curve for RM2-500.	103
Figure J.8- Stiffness degradation curve for RM4-500.	103
Figure J.9- Stiffness degradation curve for RM6-500.	103
Figure J.10- Stiffness degradation curve for SBL.	104
Figure J.11- Stiffness degradation curve for PB.	104
Figure J.12- Stiffness degradation curve for PBL.	104
Figure J.13- Stiffness degradation curve for RIF.	105

CHAPTER 1

INTRODUCTION

1.1 Background

Bangladesh is located in a highly tectonically active region, which makes the structures of the country vulnerable to earthquakes. Unreinforced masonry (URM) structures and reinforced concrete frames infilled by masonry walls are common in Bangladesh due to their affordability and availability of materials and laborers. However, these structures are weak in resisting lateral forces and have limited ductility capacity, making them susceptible to earthquake damage.

To address this issue, grouted reinforcement can be integrated into masonry structures, which can improve their earthquake resistance. In addition, the interaction between masonry infill walls and bounding frames is often ignored in design, leading to the vulnerability of the entire system under cyclic loading. To mitigate this problem, lightweight and high-strength hollow bricks can be used to reduce the weight of the infill wall, which can improve the global lateral stiffness and energy dissipation capacity of the frame.

Research should conduct to observe the behavior of reinforced masonry walls and hollow brick-infilled concrete frame walls under cyclic loading to improve the earthquake resistance of structures in Bangladesh. Additionally, as per the Bangladesh National Building Code 2020, the implementation of a minimum amount of reinforcement in masonry structures is highly recommended in most of the seismic zones in Bangladesh.

There is a significant opportunity for promoting the use of Reinforced Masonry (RM) and Reinforced Hollow Brick Infill walls for earthquake-resistant structures in Bangladesh. For this, the collaboration between industry and construction professionals are crucial to improve the seismic resilience of structures in Bangladesh. Eco Ceramics, a prominent hollow ceramic brick manufacturer in the country, can play a vital role in promoting eco-friendly construction that is both affordable and resilient to disasters. Additionally, GPH Ispat can contribute to this effort by meeting the high demand for ductile reinforcement required for such construction. This partnership can facilitate the adoption of best practices and technologies to mitigate the risk of seismic damage in the country.

1.2 Objectives of the Study

The main objectives of this research are summarized below:

- i. To conduct an experimental study among different reinforced masonry structures and infilled frame structures in terms of stiffness, ductility, load carrying capacity, energy dissipation, etc. under seismic load.
- ii. To observe different cracking patterns and failure modes of the specimens.
- iii. To investigate the performance of reinforced hollow clay brick in masonry wall in comparison with unreinforced solid clay brick.
- iv. To study the effect of installment grouted reinforcement in unreinforced masonry structures.

1.3 Methodology

Twelve 5'× 5' bare walls (Half-scale) and five infilled concrete frame walls (Half-scale) will be constructed with various parameters including different types of bricks, reinforcement and mortar ratios. After construction, an experimental setup will be established to investigate the seismic behavior of the specimen and deflections will be measured. The experimental data from different specimens will be collected and thoroughly compared to evaluate their performance.

1.4 Scope of the Investigation

This research study is conducted to investigate the behavior of reinforced masonry walls and hollow brick infilled concrete frame under cyclic loading. The study aims to address the issue of earthquake vulnerability of masonry structures in Bangladesh by exploring the use of grouted reinforcement and lightweight hollow bricks in infilled concrete frames.

All the specimens will be tested under seismic conditions to evaluate their performance, with deflections and loads being measured and compared. The experimental data will be analyzed to determine the effectiveness of grouted reinforcement and hollow bricks in improving the seismic resilience of masonry structures. This research has practical implications for the construction industry in Bangladesh, where low-strength unreinforced masonry structures are common and at high risk of earthquake damage. The results can inform the adoption of more disaster-resilient building techniques and technologies to enhance seismic safety. The study

will also involve a comparison between reinforced masonry and masonry infilled concrete frame walls by evaluating their load carrying capacity and expense of construction so that the study can provide insights into the economic feasibility of adopting new seismic-resistant construction techniques in Bangladesh.

1.5 Outline of the Study

The report is divided into five chapters, each covering different aspects of the research work.

Chapter One presents the background of the research along with the objectives, methodology, and scope of the study.

Chapter Two provides a literature review where relevant theories, codes, and concepts are described, along with previous research on reinforced masonry and infilled frame and their properties and features.

Chapter Three explains the experimental setup and summarizes the properties of the materials used. It also provides a detailed description of the preparation process of the specimens.

Chapter Four presents the test results, including proper illustrations, graphs, tables, and charts. The test results of each specimen are summarized, and a comprehensive comparison is made among the specimens based on these results.

Chapter Five concludes the report with major findings and observations of the present study, along with recommendations and suggestions for future research in the relevant field.

CHAPTER 2

LITERATURE REVIEW

2.1 Introduction

Reinforced masonry walls are commonly used in construction to provide structural strength and resistance to external cyclic forces such as wind and earthquakes. Seismic behavior of unreinforced masonry walls is a significant concern for buildings located in earthquake-prone regions. Several studies have investigated that reinforced masonry walls can provide excellent seismic resistance under lateral loads. According to these studies, reinforced masonry walls exhibit ductile behavior and can resist lateral loads through a combination of flexure and shear. Additionally, the stiffness and strength of the walls increase with increasing reinforcement ratio and compressive strength of the masonry units.

2.2 Unreinforced Masonry

Unreinforced masonry (URM) is a popular construction practice in our country. Although, because of its heavy weight, limited tensile strength, and restricted flexibility, it suffered damage to withstand seismic loads. The masonry structure exposed to lateral loading commonly showed two types of failure.

- Out-of-plane failure in which cracks showed at length the horizontal mortar bed joints.
- *In-plane failure* which is generally characterized by a diagonal tension failure with compressive crushing. (Wilson & Varkey, 2019)

Unreinforced masonry is a composite material made of bricks with mortar bed joints. The principal mechanisms of the failure modes of masonry can be classified into three types:

• Flexure Failure (Rocking failure and toe-crushing): When a load is applied perpendicular to the plane of the wall, it causes bending stress that can lead to the failure of the wall. URM walls have limited resistance to bending, and therefore, they are vulnerable to flexural failure. Crack patterns depend on the wall geometry (height/width ratio), quality of materials, the ratio of the compression shear stresses (σ/τ) , and boundary restraints.

- Sliding failure: URM wall slides or moves out of its foundation or supporting structure when horizontal forces acting on the wall, which exceed the frictional resistance between the wall and its foundation. Poor friction coefficient, low strength of mortar, seismic loads and the low vertical loads compared to the lateral loads that caused this type of failure. Thus, horizontal cracks can be seen in the mortar joints in sliding plane on the whole length of the masonry walls
- Shear failure: When a force acts parallel to the plane of the wall, it causes a shear force that can cause the wall to slide or fail in shear. The lack of reinforcement in URM walls makes them more susceptible to shear failure. Matsumura (1987); Okamoto et al (1987) found that the masonry walls with low aspect ratios showed shear strengths at failure higher than those for a much slender masonry. It is also observed that the shear strength played an important role of arching action in masonry walls with low aspect ratios, in which a large portion of the shear by compact zones which transferred large compression stresses which is defined as compression struts.

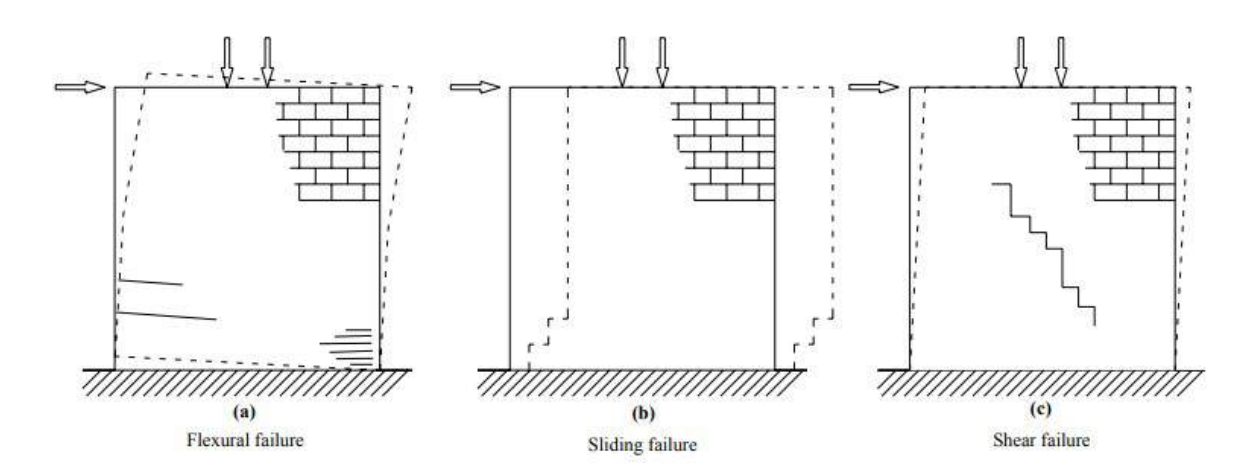


Figure 2.1- The failure modes of masonry wall (Wilson and Varkey, 2019)

2.3 Reinforced masonry

Reinforced masonry (RM) was a structural system consisting of several units that are filled with concrete or grout to anchor steel bars inside them. There are two ways of reinforcement placement in RM walls.

In first case, Reinforcement can be placed in the RM wall horizontally in the cement mortar joint between units. In this state, the serviceability limit case of the masonry could be

preserved. The second case where reinforcement are placed vertically, thus hollow units are used filled with concrete or grout to ensure the stress transfer between steel and masonry, as shown in Fig 2.2.

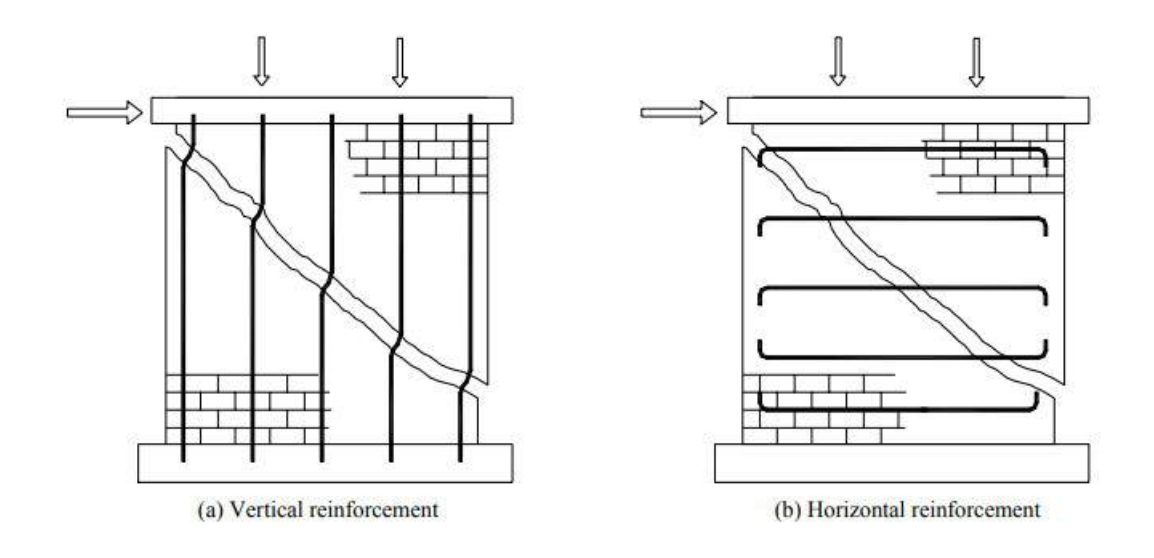


Figure 2.2- Role of reinforcement in RM (Letelier et al., 2019)

According to Haider (2007), the primary mechanism of shear failure worked when the masonry are reinforced vertically and horizontally. The reinforced masonry featured both in plane and out-of-plane with shear and bending capacities. The reinforced masonry also affected the factor of safety of the building due to the ductility rate of steel bars.

According to Samy et al. (2022), joint of reinforcement between reinforcement and masonry in RM walls can be two types:

- Bed-joint RM: In this case, two wires is welded to a persistent curvy cross wire to form a lattice truss. There are many types of joint reinforcement involving welded wire fabric, deformed reinforcing wire, and ladder or truss type joint reinforcement, as shown in Fig 2.3. The method of bed joint reinforcement depends on the anchoring of steel bars within the mortar bed joints, which beforehand excavated for a few centimeters and then refilled by a repointing material. It was observed that bed-joint reinforcement controlled the dispersion and width of cracks at the serviceability.
- Both-direction RM: in this situation, there were two main types of walls: single leaf walls and multi-leaf walls. Firstly, single-leaf walls vertical bars were anchored within the cavity of the concrete or masonry blocks filled by grout, while the horizontal bars were within the mortar joints. Secondly, the two leaf wall's two-directional reinforcement was

within the two leaves of the wall cavity by grout. Horizontal reinforcement was located anchored in the bed joints or in the bond beam units, as shown in Fig 2.4.

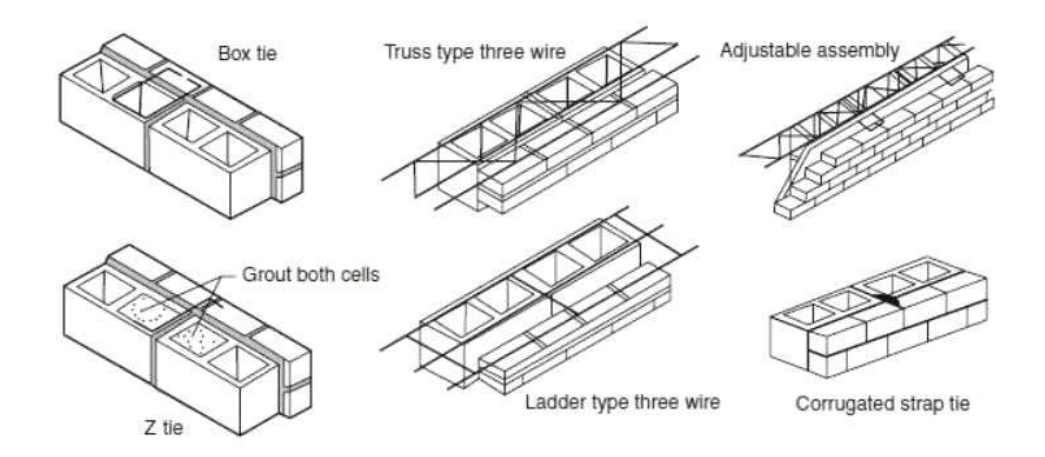


Figure 2.3- Joint Reinforcement Applications in Masonry (Fodi, 2011)

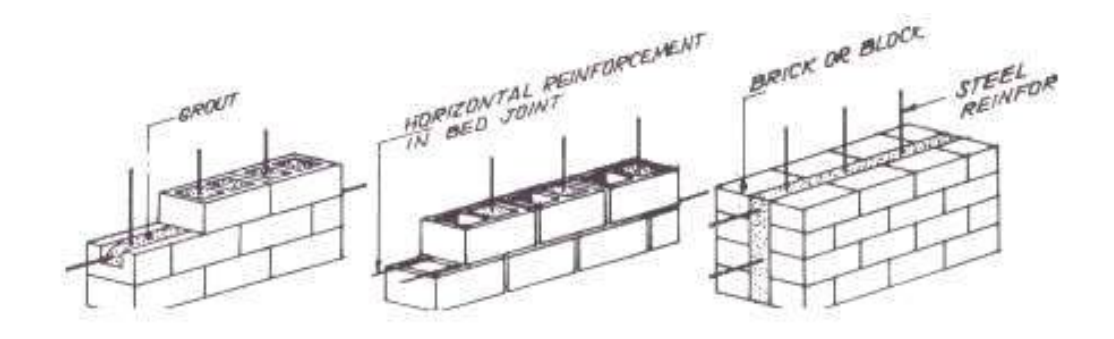


Figure 2.4- Placing of reinforcement in masonry

According to Fodi (2011), Reinforced masonry could be divided into the following classes:

- (a) *Reinforced cavity masonry:* in this situation, two leaves of a cavity wall were tied with wall ties designed to endure horizontal loads due to seismic, masonry units must be placed in running or stacked bonds. This vertically stacked was not allowed in earthquake zones;
- (b) *Reinforced solid masonry:* in this situation, bonding single-leaf walls are mainly applied externally for land retaining buildings. It was possible to reinforce the brickwork using horizontal wires.

- (c) *Reinforced hollow unit masonry:* in this situation, reinforced hollow unit brickwork featured for building in areas of high seismic due to the continuity development into the grout core and the ease of laying horizontal reinforcement bars the vertical or horizontal reinforcing bars were but to improve the tensile strength of masonry.
- (d) *Reinforced grouted masonry:* in this situation; the steel bars were tied to the masonry by grout as one system of strength loads. Composite walls contain two layes of masonry with a solid grouted collar joint with or without steel bars;
- (e) *Reinforced pocket masonry:* in this situation, the bricks were placed the so called "quetta bond". The vertical bars or stirrups must be placed in the middle of the masonry and filled out with concrete or grout, while the horizontal bars were embedded within the bed joint. This type of reinforced masonry was similar to small columns joined together, as shown in Fig 2.5.

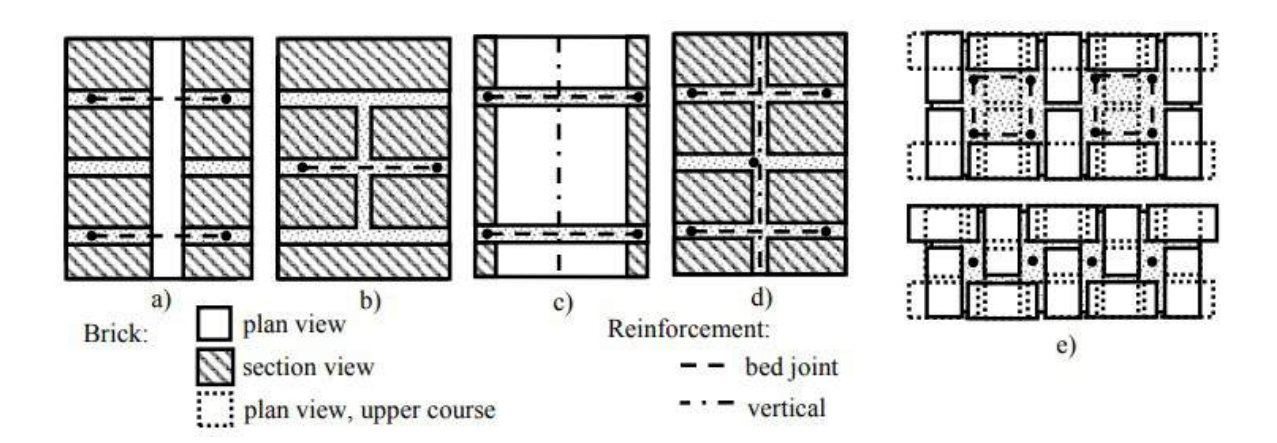


Figure 2.5- a) Reinforced cavity wall, b) Reinforced solid masonry, c) Reinforced hollow unit masonry, d) Reinforced grouted masonry, e) Reinforced pocket type wall. (Fodi, 2011).

2.3.1 Factors Affecting Reinforced Masonry walls

Load-deformation response and failures of the masonry were affected by the following factors.

• *Masonry units:* There were some standardized forms and sizes used for various masonry units used in RM walls such as concrete block, solid concrete, brick, clay block, solid or cored clay brick, clay tile, sand-lime units, and adobe units. The compressive strength of the masonry units affects the load carring capacity of RM walls. The size of the large bricks reduces the number of mortar joints that were the weakest parts of the construction.

The reduction in mortar bed joints will probably increase the strength and make the bricks economical.

• **Bonding of grout and mortar:** The compressive strength of the grout and mortar is important to ensure that the grout or mortar can transfer the compressive loads from the masonry units to the reinforcement. Figure 2.6 shows proportion of cement and fine aggregate for grout specified in ASTM C476.

Type	Parts by Volume of Portland Cement or Blended Cement	Parts by Volume of Hydrated Lime or Lime Putty	Aggregate, Measured in a Damp, Loose Condition	
			Fine	Coarse
Fine grout	1	0-1/10	2¼ –3 times the sum of the volumes of the cementitious materials	Sauth
Coarse grout	1	0-1/10	2¼ –3 times the sum of the volumes of the cementitious materials	1–2 times the sum of the volumes of the cementitious materials

Figure 2.6- ASTM specification for Grout

- Reinforcement ratio: The presence of reinforcement in masonry walls significantly improves their performance under lateral loads. The reinforcement can be in the form of steel bars or fibers, and can be placed in horizontal or vertical directions. Alcocer and Meli (1995) found that the horizontal steel bars increase the shear capacity of brick walls up to 30% compared with the quantity of horizontal reinforcement did not affect the primitive hardness of the wall despite the reinforced masonry walls resisting more forces than the unreinforced masonry walls. Xu et al. (2018) demonstrated that the horizontal and vertical reinforcement ratios for all walls were about 0.60%, 0.29%, respectively, and these ratios were considered the minimum reinforcement ratios of reinforced masonry. Sandoval et al.(2018) found the increase in horizontal reinforcement ratio led to a large increase in shear capacity and a slight increase in the lateral drift. Ghanern and Salarn (1994) found that the cracked deformations in addition to the final capacity of forced wall increased to 0.2% by increasing the horizontal reinforcement ratio.
- Modulus of elasticity of masonry and reinforcement: The modulus of elasticity is a measure of the stiffness of the materials. The modulus of elasticity of masonry and reinforcement should be determined to ensure that the wall deflects within acceptable limits under the expected loads.

- Bond strength between masonry units, grout/mortar and reinforcement: The bond strength between the masonry units, grout/mortar and reinforcement is critical for the structural integrity of the wall. The bond strength should be determined in accordance with ASTM standards.
- *Vertical Load:* According to Ghanern and Salarn (1994), the increase in vertical load led to an increase in strength, ductility, and this increase the bond strength between mortar and masonry units. In addition, the large increase in axial compressive changed the failure wall from flexure to shear. Though, Angelillo (2014) presented that allowable code values for the axial compressive affected by the properties of strength masonry.
- Aspect Ratio of wall: Sandoval et al. (2018) showed that increasing the aspect ratio led to the decrease of maximum lateral load. The aspect ratio of walls (H/L) played a significant role in the failure modes, as shown in Fig 6. For squat walls of (H/L=0.6), the shear that results from the flexural behavior mostly fails by diagonal cracking. For tall walls, a 45° crack happens in the bottom part of the walls showing flexural failure. Four square walls of (H/L=1), the diagonal crack square arises at the high corner of the wall and meets the base which the entire area by the compressive becomes effective in providing shear strength at the compression toe.

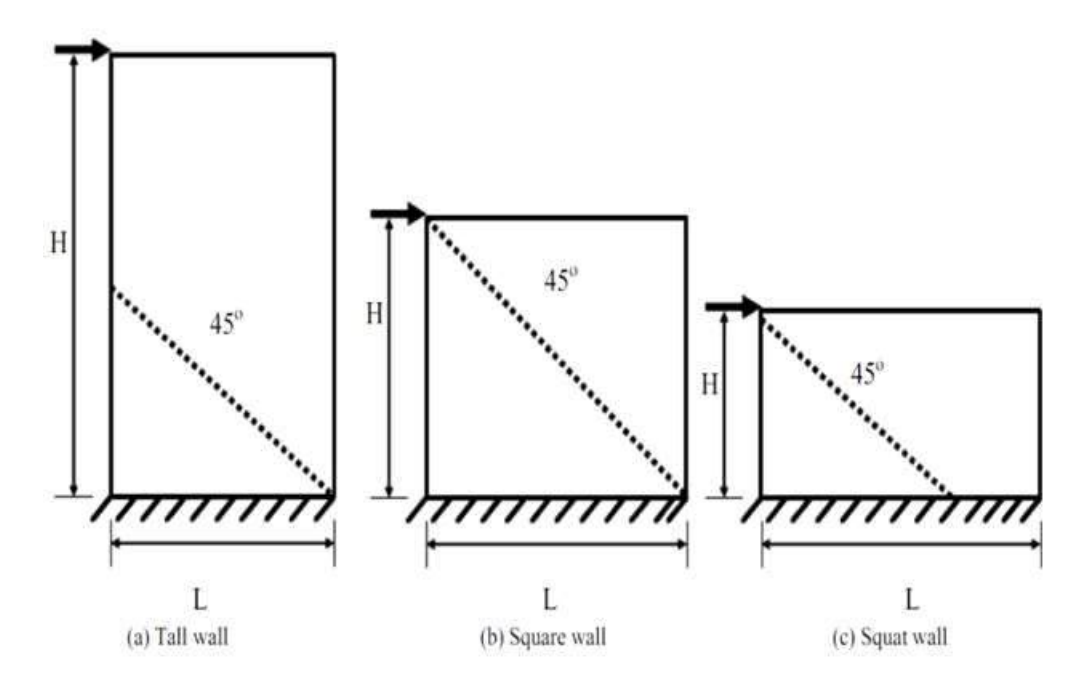


Figure 2.7- Direction of diagonal cracks in masonry shears walls (Sivaraja, 2012)

2.4 Masonry Infilled RC Frame

Infilled RC frame wall is a heterogeneous structure comprised of RC frame and masonry infill. When masonry panels are erected in line with the frames, the stiffness and strength of the frames are greatly increased. However, in seismic design calculations, the existence of masonry infill is typically overlooked on the assumption that it is a nonstructural component. This assumption may lead to erroneous assessments not only of the seismic performance, such as the lateral stiffness, strength, and ductility of the structures but also of the seismic demands associated with the dynamic properties (Maidiawati and Sanada, 2017). The contribution of infill is generally ignored because the mechanism of infill wall is not simple due to their highly nonlinear inelastic response. Furthermore, several mechanical parameters, particularly for masonry infill and the contact between the infill and the surrounding frame, are difficult to characterize (Kareem and Guneyisi, 2018). Hence, the combination and interaction between infill wall and surrounding frame are a matter of concern for engineers and researchers. According to Polyakov (1960), the full combined structure of infill and frame behaves as a braced frame because the masonry panel interacts with each side of the frame at a shorter distance from the loaded corners. This phenomenon was explained as a diagonal strut by the early researchers and engineers as presented in Figure 2.8.

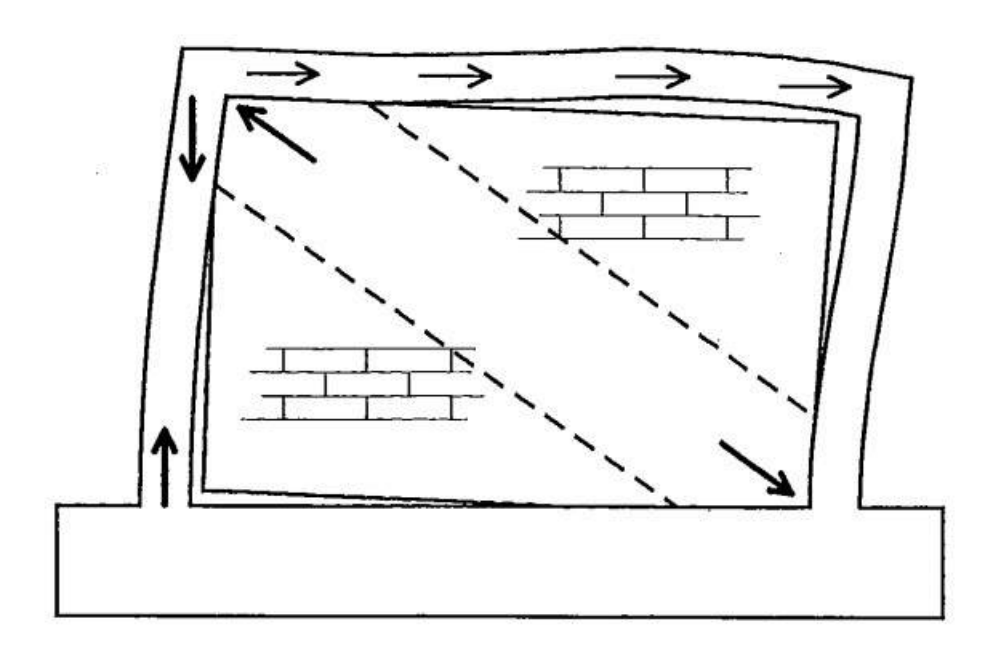


Figure 2.8- Equivalent truss mechanisms for infill frame (Polyakov, 1960).

Fardis et al. (1996) conducted a non-linear dynamic analysis and he demonstrated that the masonry infills influence positively the whole infilled frame structure, especially in the absence of irregularities. Furthermore, he showed that the masonry infill is highly beneficial to increase the stiffness and decrease the deformation of the whole system. The dynamic behavior of this type of structure is also improved because the system can dissipate sufficient energy through the slippage and friction action between the infill and the frame.

Tomazevic (1999) showed that an infilled frame operates as a monolithic load-resisting system at low lateral loads. Nevertheless, the crack is visible when there is an increment of loading. Moreover, the infill has a tendency to partially separate from the bounding frame as the load increases. This phenomenon is responsible for the formation of the compression strut mechanism. It may or may not develop into the principal load mechanism of the structure, contingent on the strength and stiffness characteristics of the infill relative to those of the frame. The behavior of this type of model is shown in Figure 2.9.

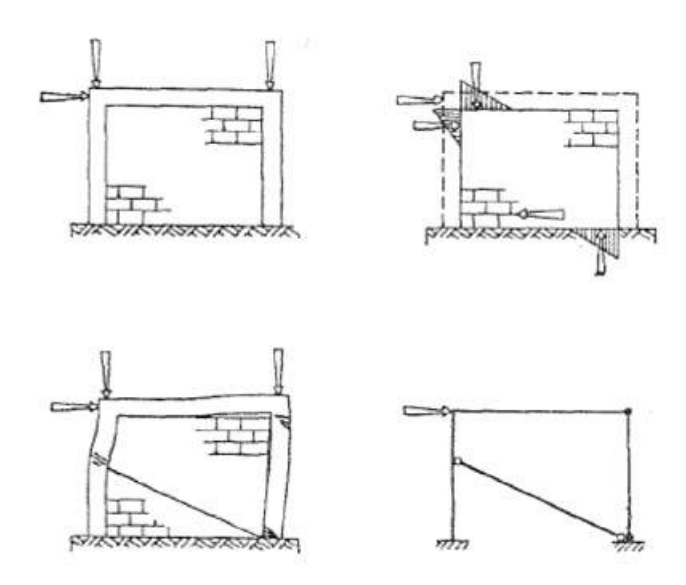


Figure 2.9- Modeling of seismic behavior before and after detachment of masonry infill (Tomazevic, 1999).

Murty and Jain (2000) stated that infills generate interference with the lateral deformations of the RC frame, which results in the segregation of the frame and the infill along one diagonal and the creation of a compression strut along the other diagonal. Therefore, infills contribute to the building's lateral rigidity. The frame action is replaced with a major truss action as the structural load transfer mechanism. As a result of this change, the frame columns are

subjected to heavy axial forces, but they are also subjected to diminished bending moments and shear forces. The phenomenon is presented in Figure 2.10.

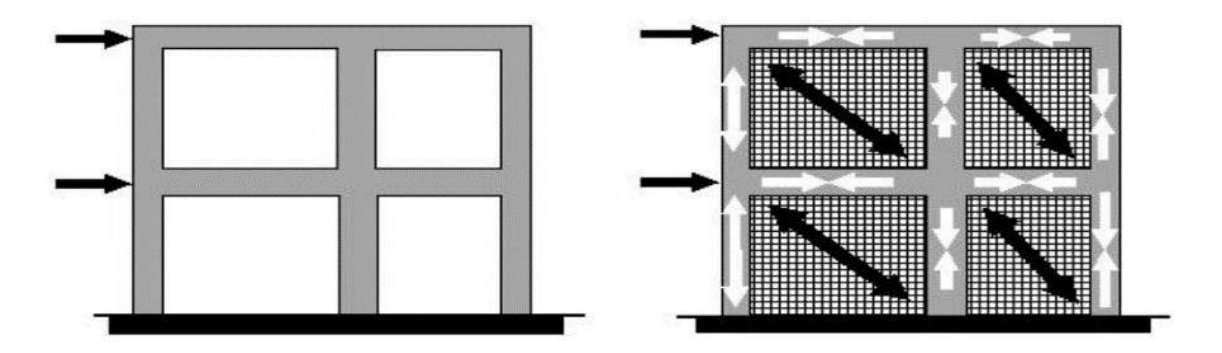


Figure 2.10- Change in the lateral load transfer mechanism owing to the inclusion of masonry infill walls (Murty and Jain, 2000).

2.4.1 Different Failure Modes of Masonry Infilled RC Frame Structures

In FEMA 306 (1998), four basic types of failures have been described.

- Bed joint sliding
- Corner crushing
- Diagonal tension cracking
- Cracking due to both corner crushing and diagonal cracking

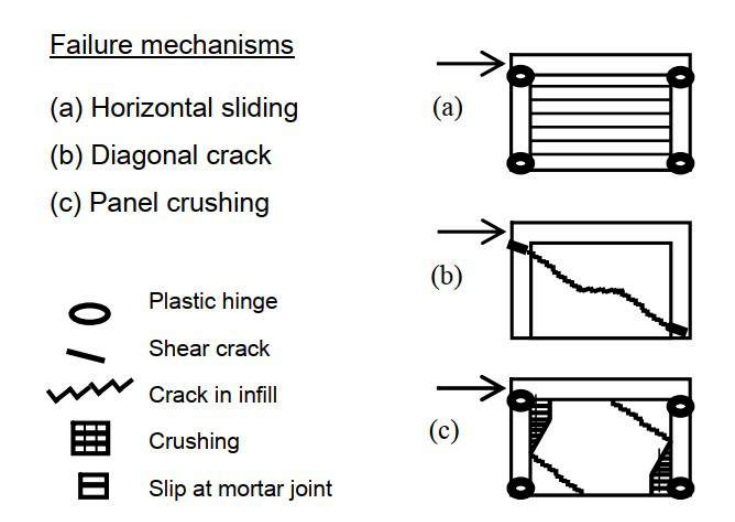


Figure 2.11- Failure mechanisms of infilled frames (Mehrabi et al., 1994).

2.5 Standards and Codes

Building codes provide minimum requirements for the design and construction of reinforced masonry walls to ensure adequate safety and performance. Most building codes for reinforced masonry walls are based on the International Building Code (IBC) and the Building Code Requirements for Masonry Structures (TMS 402).

The International Building Code (IBC) is a model code developed by the International Code Council (ICC) that provides minimum requirements for the design, construction, and maintenance of buildings and structures. Chapter 21 of the IBC provides specific requirements for masonry construction, including reinforced masonry walls. On the other hand, The Building Code requirements for Masonry Structures (TMS 402) is a consensus-based standard developed by the Masonry Standards Joint Committee (MSJC) that provides minimum requirements for the design and construction of masonry structures, including reinforced masonry walls. TMS 402 provides guidance on materials, design, construction, and inspection of masonry structures and referenced by many building codes in the United States.

In Bangladesh, The Bangladesh National Building Code (BNBC) 2020 provides guidelines for the design and construction of reinforced masonry walls in Bangladesh. According to BNBC, Two assumption have to be followed while designing reinforced masonry.

- a) Masonry carries no tensile stress.
- b) Reinforcement is completely bonded.

Members will be designed for specific loading condition. Stress calculation for different loading condition specified in BNBC 2020 (section 7.6) is discussed below.

Design of Members Subjected to Axial Compression:

Stresses due to compressive forces applied at the centroid of load bearing wall, column and pilaster may be computed assuming uniform distribution over the effective area.

$$f_a = \frac{P}{A_a}$$

Design of Members Subjected to Shear Force:

Shearing stresses in flexural members and shear walls shall be computed by the following equation.

$$f_v = \frac{V}{bjd}$$
; $A_v = \frac{sV}{A_sjd}$; $s \le \frac{d}{2}$ or 600 m

When the computed shear stress f_v exceeds the allowable value, web reinforcement shall be provided and designed to carry the total shear force. The area required for shear reinforcement placed perpendicular to the longitudinal Reinforcement is A_v . Spacing of vertical shear reinforcement shall not exceed d/2, nor 600 mm.

Design of Members Subjected to Flexural Stress:

Rectangular flexural elements shall be designed in accordance with the following equations or other methods based on the simplified assumptions.

Compressive stress in the masonry,
$$f_b = \frac{M}{bd^2} (\frac{2}{jk})$$

Tensile stress in the longitudinal reinforcement,
$$f_s = \frac{M}{A_{sjd}}$$

2.5.1 Reinforcement Detailing of Reinforced Masonry Wall

Some of the design guidelines reinforcement requirement specified for reinforced masonry walls in the BNBC 2020 are mentioned below.

Maximum size of the reinforcement used in RM walls will be 35 mm. Maximum steel area in cell shall be 6 percent of the cell area without splices and 12 percent of cell area with splices. The clear distance between parallel bars, except in columns, shall not be less than the nominal diameter of the bars or 25 mm. The minimum clear distance between parallel bars in columns shall be two and one-half times the bar diameter. The clear distance between the surface of a bar and any surface of a masonry unit shall not be less than 6 mm for fine grout and 12 mm for coarse grout. Cross webs of hollow units may be used as support for horizontal reinforcement. All reinforcing bars, except joint reinforcing, shall be completely embedded in mortar or grout and have a minimum cover, including the masonry unit, as specified below:

- (a) 20 mm when not exposed to weather
- (b) 40 mm when exposed to weather
- (c) 50 mm when exposed to soil

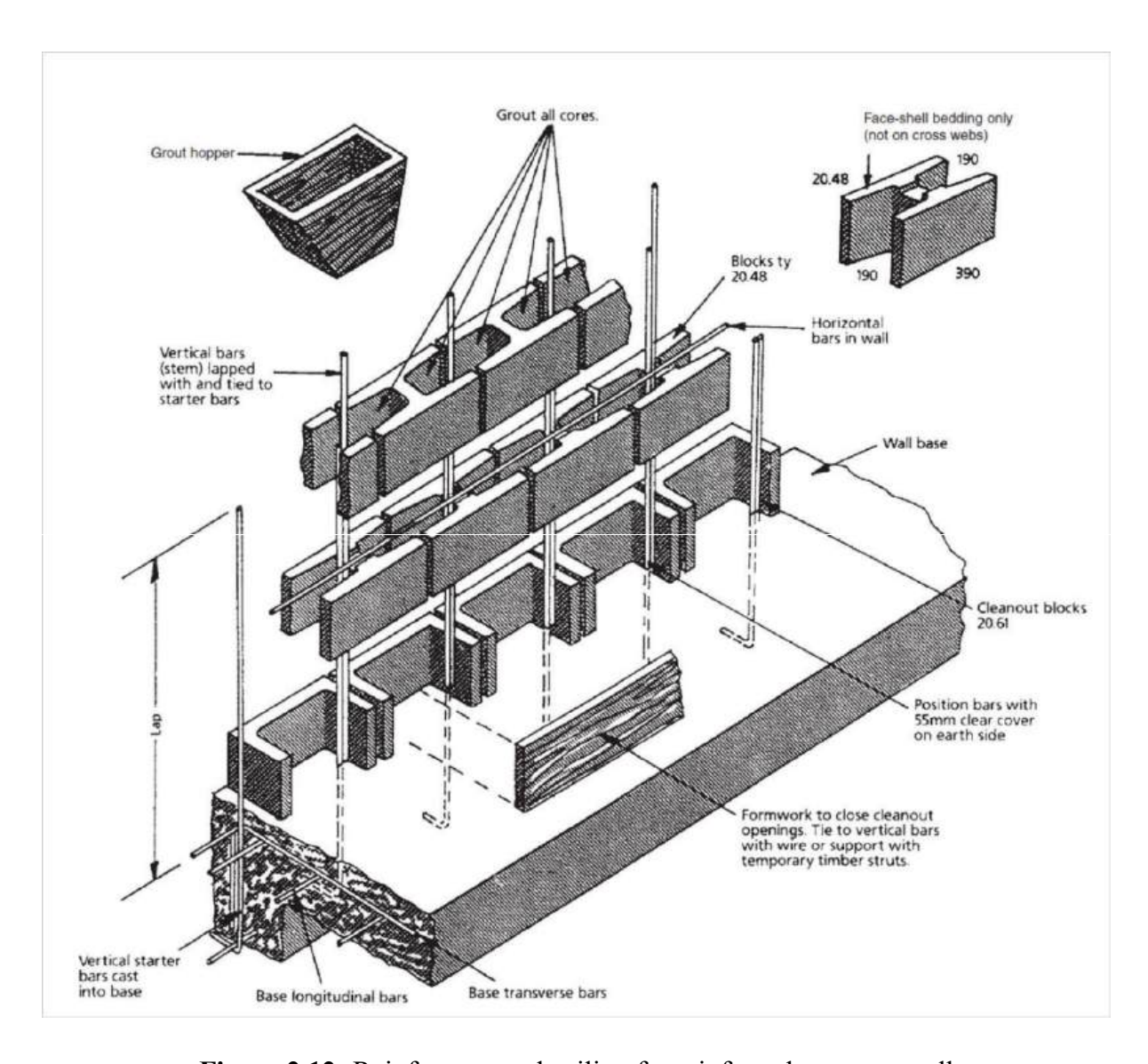


Figure 2.12- Reinforcement detailing for reinforced masonry wall

CHAPTER 3

EXPERIMENTAL STUDY

v3.1 Introduction

This research has been carried out to study the behavior of reinforced masonry walls having different materials and structural properties under cyclic load and compare the results with unreinforced masonry walls.

This chapter covers the characteristics of the materials used in the research, the specifics of the specimens chosen, their description and method of preparation, as well as the specifics of the experimental setup and instruments.

3.2 Material Properties

The major components of reinforced masonry and infilled frame walls are clay brick, cement, fine aggregate, coarse aggregate, and steel reinforcement. The properties of these materials were tested in the laboratory to ensure proper quality.

3.2.1 Cement

Crown Portland Cement (BDS EN 197-1:2003) has been used in this research. Some essential properties of this cement have been determined in the concrete laboratory. The properties are shown in Table 3.1.

Table 3.1- Properties of cement

Normal Consistency (%)	25
Initial setting time (minutes)	162
Final setting time (minutes)	358
Cement mortar compressive strength (MPa)	35.4 (7 Days)
cement mortal compressive strength (wir a)	46.2 (28 Days)

3.2.2 Fine Aggregate

Sand used as fine aggregate that was strong, clean, and free of toxic components and organic substances according to ASTM C33, 2020. In this study, two different kinds of fine aggregates have been used including local sand having FM 2.7 and sylhet sand having FM 1.5.

3.2.3 Coarse Aggregate

12.5 mm and downgraded stones have been used as coarse aggregate for infilled frame which comply with characteristics mentioned in ASTM C33, 2020.

3.2.4 Reinforcement

In this experiment, 8 mm and 12 mm diameter B420DWR rebars and 8 mm 500CWR rebers have been used. Table 3.2 displays the results of tension tests. In Appendix-A, detailed results of the reinforcement testing are illustrated.

 Table 3.2- Tension test results of reinforcement

Reber Grade	Diameter	Average Yield Strength	Average Ultimate
		(MPa)	Strength (MPa)
B420DWR	8	472	686
B420DWR	12	465	637
B500CWR	8	555	660

3.2.5 Clay Brick

In this experiment, both solid and perforated clay bricks have been used. In order to create eight half-scale solid clay bricks, a full-scale solid clay brick (240 mm \times 115 mm \times 67 mm) was cut along the dotted lines in Figure 3.1. Dimensions of each half-scale solid clay brick were 120 mm \times 57.5 mm \times 33.5 mm.

A full-sized perforated clay brick has ten holes in it, each measuring 23 mm in diameter. Its dimensions (240 mm \times 115 mm \times 67 mm) were cut to make eight half-scale perforated clay bricks by following the dotted lines in Figure 3.2. The middle hatched portion was deducted due to maintaining the uniformity of all half scale brick. Each half-scale perforated clay brick measured 104 mm \times 57.5 mm \times 33.5 mm and had two holes (each 23 mm in diameter) in it.

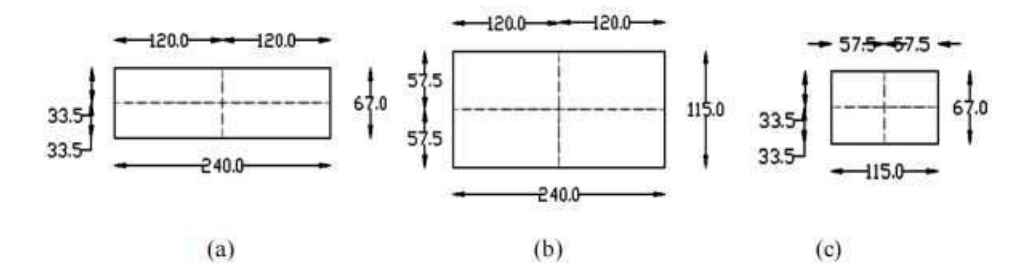


Figure 3.1- (a) Front / back elevation, (b) plan view, (c) side elevation of a full scale solid clay brick (Every unit is in mm).

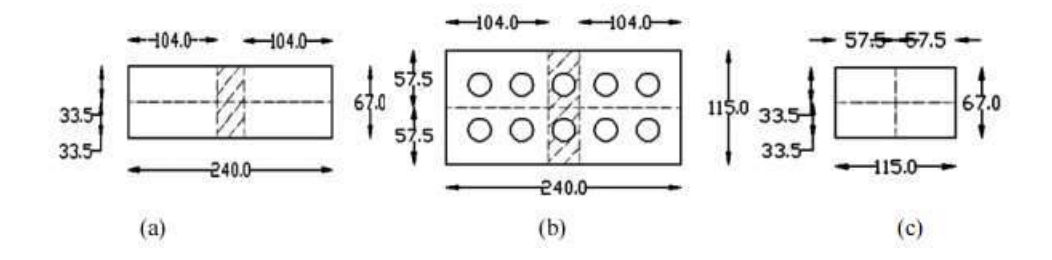


Figure 3.2- (a) Front / back elevation, (b) plan view, (c) side elevation of a full scale perforated clay brick (Every unit is in mm).

The compressive strength and water absorption capacity of the brick samples were determined in the laboratory according to ASTM C67, 2020. The test results are summarized in Table 3.3. Details of these results are illustrated in Appendix-B and C.

Table 3.3- Properties of clay brick

Compressive Strength		Water Absorption	
Solid Brick	Perforated Brick	Solid Brick	Perforated Brick
40.4 Mpa	26.8 Mpa	14.7%	12.8%

3.2.6 Mortar

Three different cement to sand ratio for mortar have been used in this study which are commonly used in local construction practice in Bangladesh. Cement and local sand were mixed at 1:2, 1:4 and 1:6 ratio to cast mortar. The water/cement ratio has been maintained as 0.45 in every case. The compressive strengths of mortar cubes are determined according to ASTM C109, 2020. The results are shown in Figure 3.3, Figure 3.4 and Figure 3.5 for different cement to sand ratio. Detailed test results are illustrated in Appendix-D.

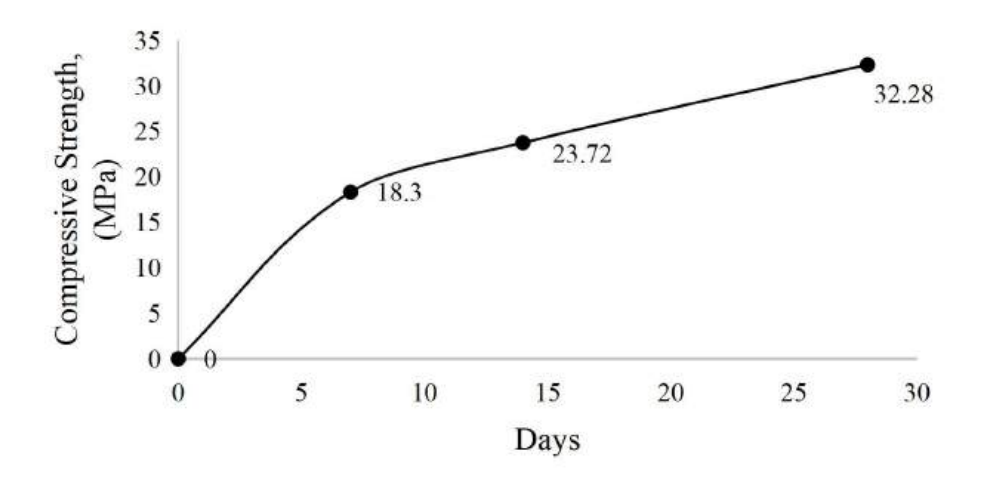


Figure 3.3- Compressive strength of mortar cube for mix ratio 1:2.

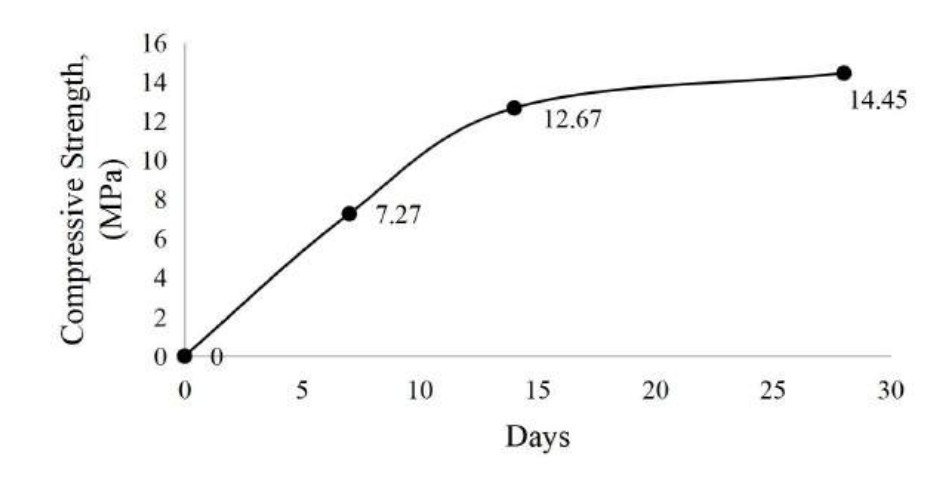


Figure 3.4- Compressive strength of mortar cube for mix ratio 1:4.

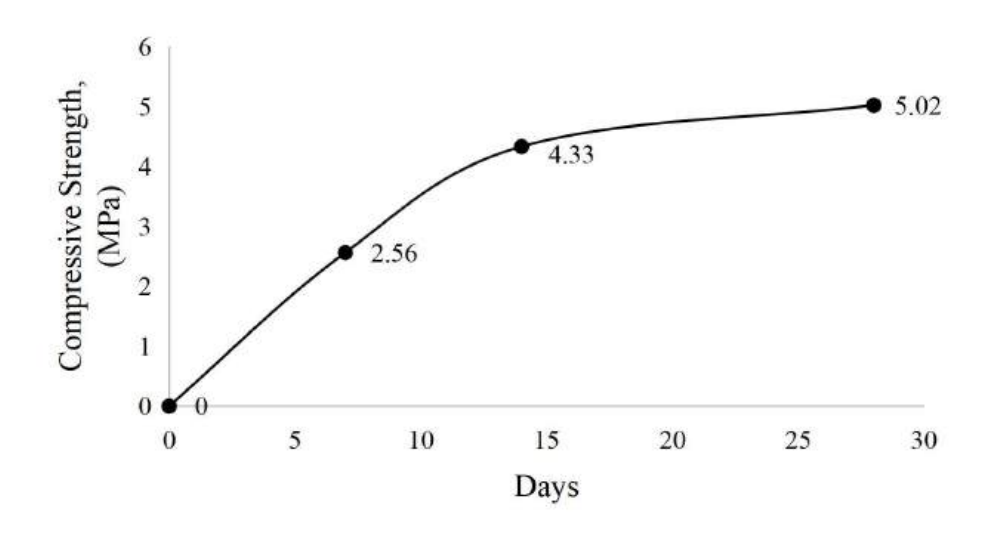


Figure 3.5- Compressive strength of mortar cube for mix ratio 1:6.

3.2.7 Prism Test

Clay bricks and mortar has been used to construct the masonry prism to estimate the capacity of masonry. Ten solid bricks and ten perforated bricks were placed in a set of solid and perforated masonry prisms respectively which were bound by mortar. After 28 days curing period, these prisms were tested in compression testing machine for determining compressive strength of masonry unit. The compressive strength test of brick prisms were conducted according to ASTM C1314, 2020. Results are shown in Table 3.4. Detailed test results are illustrated in Appendix-E.

Table 3.4- Compressive strength of brick prism

Mix Ratio (Cement: Sand)	Brick Type	Average Compressive Strength (MPa)
1:2	Solid	11.56
	Perforated	6.55
1:4	Solid	10.48
	Perforated	4.85
1:6	Solid	6.92
	Perforated	3.96

3.2.8 Grout

For reinforcement and masonry unit bonding, grouting were used to fill the space between brick and reber. Fine grout having cement to local sand mix ratio of 1:3 were used and water/cement ratio was 0.7. (according to ASTM C476, 2020).

3.2.9 Concrete

For infilled frame walls and base of masonry wall, a mixture of cement, sylhet sand, and coarse aggregate was mixed at a ratio of 1:1.5:3 while beam column concrete casting. The water to cement ratio was maintained as 0.45. Slump value 75-100 mm were achieved to ensure sufficient workability. After 28 days curing period, these cylinders were tested in compression testing machine. Figure 3.6 displays the compressive strength of concrete cylinder on several days tested according to ASTM C39, 2020. Details of the test results for the reinforcement are shown in Appendix-F.

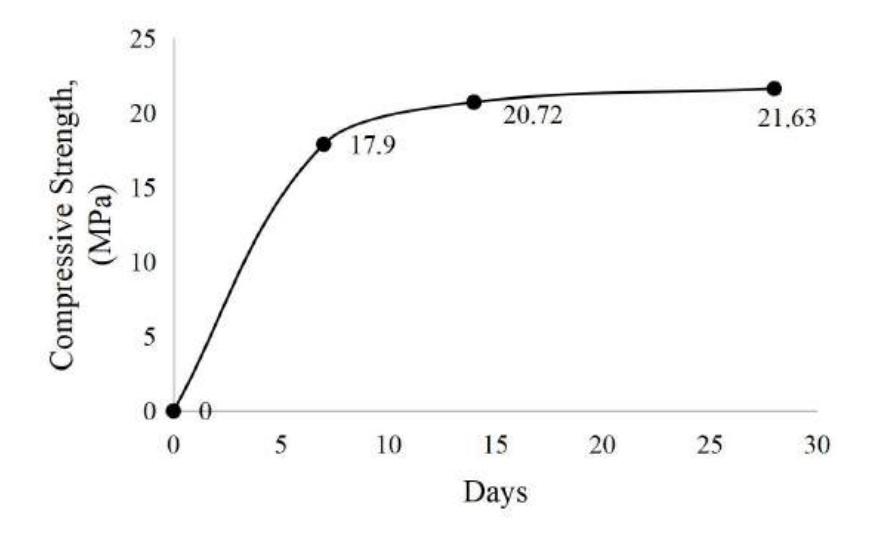


Figure 3.6- Compressive strength of concrete cylinder.

3.3 Details of Specimens

All the test samples were prepared in the concrete laboratory of the Department of Civil Engineering, BUET.

3.3.1 Reinforced Masonry walls

In this experiment, six reinforced masonry (RM) wall were constructed with perforated brick and tested under in plane lateral cyclic loading. Among seven specimens, the core variation was introduced in mortar type and reinforcement grade. Four walls were having 420DWR reber while other three walls contained 500CWR as tension reinforcement. Six specimens having 420DWR and 500CWR reber were constructed for three different cement to sand ratio (1:2, 1:4 and 1:6). Dimension of each walls are 1524mm × 1524 mm × 127mm. In each wall, 8 mm diameter bar were used as vertical and horizontal reinforcement in zigzag pattern. Horizontal reinforcement used in every four layers. All the walls are constructed on a strong firm concrete base. The details of these specimens are illustrated in Table 3.5. The schematic drawings of the specimens are presented in Figures 3.7.

Table 3.5- Details of the reinforced masonry walls

Wall No	Wall Name	Brick Used	Mortar (Cement : Sand)	Reinforcement
1	RM2-420	Perforated	1:2	420 DWR
2	RM4-420	Perforated	1:4	420 DWR
3	RM6-420	Perforated	1:6	420 DWR
5	RM2-500	Perforated	1:2	500 CWR
6	RM4-500	Perforated	1:4	500 CWR
7	RM6-500	Perforated	1:6	500 CWR

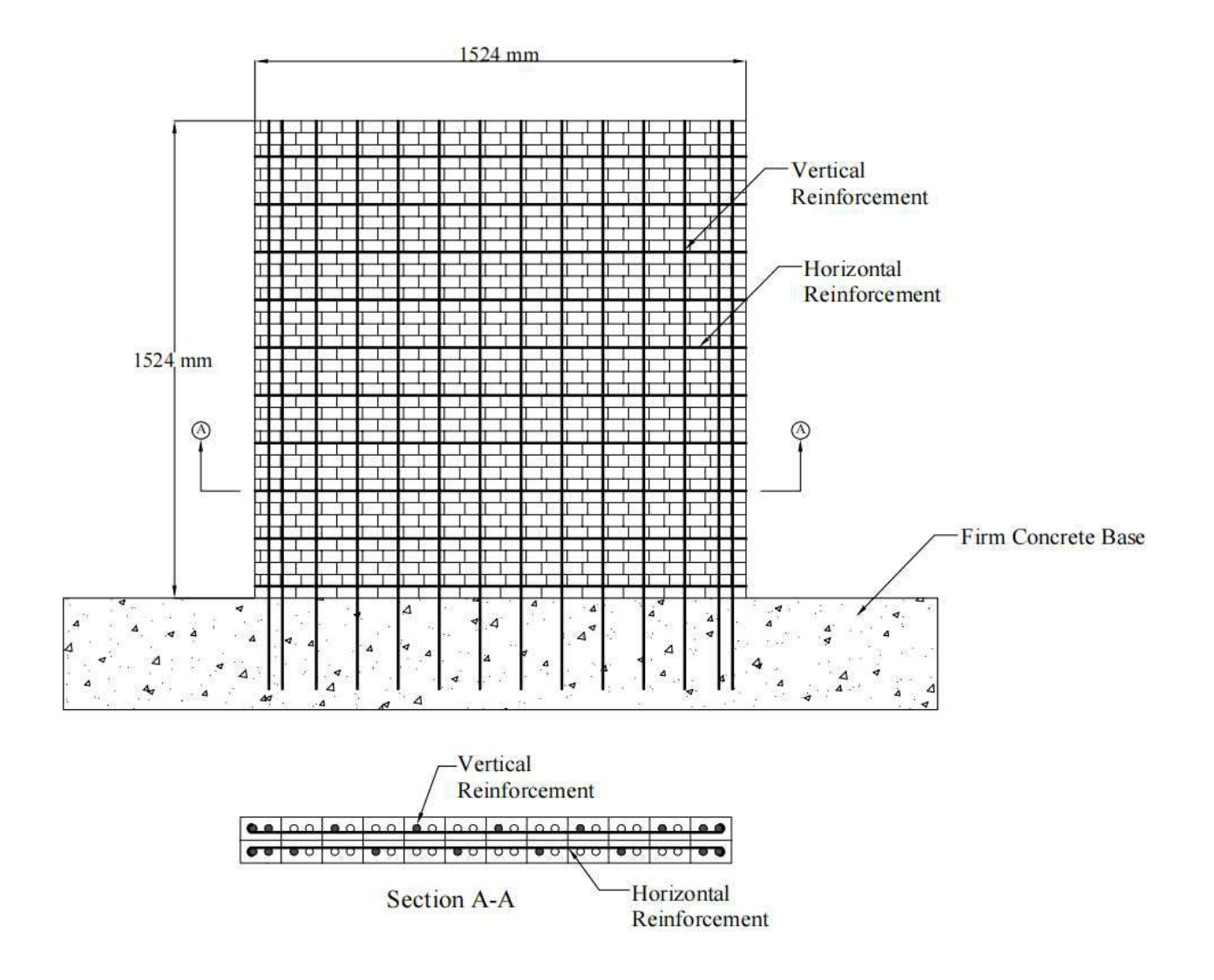


Figure 3.7- Schematic drawing of Reinforced Masonry wall (Every unit is in mm).

3.3.2 Unreinforced Masonry

In this experiment, six unreinforced masonry (URM) wall were constructed and tested under in plane lateral cyclic loading same as RM walls. Among six specimens, the core variation was introduced in mortar type and brick type. Three walls were constructed with solid brick while perforated bricks were used for other three walls. All six walls were constructed for three different cement to sand ratio (1:2, 1:4 and 1:6). Dimension of each walls are 1524mm × 1524 mm × 127mm. All the walls are constructed on a strong firm concrete base. The details of these specimens are illustrated in Table 3.6. The schematic drawings of the specimens are presented in Figures 3.8 and 3.9.

Table 3.6- Details of the unreinforced masonry walls

Wall No	Wall name	Brick Used	Mortar (Cement : Sand)
1	SURM2	Solid	1:2
2	SURM4	Solid	1:4
3	SURM6	Solid	1:6
4	HURM2	Perforated	1:2
5	HURM4	Perforated	1:4
6	HURM6	Perforated	1:6

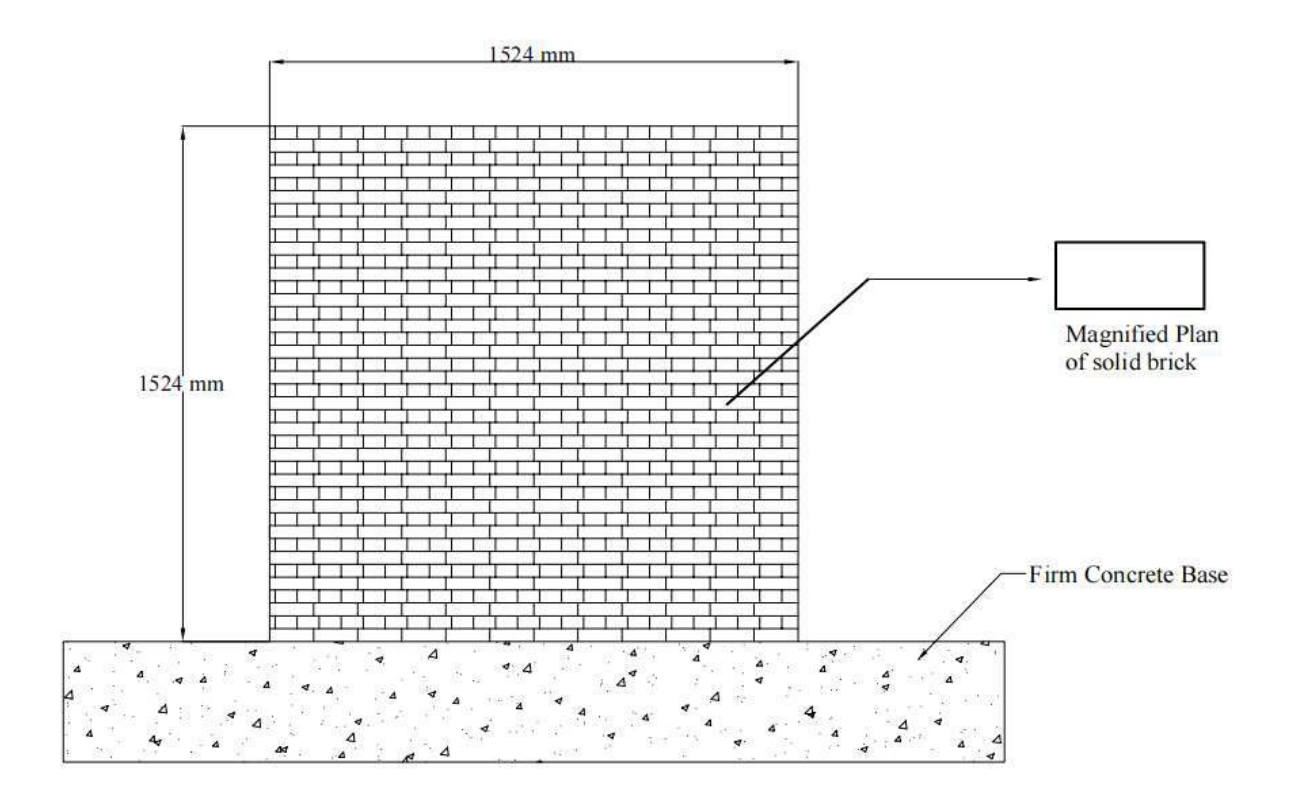


Figure 3.8- Schematic drawing of perforated unreinforced Masonry wall (Every unit is in mm).

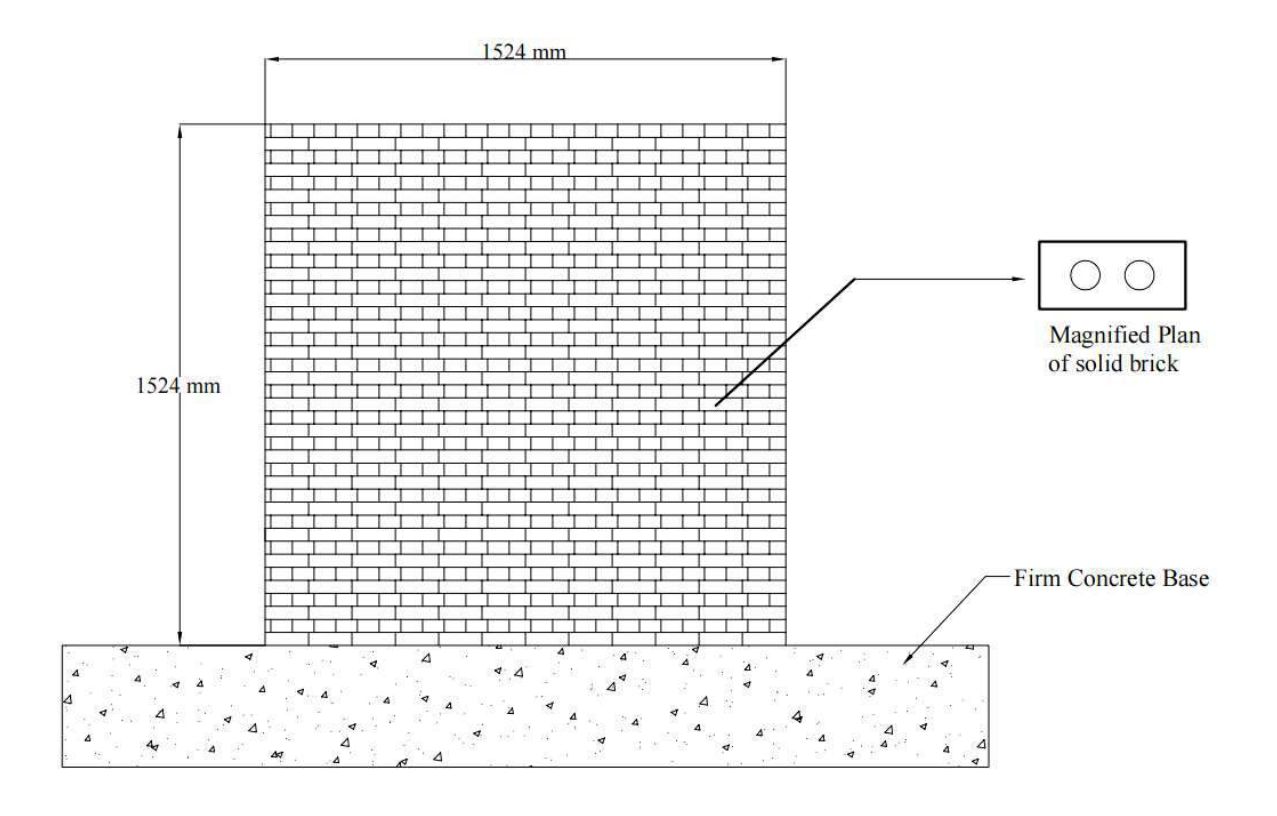


Figure 3.9- Schematic drawing of solid unreinforced Masonry wall (Every unit is in mm).

3.3.3 Infilled Frame

In this experiment, four single bay single-story half-scale unreinforced masonry infilled concrete frame and one reinforced masonry infilled concrete frame structures were constructed and they were tested under in-plane lateral cyclic loading. Among four unreinforced masonry infilled walls, the core variation was introduced in masonry materials and the existence of lintel. Two of the specimens contained lintel and the rest two were constructed without lintel. Again, solid clay bricks were used in two specimens and the masonry work of the rest two structures were built with perforated clay bricks. Each frame consisted of two columns (150 mm × 150 cross sectional area) and one beam (150 mm × 150 cross-sectional area). In both the beam and columns, 12 mm diameter and 8 mm diameter bar were used as main bar and shear reinforcement respectively. The main frame was the same in all five specimens. The cross-sectional dimension of the lintel was 125 mm × 100 mm and it contained 8 mm diameter reinforcement both as the main bar and stirrup. For reinforced masonry infilled wall 8 mm diameter reinforcement were used in perforated masonry unit as

vertical and horizontal reber. The details of the specimens are illustrated in Table 3.7. The schematic drawings of the specimens are presented in Figures 3.10 to 3.12.

Table 3.7- Details of the masonry infilled frame walls

Wall no	Wall Name	Brick type	Existence of lintel
1	SB	Solid	No
2	PB	Perforated	No
3	SBL	Solid	Yes
4	PBL	Perforated	Yes
5	RIF	Perforated	No

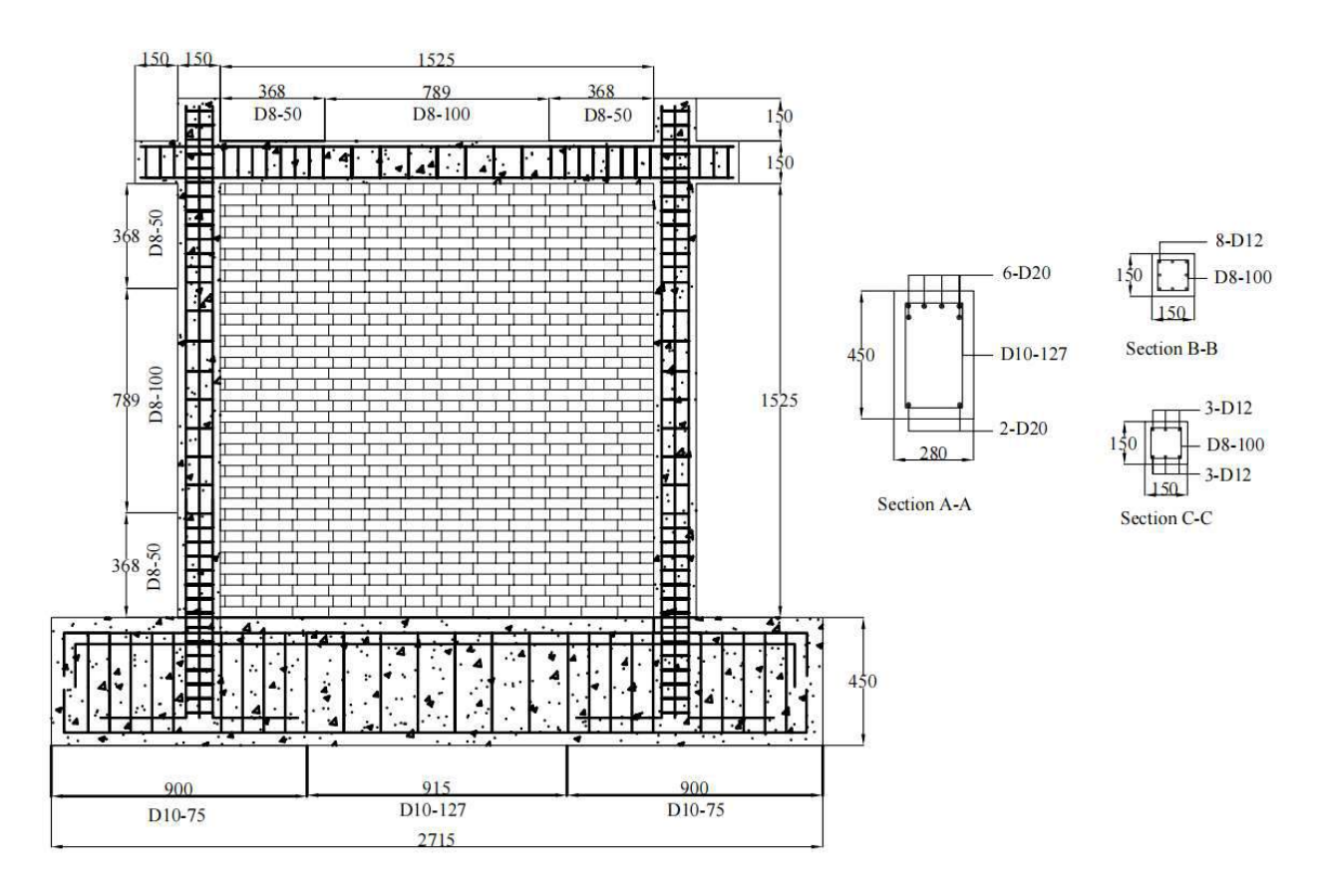


Figure 3.10- Schematic drawing of infilled frame without lintel (Every unit is in mm).

[Note: Section A-A, B-B and C-C are the midsection of base, column and beam respectively].

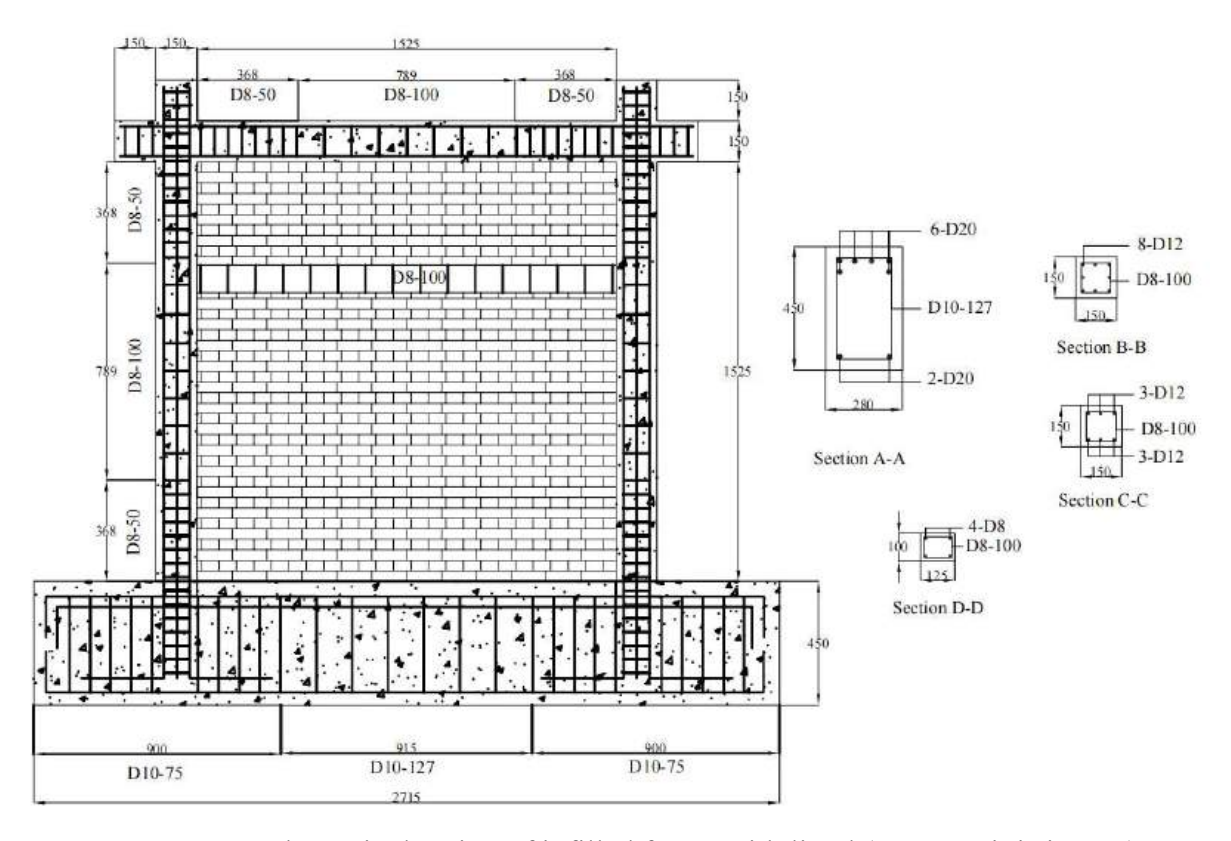


Figure 3.11- Schematic drawing of infilled frame with lintel (Every unit is in mm)

[Note: Section A-A, B-B, C-C and D-D are the midsection of base, column, Beam and lintel respectively].

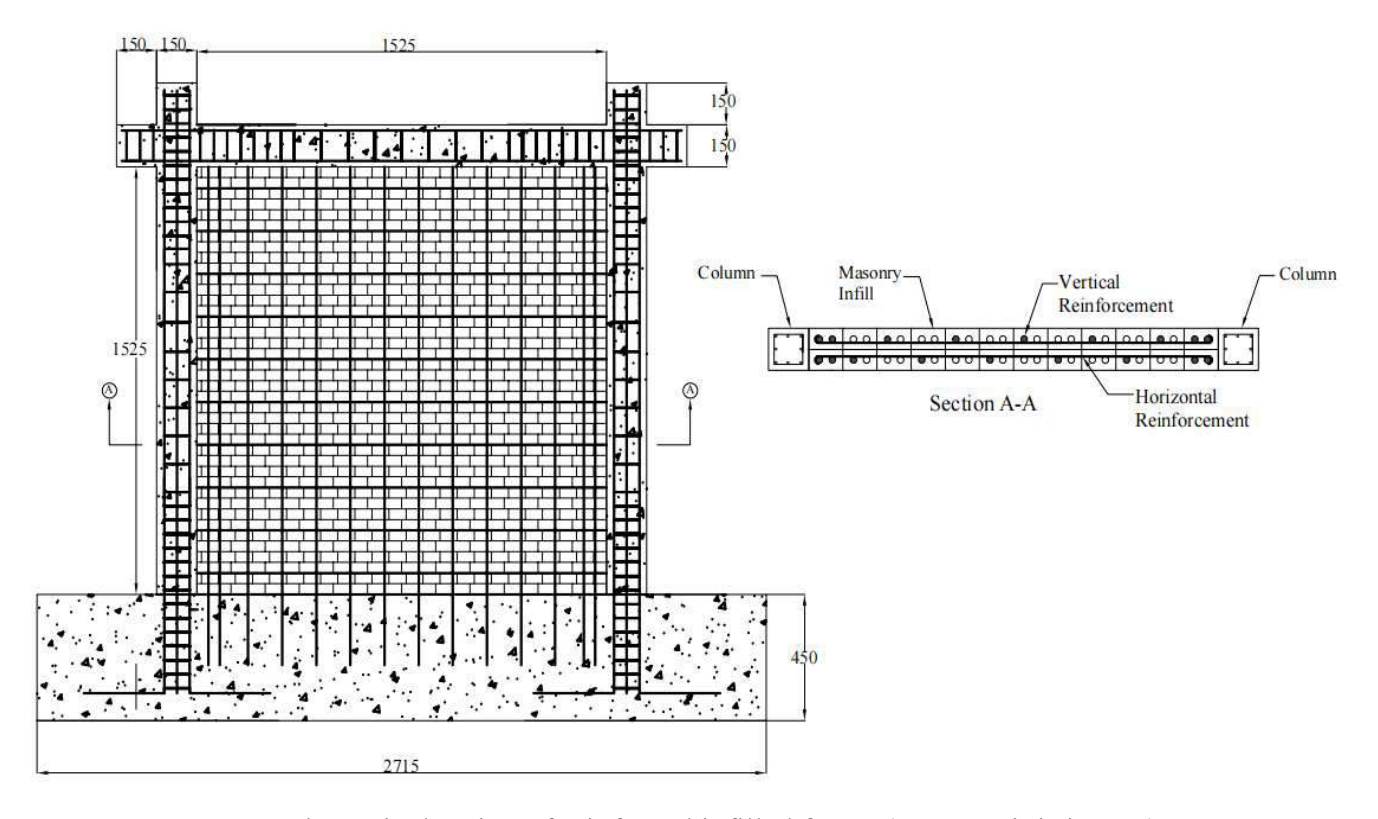


Figure 3.12- Schematic drawing of reinforced infilled frame (Every unit is in mm).

3.4 Preparation of Specimens

All the specimens have been precisely prepared in order to get satisfactory testing results. Steps of specimen preparation is different for RM, URM and MIRCF. This section covers the procedure for sample preparation of each type of walls which is followed by step-by-step illustrated instructions for preparing specimens.

3.4.1 Reinforced Masonry wall Preparation

All seven reinforced masonry walls were prepared on individual concrete base. So the step 1 is to arrange the reinforcement, bent them and fastened to form the base. 20 mm diameter bars were used for longitudinal reinforcement and 10 mm diameter bars were used as shear reinforcement. Different phases of these processes are displayed in Figure 3.13.







Figure 3.13- Reinforcement Preparation for base of RM walls.

In step 2, 8 mm diameter vertical reinforcement were embedded into the base keeping proper alignment and spacing. Development length for vertical reinforcement was kept 150 mm. Details of this phase are shown in Figure 3.14.





Figure 3.14- Vertical Reinforcement Preparation for base of RM

In step 3, wooden formwork was prepared and the base were inserted inside the formworks to provided a suitable clear cover using cement concrete blocks. With a plastic cover, it was made sure that the joints of the formworks were impermeable to leaks.



Figure 3.15- Formwork Preparation of RM walls

In step 4, cement, sylhet sand, and coarse aggregate were mixed at 1:1.5:3 ratio by volume in a mixture machine to prepare concrete. The water/cement ratio was kept at 0.45. During casting slump was kept between the range of 75 mm to 100 mm. After preparing fresh concrete, they were poured carefully in the formwork and compacted cautiously with a vibrator. Different stages of these processes are presented in Figure 3.16.







Figure 3.16- Measuring slump and concrete casting of RM walls.





Figure 3.17- Base of RM walls after 28days of casting.

In step 5, perforated bricks were cut through predetermined lines as shown in Figure 3.2

so that a full-scale brick (240 mm \times 115 mm \times 67 mm in dimension each) can be converted to eight half-scale bricks 104 mm \times 57.5 mm \times 33.5 mm in dimension each). Eight half-scale perforated clay bricks produced from a single full-scale perforated clay brick are shown in Figure 3.18.

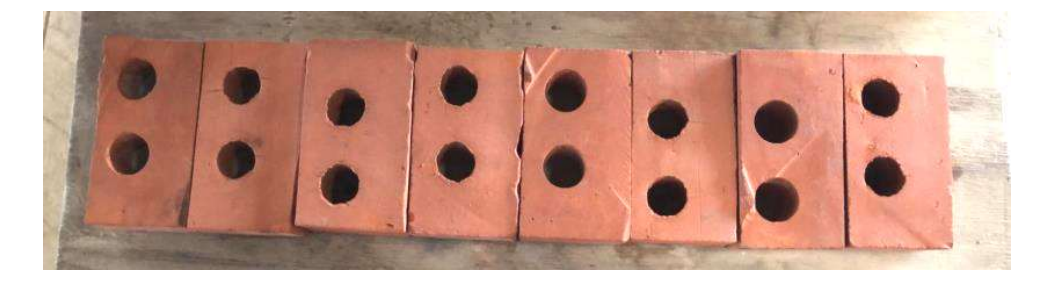


Figure 3.18- Eight half-scale bricks produced from a single full-scale brick

In step 6, bricks, cement, local sand, and water were prepared to commence masonry work. Cement and local sand were mixed at a specific ratio (1;2, 1:4 and 1:6) by volume for mortar for each wall and the water/cement ratio was maintained at 0.45. After that, bricks were placed carefully so that the vertical reinforcement could be inserted into exact hole of the brick. Horizontal reinforcement were placed at first layer of masonry and on every four layer after that. The space between brick hole and reber were filled with grouting (specified in

3.2.7). The whole 1524 mm \times 1524 mm \times 125 mm wall of each specimen was filled up with bricks in two layers. Masonry units were joined using english bond.





Figure 3.19- Masonry work of RM walls.

After completing the masonry work, the specimens were kept 28 days more before testing. In the last step, all the specimens were whitewashed such as in Figure 3.20 to identify the cracks properly during testing.



Figure 3.20- Reinforced Masonry Wall after whitewash.

3.4.2 Unreinforced Masonry wall Preparation

All 6 walls were constructed on individual concrete base. So in step 1, reinforcements were prepared for base. Ten 20 mm diameter bar were used as longitudinal reinforcement while 10 mm bar were used a shear reinforcement for base. The length of the each base were 2130 mm. After reinforcement work base were casted maintaining mix ratio specified in section 3.2.8.







Figure 3.21- Base Construction for URM.

In step 2, The URM walls were constructed on the centrally marked place of beams top surface after 28 days of curing of the base. The English bond for masonry wall was used with one layer of stretcher and another layer of header and so on. As the wall samples were so prepared that replicate a 10 in. wall being used in conventional construction work.





Figure 3.22- URM wall construction

In step 4, after 28 days of mortar curing, all URM walls were whitewashed and ready for setup.



Figure 3.23- URM wall after whitewash.

3.4.3 Masonry Infilled Frame Wall Preparation

In step 1, reinforcements were bent and fastened to form a reinforced structure. Mainly, 8 mm and 12 mm dia rebars were used in the frame and lintel. Only 8 mm bars were used in lintel

in all cases. However, in the beam and columns, 12 mm bar and 8 mm bar were used as the longitudinal reinforcement and stirrup respectively. Different stages of these processes are presented in Figure 3.24.



Figure 3.24- (a) lintel, (b) beam-column joint, (c) stirrups / ties, (d) column-base joint, (e) a full reinforced structure.

In step 2, a wooden formwork is constructed to facilitate the concrete casting. Afterward, the previously built reinforced structure was placed in the wooden formwork as shown in Figure 3.25.



Figure 3.25- Shuttering work.

In step 3, cement, sylhet sand, and coarse aggregate were mixed at 1:1.5:3 ratio by volume in a mixture machine to prepare concrete. The water/cement ratio was kept at 0.45. During casting slump was kept between the range of 75 mm to 100 mm. After preparing fresh concrete, they were poured carefully in the formwork and compacted cautiously with a vibrator. Different stages of these processes are presented in Figure 3.26.





Figure 3.26- Measuring slump and concrete casting.

In step 4, the concrete was led to curing for 28 days as shown in Figure 3.27 (a). Curing provided enough scope for hydration. Wet gunny bags were used for curing. After 28 days of casting, the concrete became strong enough for commencing the masonry work. The full concrete frame is shown in Figure 3.27 (b)





Figure 3.27- (a) curing, (b) a concrete frame after 28 days of casting.

In step 5, bricks, cement, local sand, and water were prepared to commence masonry work. Cement and local sand were mixed at 1:4 ratio by volume for mortar and the water/cement ratio was maintained at 0.45. After that, the whole 1525 mm × 1525 mm × 125 mm wall of each specimen was filled up with bricks in two layers. Masonry units were joined using english bond. The lintel (1525 mm × 125 mm × 100 mm) was connected both with masonry and column at two sides by mortar. After completing the masonry work, the specimens were kept 28 days more before testing. Different stages of masonry work are presented in Figure 3.28.



Figure 3.28- Masonry work for Infilled Frame.

In the last step, all the specimens were whitewashed such as in Figure 3.29 to identify the cracks properly during testing.



Figure 3.29- Infilled Frame after whitewash.

3.5 Experimental Setup

After completing the full construction of all four specimens, they were transported to the 'Strength of Materials Laboratory' of Bangladesh University of Engineering and Technology one by one and prepared for the experiment. The schematic diagram of the experimental setup for infilled frame walls and masonry walls and infilled frame walls are shown in Figure 3.30 and Figure 3.31.

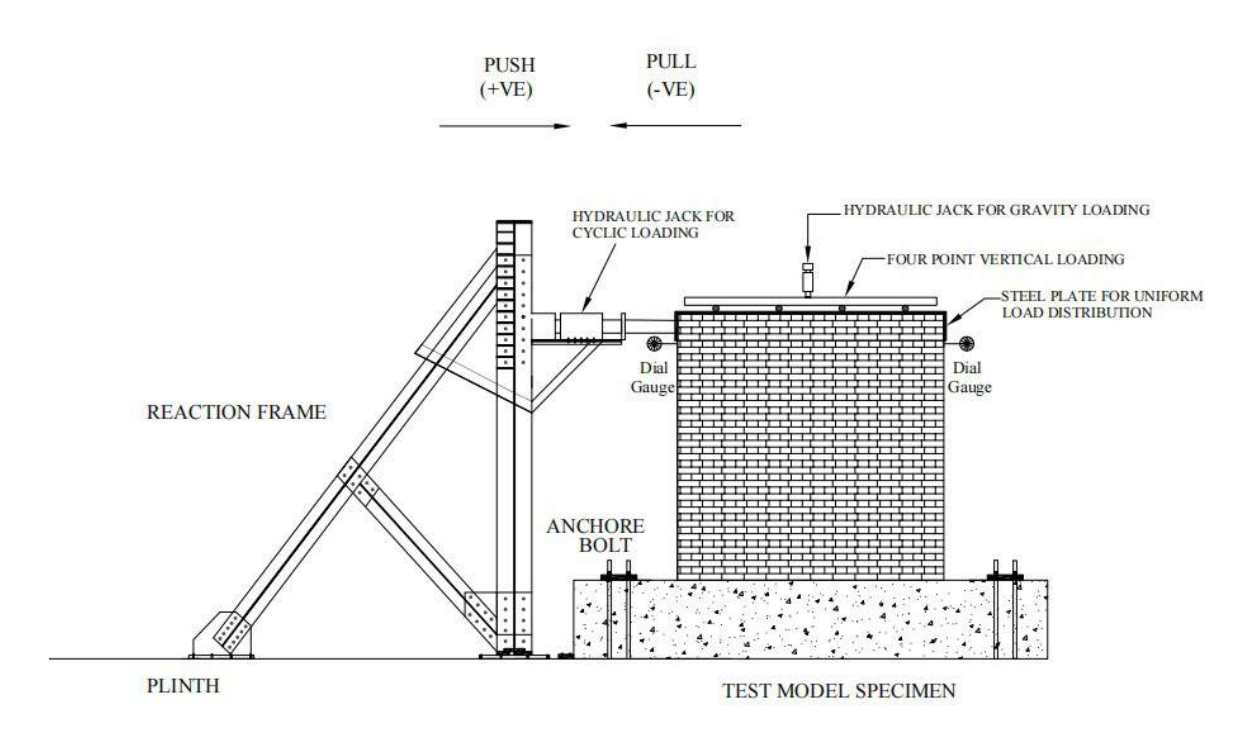


Figure 3.30- Schematic diagram of the experimental setup for masonry wall.

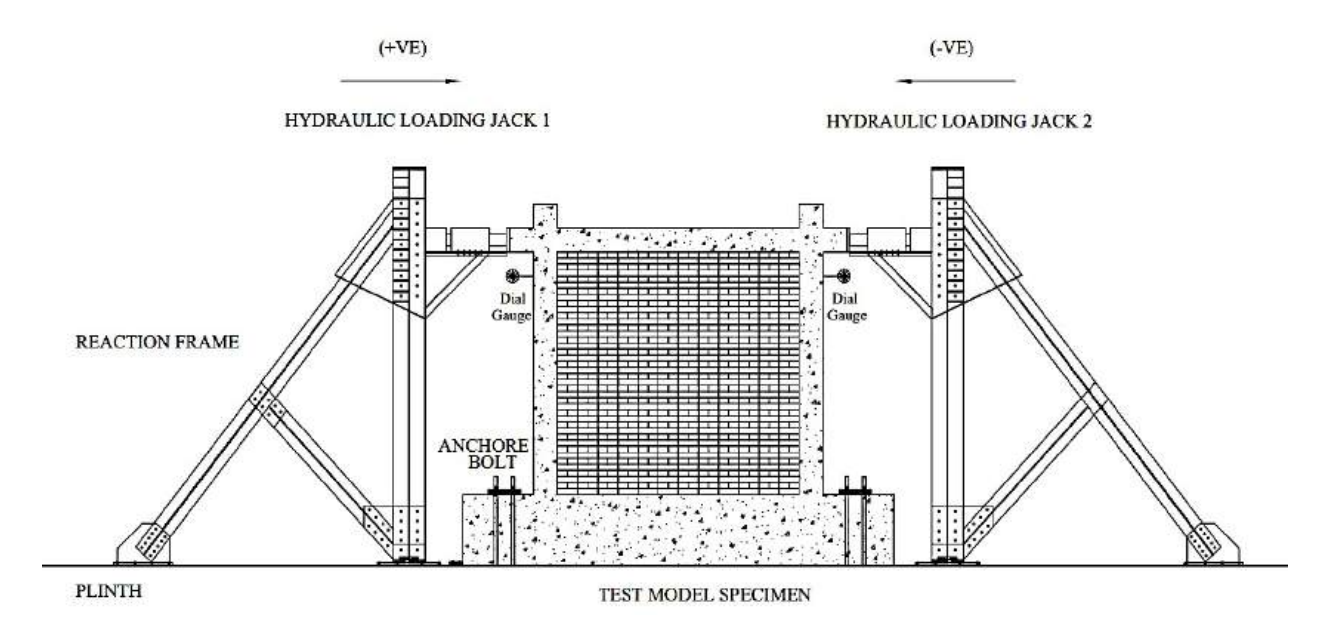


Figure 3.31- Schematic diagram of the experimental setup for infilled frame wall.

3.5.1 Hydraulic Jack

For infilled frame walls, Two Hydraulic jacks were utilized in this experiment for applying lateral load. Hydraulic jack 1 (Capacity: 50 ton) was attached to the left reaction frame and the Hydraulic jack 2 (Capacity: 30 ton) was attached to the right reaction frame. The jacks are shown in Figure 3.32. The deformation of the specimen due to the applied load by hydraulic jack 1 is assumed as positive direction. On the contrary, the deformation of the specimen due to the applied load by hydraulic jack 2 is assumed negative direction.

For masonry wall, another hydraulic jacks were utilized for applying cyclic load. The jack (capacity: 50 ton) was attached to the reaction frame. The jack are shown in Figure 3.33. A MS steel plate was placed over the top surface of the wall to evenly distribute the gravity load over the structure. The top plates were designed in such a way that they could exert pressures on the wall during both pushing and pulling. Four cylindrical rollers were fitted with chambers on the upper surface of the top plate which could move freely throughout the test. Another beam (box section) of adequate length was located above the four rollers and a 30 Ton jack was used to apply the gravity force there. Details of the hydraulic jacks are illustrated in Appendix-G.

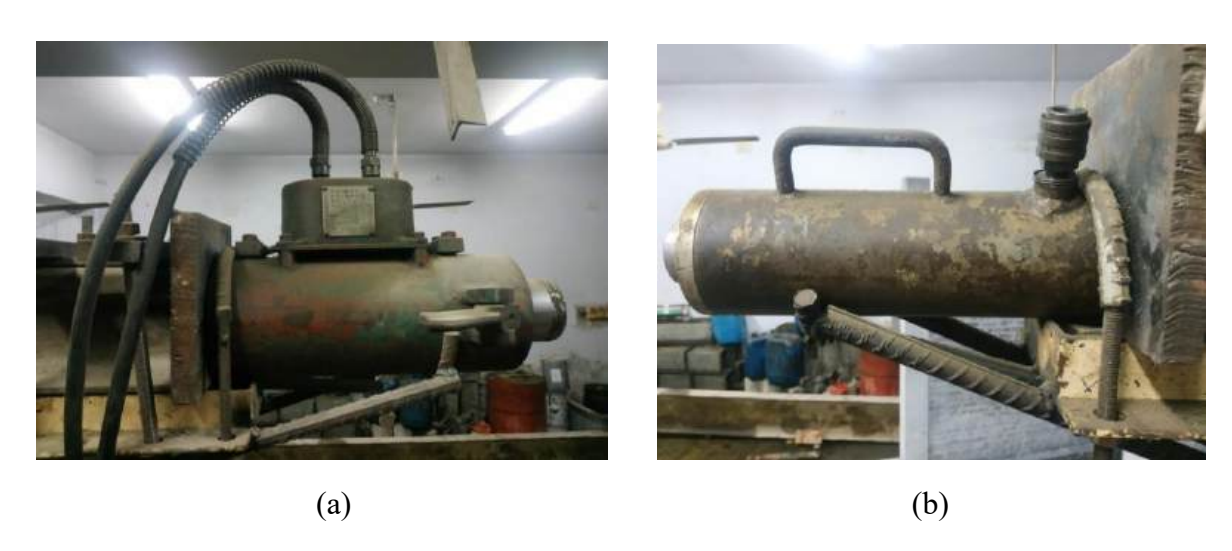


Figure 3.32- (a) Hydraulic Jack 1, (b) hydraulic jack 2 for infilled frame.





Figure 3.33- Hydraulic Jack for masonry wall (a) Horizontal Loading (b) Gravity Loading.

Four pairs of anchor bolts were used to fasten the base with the ground as shown in Figure 3.34. Each pair of anchor bolts was accompanied by a 475 mm × 75 mm × 50 mm steel plate. Each anchor bolt was 24 mm in dimension. Each side of the base was attached with two pairs of bolts. The bolts were strong enough to restrain the base from moving when the specimen is subjected to in-plane lateral loading.



Figure 3.34-Anchor bolt and steel plate

Three dial gauges were used to measure the displacement of the specimens during the cyclic excitation. They were set on the specimens with the help of the tripod stands. One dial gauge was set at the top-left corner and the other was set at the top-right corner of the specimens. The third dial gauge was set at the bottom right corner of the base to identify the base movement.



Figure 3.35- Full experimental setup of infilled frame wall



Figure 3.36- Full experimental setup of masonry wall

3.6 Test Procedure

In this study, specimens were subjected to cyclic lateral loads to investigate their performance under seismic conditions. The test was conducted using a load-controlled test scheme where different loading patterns were applied to masonry walls and infilled frame walls. Each cycle of the load had an equal amount of positive and negative portions. In the case of the infilled frame, the positive portion was applied by hydraulic jack 1, and the negative portion was applied by hydraulic jack 2. For the masonry wall, both positive and negative loads were applied by hydraulic jack 3. During the test, a jack was used to apply a vertical gravity load, which was maintained at a constant value of 40 kN. The loading value and increment for masonry wall and infilled frame are shown in Figure 3.37 and Figure 3.38.

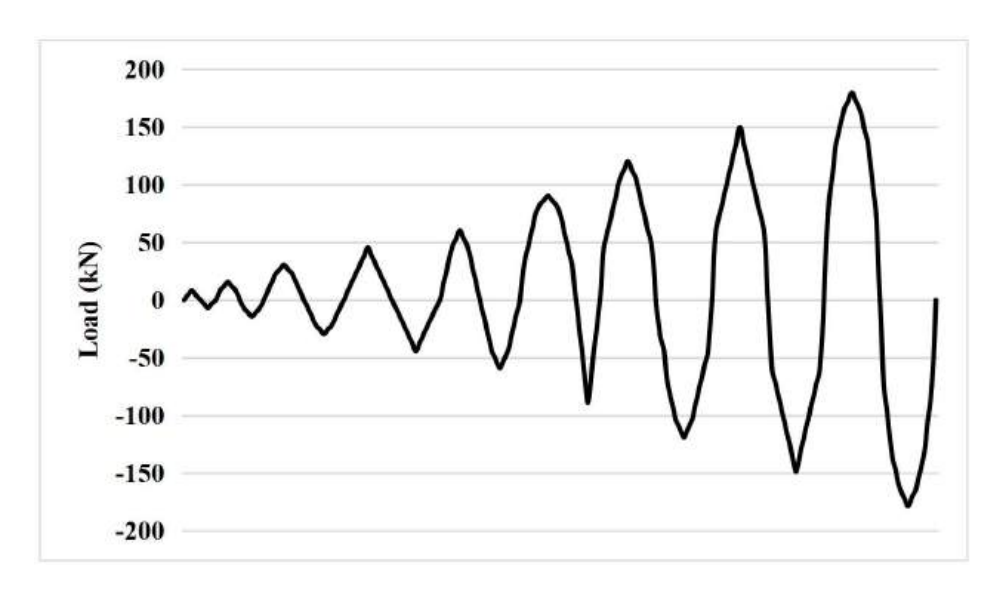


Figure 3.37- Applied loading pattern of Masonry wall during testing.

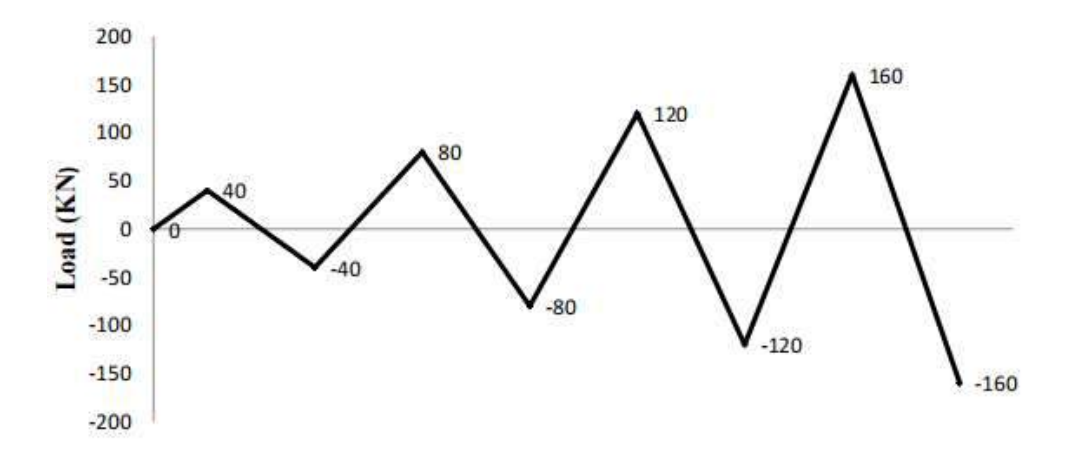


Figure 3.38- Applied loading pattern of Infilled Frame Wall during testing.

CHAPTER 4

RESULTS AND DISCUSSIONS

4.1 Introduction

The key objective of this study is to investigate the influence of reinforcement embedded in masonry under cyclic loading. In this chapter, initially, the damage and failure patterns of the specimens are assessed. Later, extensive comparative studies are conducted to identify the behavior of the reinforced masonry wall and compare the results with equivalent unreinforced masonry wall. The comparison will be based on the relevant parameters such as – ultimate load, energy dissipation, ductility and stiffness degradation.

4.2 Damage Assessment and Failure Mode of the Specimens

The pattern of cracking and the resulting damage of unreinforced masonry (SURM4 & HURM4), reinforced masonry (RM-420) and infilled frame (SB) in each cycle of the specimens are described in detail below.

4.2.1 Failure Analysis of SURM4

SURM4 is subjected to the experimental setup for cyclic loading specified in Figure 3.30 and it underwent a total of four cycles (specified in Figure 3.37), with failure occurring in the fourth cycle.

During the first cycle, a maximum load of 8.1 kN was applied to the specimen through push and pull and no significant changes or cracks were identified. In the second cycle, a maximum load of 15.6 kN was applied and still no notable crack or changes observed.

In the third cycle, a maximum load of 30.5 kN was applied to the specimen. At maximum push load (30.5 kN), a horizontal crack formed in mortar near base. Another crack formed in the same layer of the specimen when it was subjected to reverse loading, and this crack intersected the previously formed cracks.

In cycle 4, The cracks that had already formed in the wall widened upto 4.5 mm and lengthened and spreading throughout the entire length of the wall. The maximum load applied in the reverse direction was 41.7 kN, after which no further loading was applied because there was a risk of the entire wall collapsing. The maximum lateral displacement at top was recorded to be 8.475 mm at that stress level. Figure 4.1 illustrates the state of the

specimen after failure in cycle 4. The area marked in red indicates the location where the crack appeared and ultimately led to failure. A more detailed view of the zone are shown in Figure 4.2 where failure occurred.



Figure 4.1- SURM4 at complete failure.



Figure 4.2- Cracks at final state of SURM4 (Sliding).

The total hysteretic graph of load vs. displacement is shown in Figure 4.3.

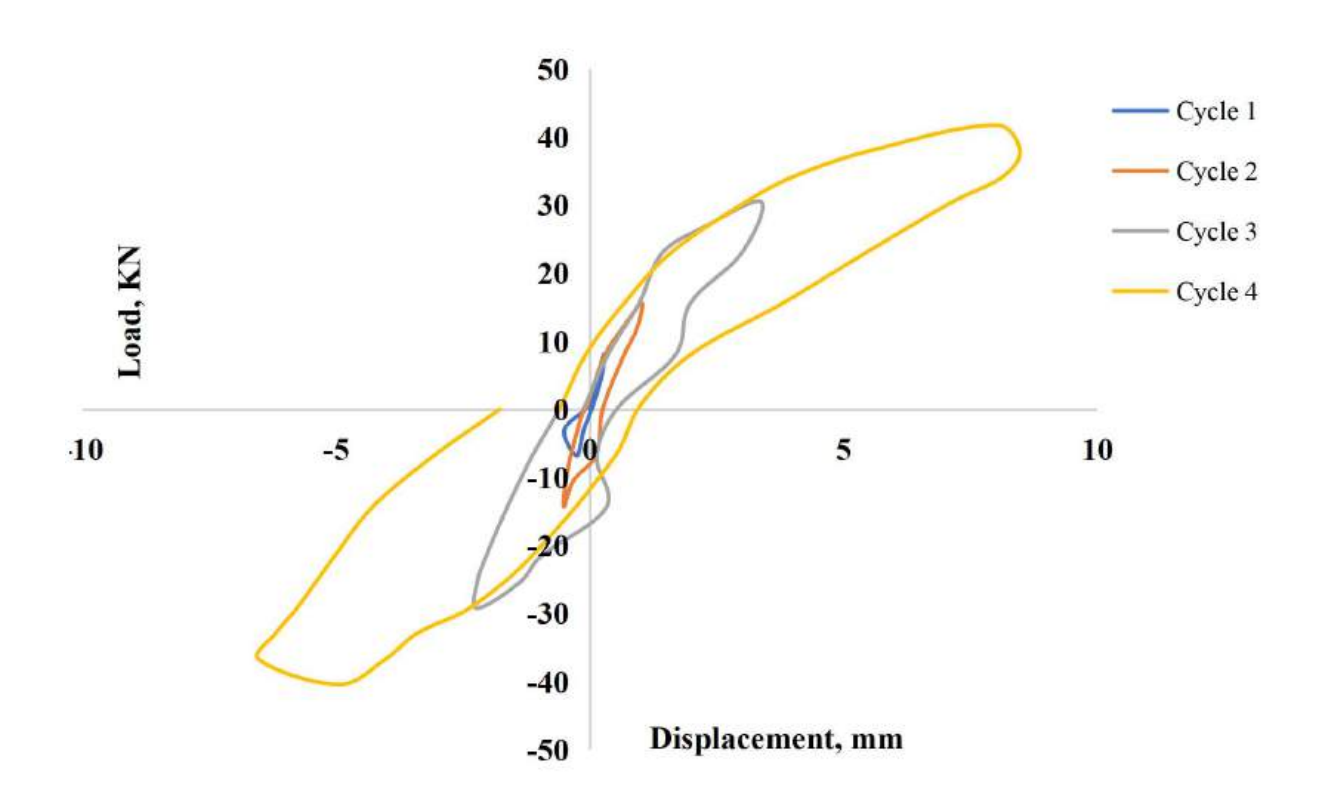


Figure 4.3- Hysteretic load-displacement curve for SURM4.

Stiffness degradation in each cycle with increasing top displacement are presented in Figure 4.4.

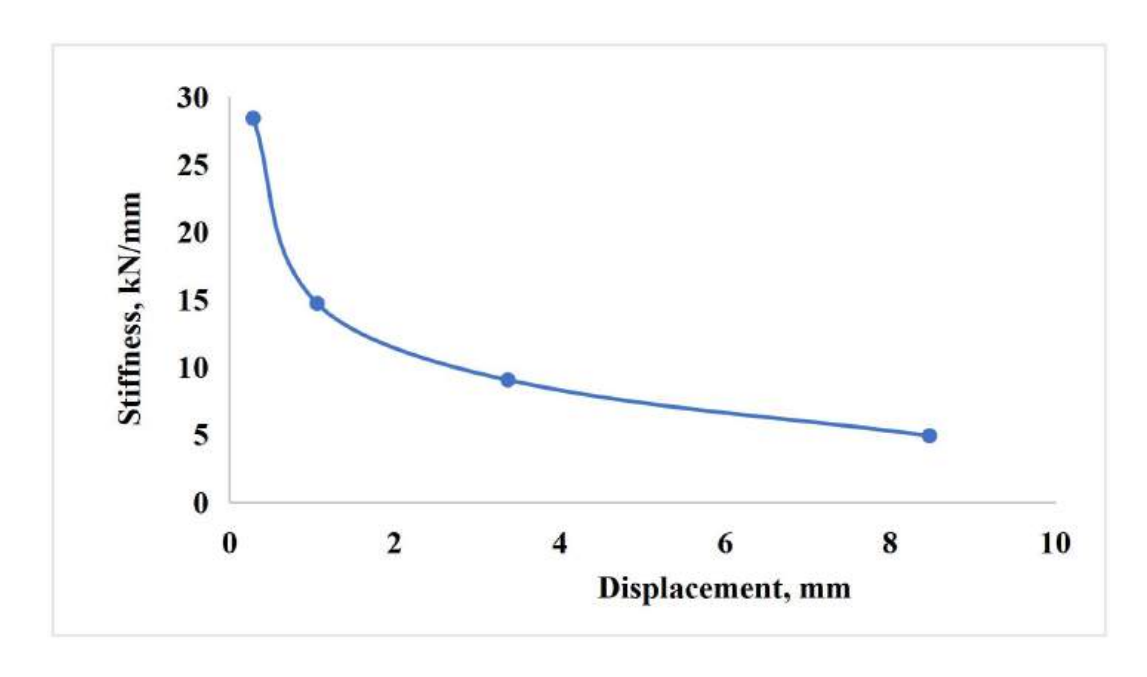


Figure 4.4- Stiffness degradation curve for SURM4.

4.2.2 Failure Analysis of HURM4

HURM4 is subjected to the experimental setup for cyclic loading specified in Figure 3.30 and it underwent a total of four cycles (specified in Figure 3.37), with failure occurring in the fourth cycle.

During the first two cycles, maximum loads of 8.1 kN and 15.6 kN were applied through push and pull respectively and no significant changes or cracks were observed.

In the third cycle, a maximum load of 30.5 kN was applied to the specimen. At push load 23.1 kN, a horizontal crack formed in mortar near base. Another crack formed in the same layer of the specimen when it was subjected to maximum reverse loading, and this crack intersected the previously formed cracks.

During the fourth cycle, the cracks that had already formed in the wall widened up to 5 mm and continued to lengthen and spread throughout the entire length of the wall. The maximum load applied in the reverse direction was 38 kN, which caused the bricks below the cracked layer to start crushing due to the uplifting of the other side of the wall. It state that they were experiencing stress beyond their compressive strength. As a result, further loading was stopped to avoid the risk of the entire wall collapsing.

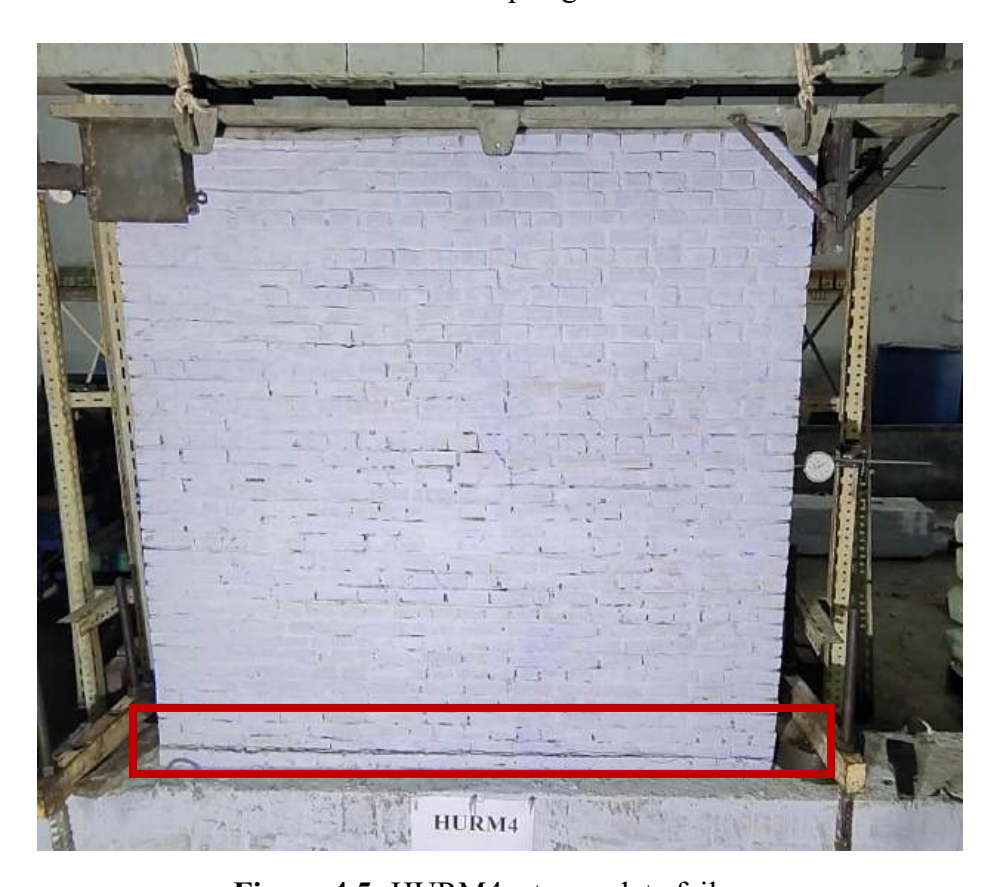


Figure 4.5- HURM4 at complete failure.

At the stress level where failure occurred, the maximum lateral displacement at the top of the wall was recorded to be 9.3 mm. Figure 4.5 illustrates the state of the specimen after failure in cycle 4, with the area marked in red indicating the location where the crack initially appeared and ultimately led to failure. A more detailed view of this zone is shown in Figure 4.6, where the failure occurred.

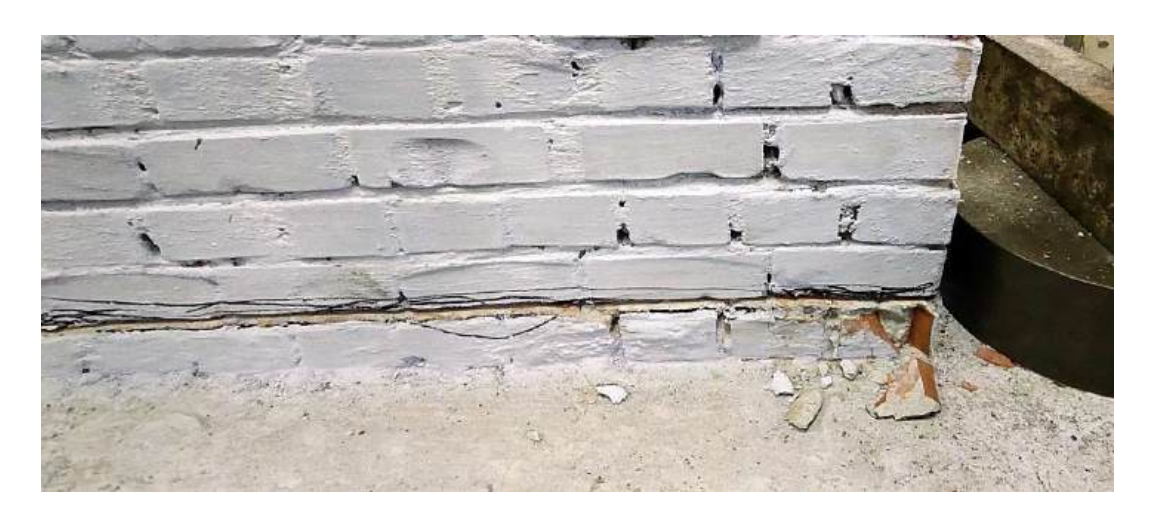


Figure 4.6- Cracks at final state of HURM4 (Rocking).

The total hysteretic graph of load vs. displacement is shown in Figure 4.7.

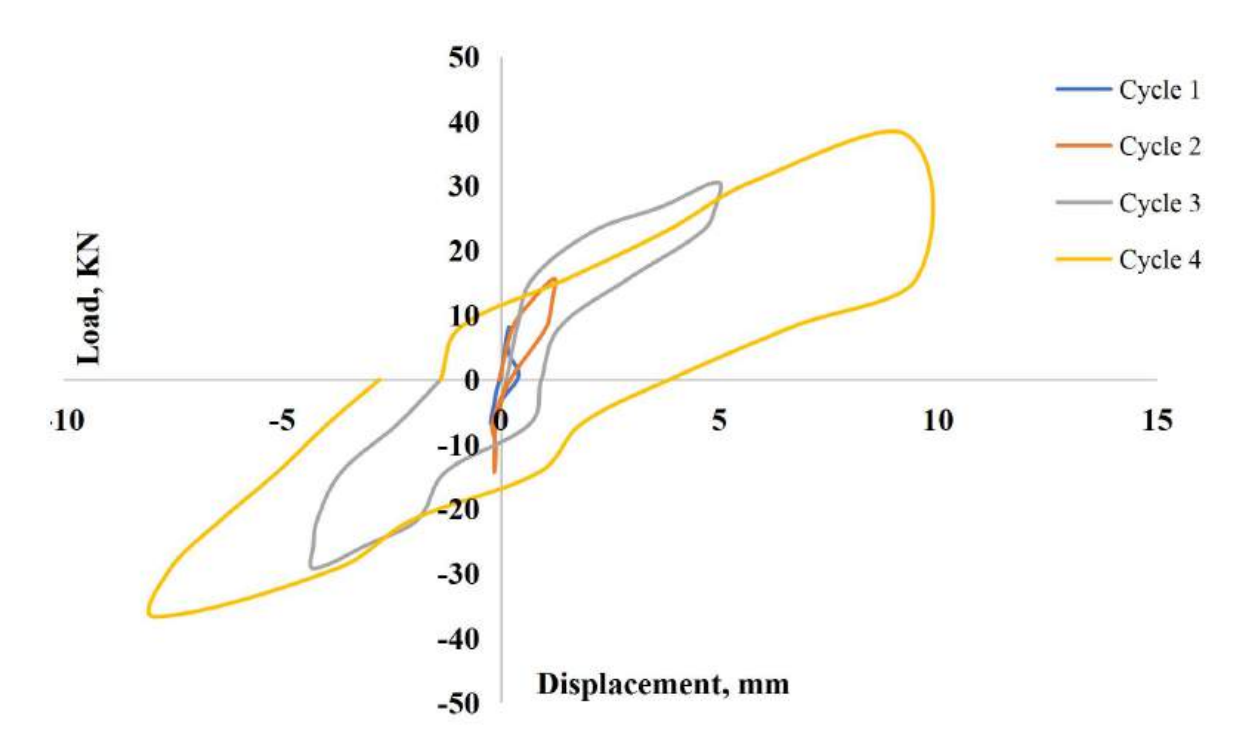


Figure 4.7- Hysteretic load-displacement curve for HURM4.

Stiffness degradation of HURM4 in each cycle with increasing top displacement are presented in Figure 4.8.

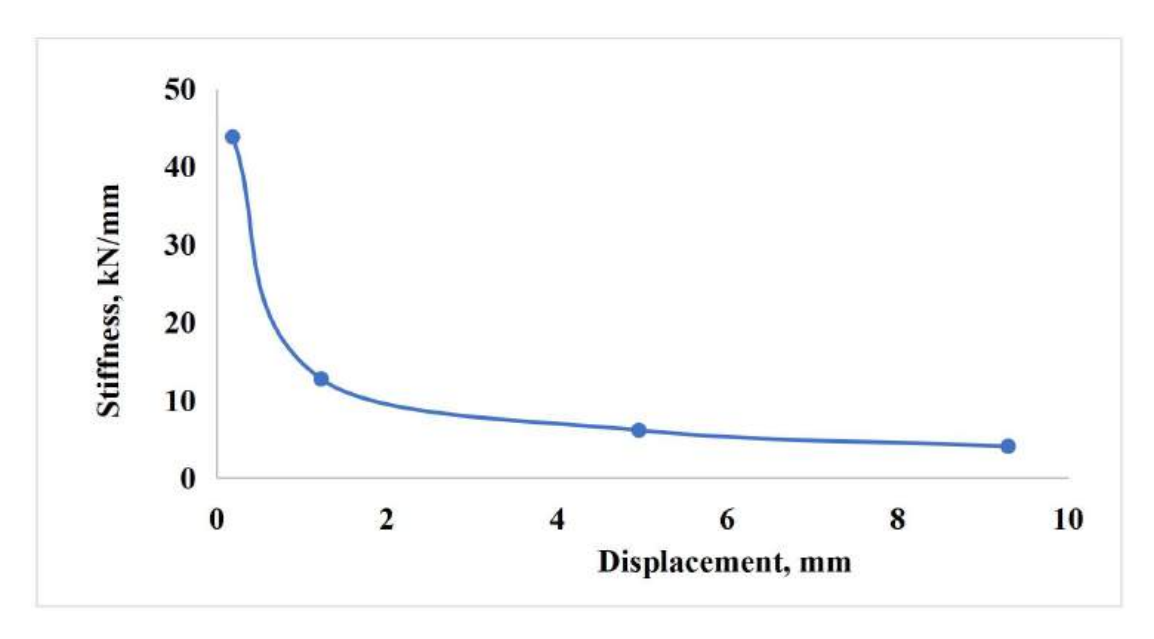


Figure 4.8- Stiffness degradation curve for HURM4.

4.2.3 Failure Analysis of RM4-420

Rm4-420 was also subjected to the experimental setup as SURM4 and HURM4 but it sustained a total of eight cycles with failure occurring in the eighth cycle.

During the first five cycles, maximum loads of 8.1 kN, 15.6 kN, 30.5 kN, 45.5 kN and 60.4 kN were applied through push and pull respectively and no significant changes or cracks were observed while SURM4 and HURM4 were already failed at this stage having same loading condition.

In the sixth cycle, a maximum load of 90kN kN was applied to the specimen. When maximum load was applied in positive direction, a micro horizontal crack was identified along the mortar which indicates that the mortar was weaker at that layer. Another horizontal crack was formed on the opposite side when maximum reverse load applied in this cycle.

In cycle 7, when 105.2 kN load was applied in positive direction, previously formed horizontal crack extended to the left in this cycle and resulted in a diagonal shear crack. It refers that reinforcement in masonry was transferring maximum shear stress from the lateral load which caused diagonal tensile stress on the wall. This crack expanded upto 0.5 mm

when maximum positive (push) load of 120.1 kN applied in this cycle. Other than that, several horizontal micro cracks became visible through out the height of the wall at maximum positive load. At maximum reverse load of 120.1 kN, a vertical shear crack had formed from the earlier horizontal crack and had crossed the previously formed primary diagonal crack. Status after completion of the cycle seven is shown in Figure 4.9.



Figure 4.9- RM4-420 after the completion of cycle 7.

In cycle 8, the specimen resulted in failure at maximum intended load of 160 kN. Before that, the specimen experienced several flexural crack and diagonal shear crack which spanned throughout the specimen. Previously formed diagonal crack was widened upto 1 mm and horizontal micro cracks widened upto 0.1 mm and extended in length at this point. At maximum positive load, bottom layer brick started to crush and could not take any further load. At the maximum stress level, the maximum lateral displacement at the top of the wall was recorded to be 14.3 mm. The state of the specimen after failure in eighth cycle illustrates in Figure 4.10 where the area marked in red indicating the location where the brick started to crush and the specimen ultimately led to failure.

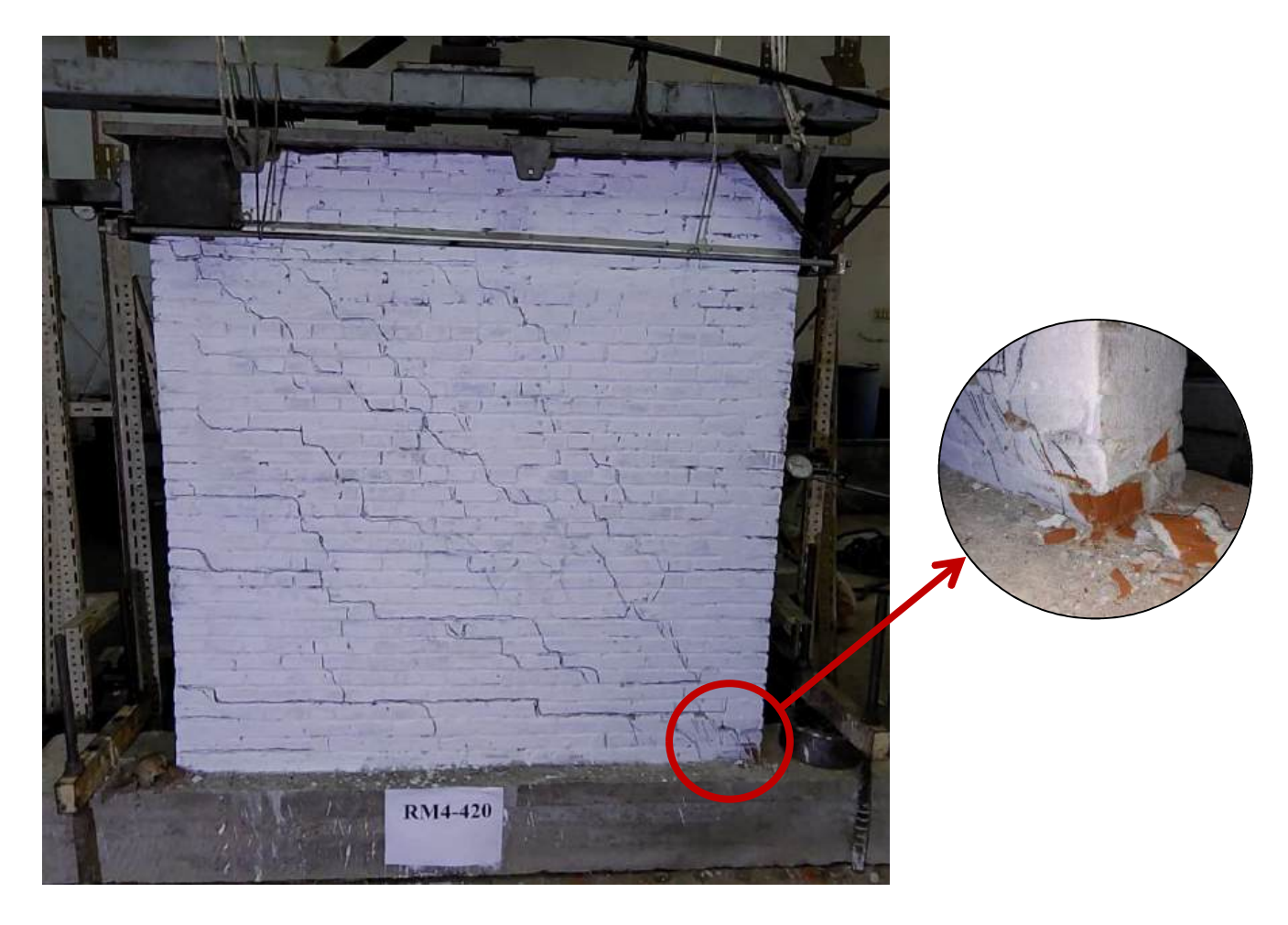


Figure 4.10- RM4-420 at complete failure.

The total hysteretic graph of load vs. displacement and stiffness degradation of RM-420 in each cycle with increasing top displacement are presented in Figure 4.11 and Figure 4.12.

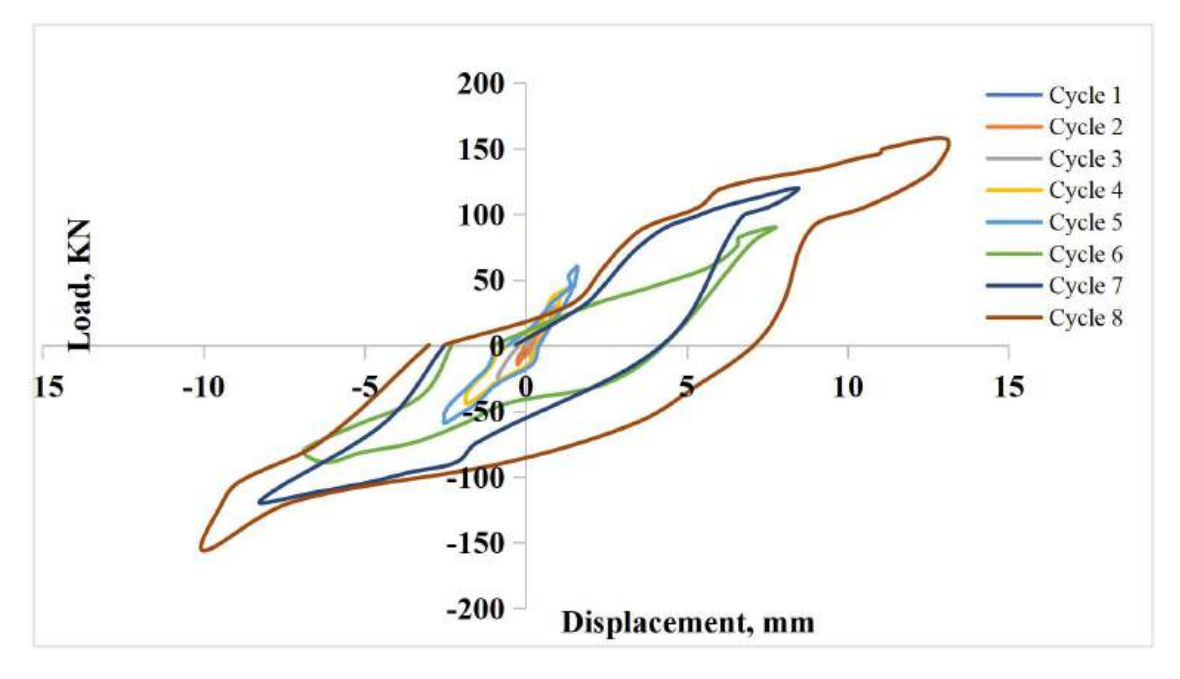


Figure 4.11- Hysteretic load-displacement curve for RM4-420.

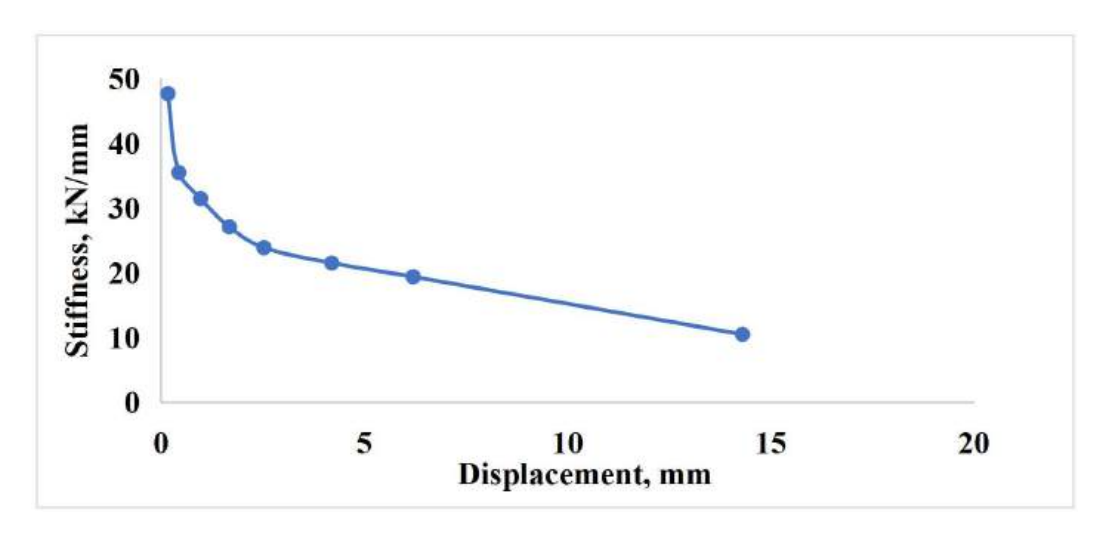


Figure 4.12- Stiffness degradation curve for RM4-420.

4.2.4 Failure Analysis of SB

SB subjected to the experimental setup for cyclic loading is specified in Figure 3.31 and it underwent a total of four cycles (specified in Figure 3.38), with failure occurring in the fourth cycle.

During the first cycle, a maximum load of 40 kN was applied to each side of the specimen, and no significant changes or cracks were identified.

In the second cycle, a maximum load of 80 kN was applied in each direction. A long horizontal crack was detected along the mortar, indicating that the mortar was weaker at that point, and a mild shear crack was also found at the beam-column joint. When the load was reduced to 40 kN in the opposite direction, the horizontal crack extended to the right and stopped at the column. At 80 kN in the opposite direction, the vertical crack expanded to 0.05 mm and moved. A minor crack was also detected at the base-column joint.

In the third cycle, a maximum load of 120 kN was applied in both directions. At 80 kN, wider cracks, up to 4 mm, appeared in the bricks, indicating that they were experiencing stress beyond their compressive strength. By 120 kN, a vertical shear crack had formed from the earlier horizontal crack. Additionally, numerous flexural cracks appeared on both columns and beam-column joints.

In cycle 4, the intended maximum load of 160 kN from each direction but the specimen resulted in failure at 150 kN. At 60 KN (towards positive direction) load, the segregated hairline cracks formed in the previous cycle connected and created a long diagonal crack.

More flexural cracks were identified on both of the columns. The previously formed diagonal tensile crack extended to the top upper-left corner and reached the beam-column (left) joint. At 120 kN (positive direction), flexural cracks appeared on the beam, indicating that it was experiencing a significant amount of moment from the lateral load. At 150 kN, cracks up to 5 mm wide appeared in the wall, and significant damage was observed on the base-column joint on the left. All previously formed cracks widened and extended in length leading to the eventual failure of the entire specimen. At the time of failure, the maximum lateral displacement at the top of the wall was recorded to be 17.25 mm. The state after failure (at cycle 4) is presented in Figure 4.13.



Figure 4.13- SB at complete failure (at cycle 4).

The total hysteretic graph of load vs. displacement and stiffness degradation of SB in each cycle with increasing top displacement are illustrated in Figure 4.14 and Figure 4.15.

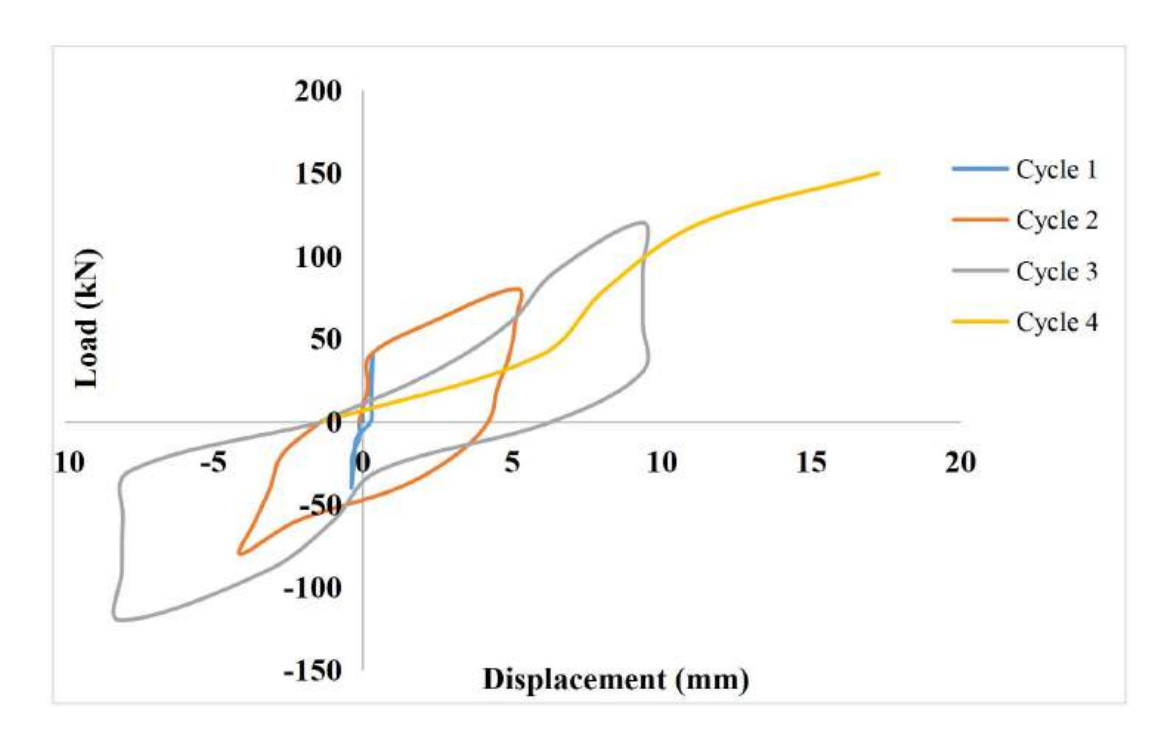


Figure 4.14- Hysteretic load-displacement curve for SB.

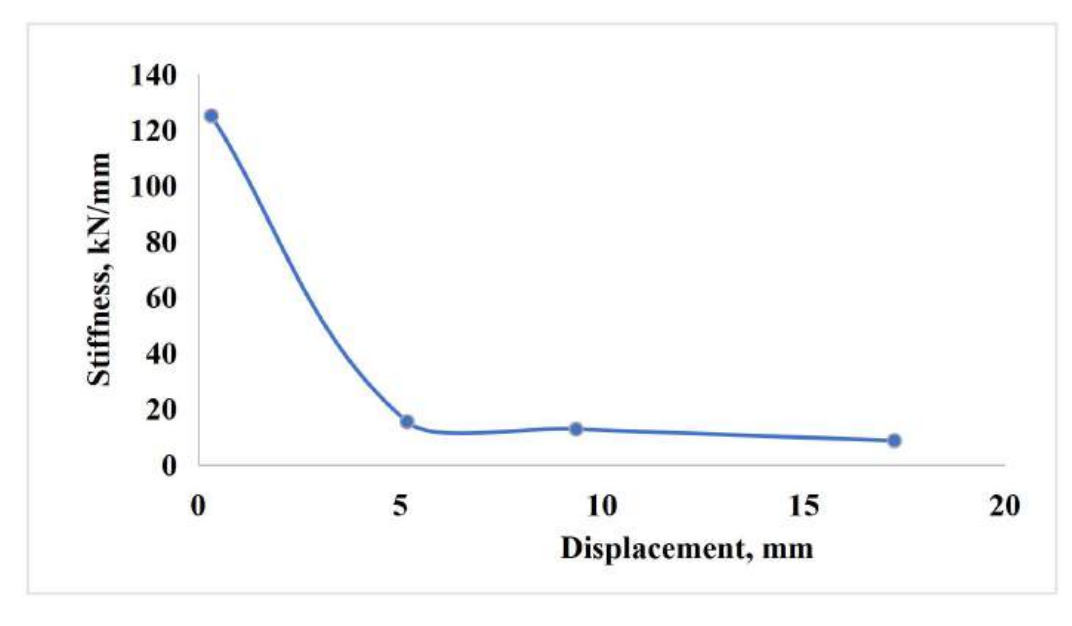


Figure 4.15- Stiffness degradation curve for SB.

Details of the failure pattern, hysteretic graph of load vs. displacement and stiffness degradation of other specimen are presented in Appendix-H, I & J.

4.3 Summary of The Experimental Results of The Specimens

The summary of the experimental results and failure mode (according to FEMA 306 and 307) of reinforced masonry walls, unreinforced masonry walls and infilled frame walls are provided in Table 4.1, Table 4.2 and Table 4.3.

Table 4.1- Summary of The Experimental Results of unreinforced masonry walls

Parameters	SURM2	HURM2	SURM4	HURM4	SURM6	HURM6
First cracking load (kN)	34.2	26.8	30.5	26.8	26.8	23.1
Displacement at first cracking (mm)	3.3	3.8	3.37	4.2	2.95	3.13
Stiffness at first infill cracking (kN/mm)	10.4	7.1	9.1	6.4	9.1	7.4
Ultimate load at specimen failure (kN)	45.5	41.7	41.7	38	34.2	34.2
Displacement at specimen failure (mm)	9.02	10.1	8.47	9.3	10.2	11.06
Stiffness at specimen failure (kN/mm)	5.04	4.13	4.9	4.09	3.35	3.1
Cumulative Energy Dissipation (kN-mm)	523.6	568.5	475	525.3	541.4	562.2
Cycle sustained	4	4	4	4	4	4
Component type	URM1B	URM1C	URM1B	URM1B	URM2G	URM2G
Behavior mode	Bed joint sliding	Bed joint sliding at wall base	Bed joint sliding	Bed joint sliding	Rocking / Toe crushing	Rocking / Toe crushing
Damage Severity	Moderate	Moderate	Moderate	Moderate	Heavy	Heavy

 Table 4.2- Summary of The Experimental Results of Reinforced masonry walls

D 4	RM2-	RM2-	RM4-		RM6-	RM6-
Parameters	420	500	420	RM4-500	420	500
First cracking load (kN)	98	120	90	94	57	57
Displacement at first cracking (mm)	4.95	5.9	4.2	6.9	2.6	4.1
Stiffness at first infill cracking (kN/mm)	19.8	20.3	21.4	13.6	21.9	13.9
Ultimate load at specimen failure (kN)	180	180	160	160	90	90
Displacement at specimen failure (mm)	12.5	15.2	14.3	15.8	6.3	7.2
Stiffness at specimen failure (kN/mm)	14.4	11.8	11.2	10.1	16.9	12.5
Cumulative Energy Dissipation (kN-mm)	1711	2216	1390	1985	930	1117
Cycle completed	9	9	8	8	6	6
Component type	RM1A	RM1C	RM1B	RM2G	RM1C	RM1C
Behavior mode	Ductile Flexure	Flexure/ Sliding Shear	Flexure / Diagonal Shear	Preempitive shear	Flexure/ Sliding Shear	Flexure/ Sliding Shear
Damage Severity	Moderate	Moderate	Moderate	Slight	Moderat e	Slight

 Table 4.3- Summary of The Experimental Results of infilled frame walls.

Parameters	SB	SBL	PB	PBL	RIF
First infill cracking load (kN)	80	80	80	80	200
Displacement at first infill cracking (mm)	5.17	5.29	5.7	6.14	9.3
Stiffness at first infill cracking (kN/mm)	15.47	15.12	14.04	13.03	21.51
First cracking load at frame (KN)	80	120	120	80	160
Displacement at first frame cracking (mm)	5.17	15.26	10	6.14	6.1
Stiffness at first frame cracking (KN/mm)	15.47	7.86	12	13.03	26.23
Ultimate load at specimen failure (KN)	150	160	130	160	220
Displacement at specimen failure (mm)	17.25	31.14	22.41	34.12	15.7
Stiffness at specimen failure (KN/mm)	8.7	5.14	5.8	4.69	14.01
Cumulative Energy Dissipation (KN-mm)	1549.6	2268.4	1676	2639.2	3261
Cycle completed	4	4	4	4	6
Component type	RC1A	RC1D	RC1B	RC1A	RC1D
Behavior mode	Ductile flexure	Flexure/ Sliding Shear	Flexure/ Diagonal tension	Ductile flexure	Flexure/ Sliding Shear
Damage Severity	Moderate	Heavy	Moderate	Moderate	Heavy

4.4 Comparative Study

From section 4.3, a preview of the test results for various type of masonry wall under cyclic loading conditions can be obtained. Based on these information, a comparison will be carried out between hollow brick masonry wall, solid brick masonry wall, reinforced masonry wall, and infilled frame wall to better understand their respective performance under cyclic loading conditions and draw a definitive conclusions.

4.4.1 Comparison between Solid Brick Masonry and Hollow brick Masonry

The purpose of this comparison is to evaluate the impact of using perforated clay brick as a substitute for solid clay brick.

From summary of the test results, it is demonstrated that HURM2, HURM4 and HURM6 showed 15%, 24% and 6% more displacement than SURM2, SURM4 and SURM6 respectively at first cracking. On the other hand, perforated brick masonry walls showed 19% to 30% less stiffness than solid bricks walls.

Eventually, the ultimate load-carrying capacity of perforated brick masonry was found about 8% - 9% less than solid brick masonry. But in case of HURM6 and SURM6, ultimate load carrying capacity was found same. Because of their lower mortar strength, brick type could not make significant impact on their ultimate load. At failure, hollow bricks masonry exhibited 9% - 11% more displacement and 7% - 18% less stiffness than their respective solid bricks masonry walls. Furthermore, HURM walls dissipated 3% - 10% more cumulative energy than SURM walls.

In case of infilled frame wall, at frame first cracking, PB showed 93% more displacement and 22% less stiffness than SB. The ultimate load-carrying capacity of PB was found about 13% less than SB. At this point, PB exhibited 30% more displacement and 33% less stiffness than SB. For energy dissipation, PB dissipated 8% more cumulative energy than SB.

For infilled frame with lintel, at first cracking of the infill, PBL showed 16% more displacement and 14% less stiffness than SBL. Eventually, they both displayed identical ultimate load-carrying capacity. At this point, PBL exhibited 10% more displacement and 9% less stiffness than SBL. Furthermore, PBL dissipated about 16% more cumulative energy than SBL.

The relation of stiffness and cumulative energy dissipation in each cycle of perforated brick walls and respective solid brick walls are illustrated below.

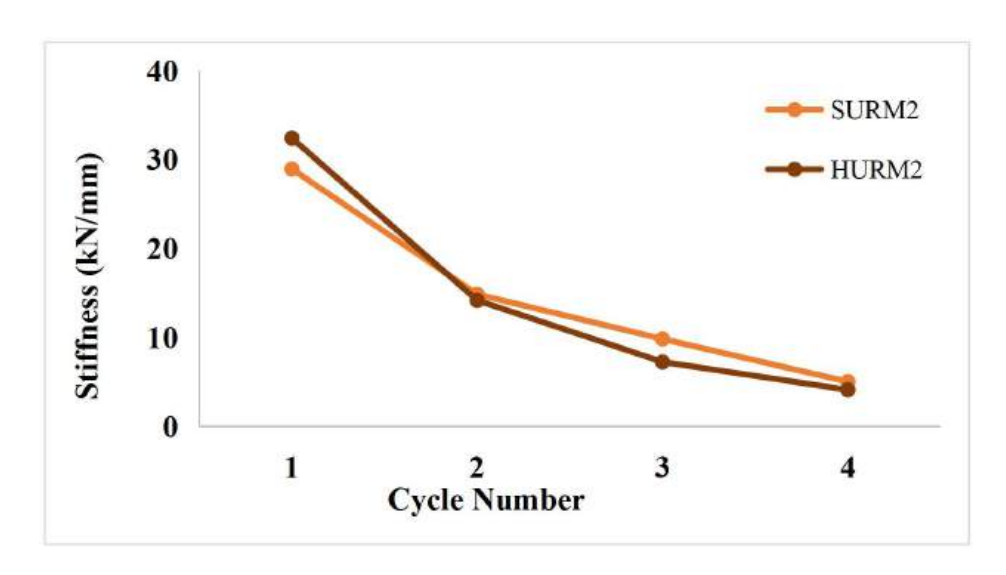


Figure 4.16- Stiffness degradation of SURM2 & HURM2

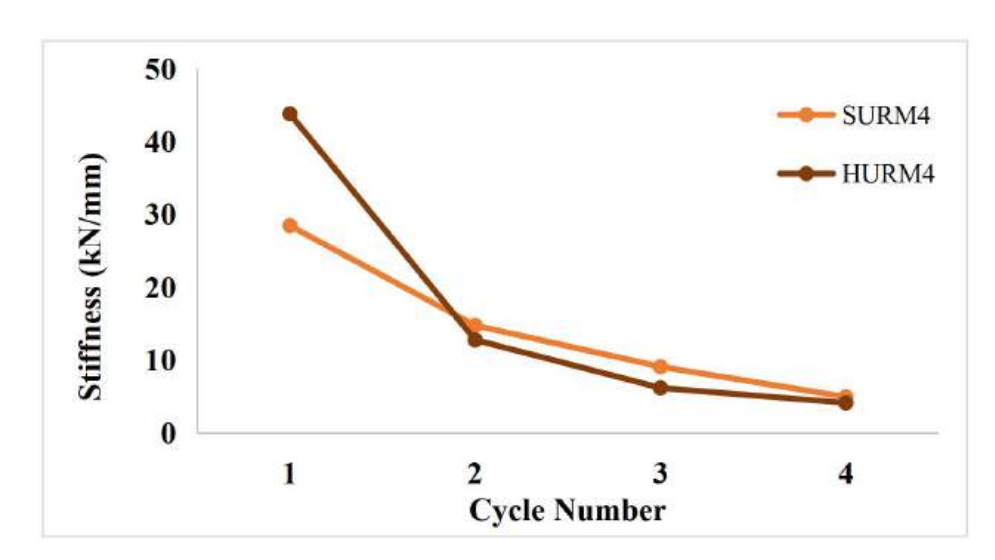


Figure 4.17- Stiffness degradation of SURM4 & HURM4.

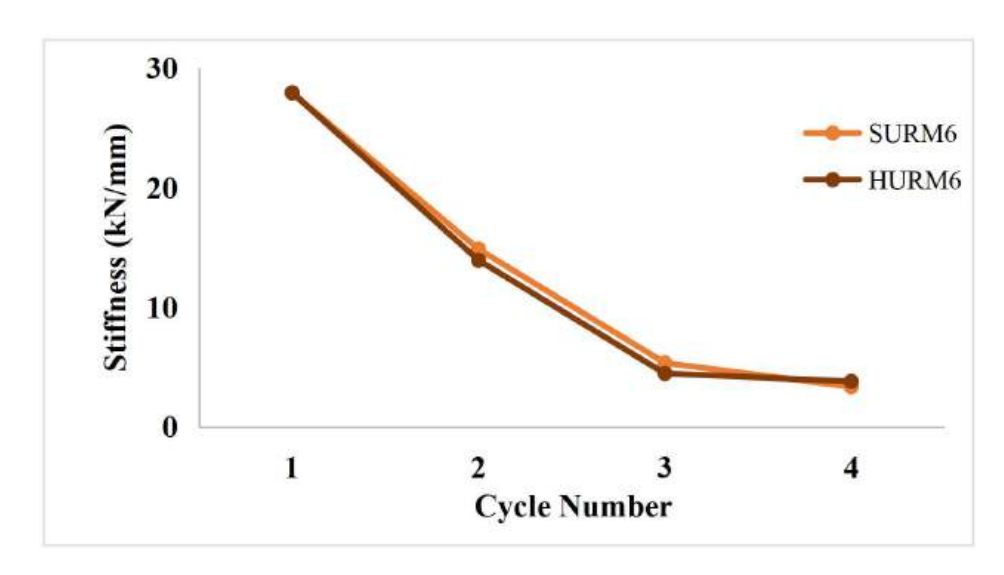


Figure 4.18- Stiffness degradation of SURM6 & HURM6.

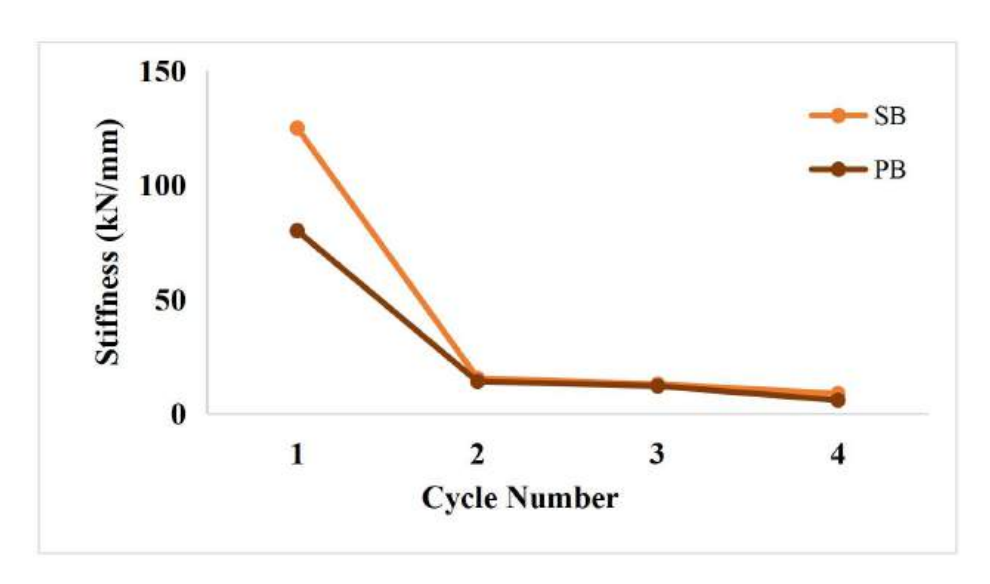


Figure 4.19- Stiffness degradation of SB & PB.

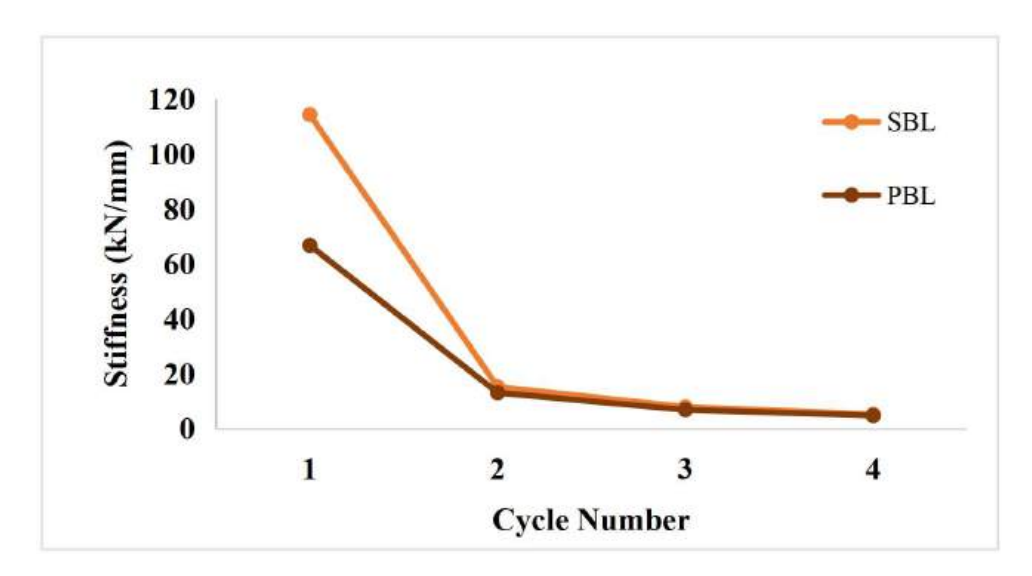


Figure 4.20- Stiffness degradation of SBL & PBL.

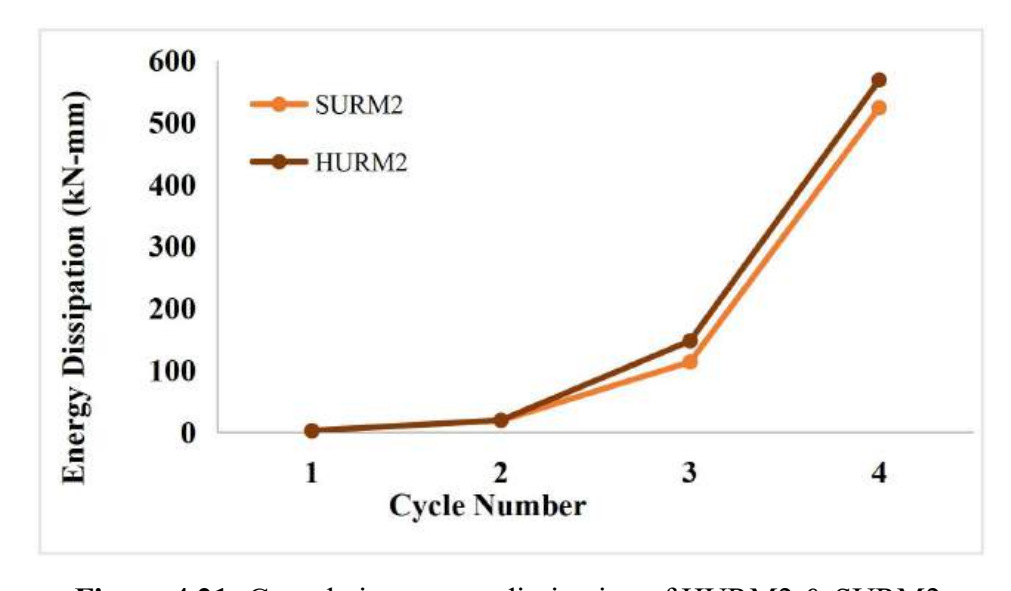


Figure 4.21- Cumulative energy dissipation of HURM2 & SURM2.

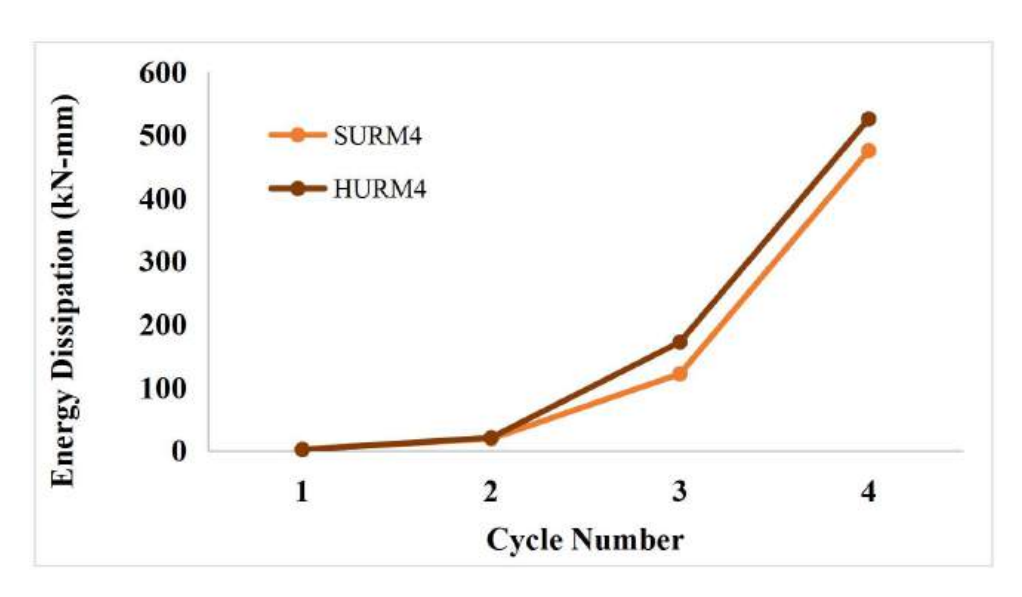


Figure 4.23- Cumulative energy dissipation of HURM4 & SURM4.

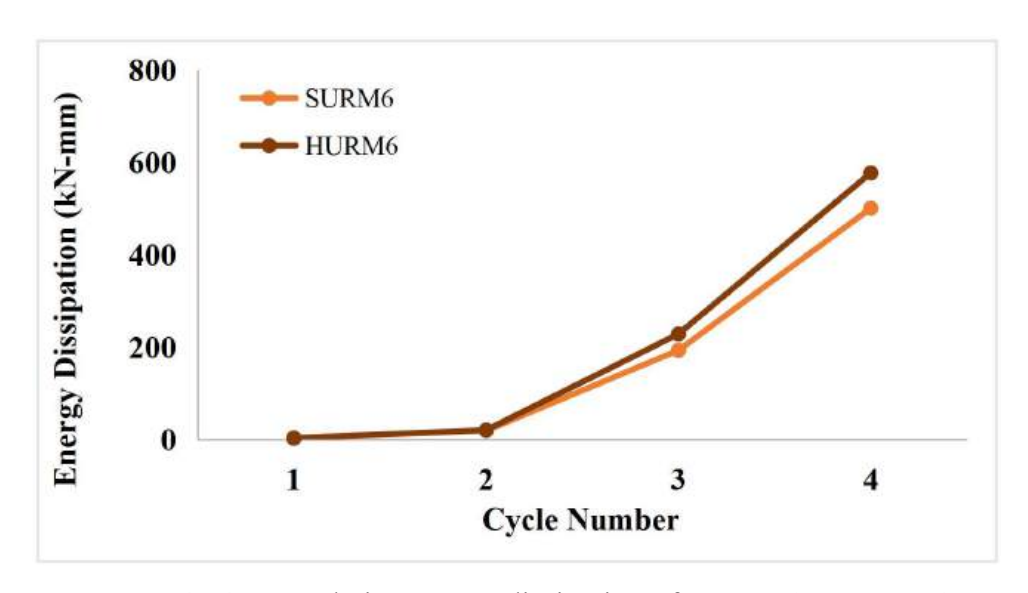


Figure 4.24- Cumulative energy dissipation of HURM6 & SURM6.

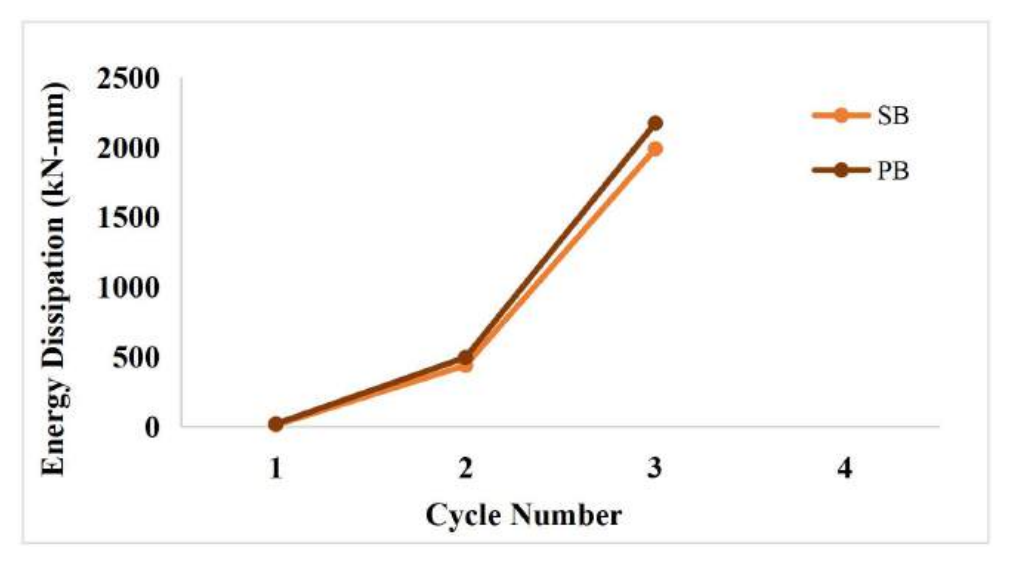


Figure 4.25- Cumulative energy dissipation of SB & PB.

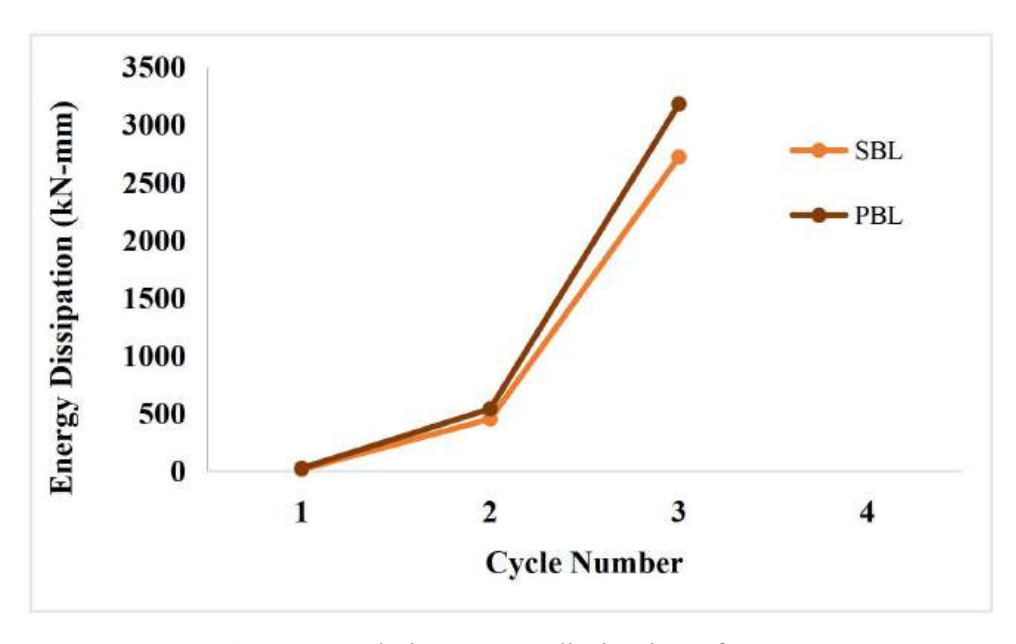


Figure 4.26- Cumulative energy dissipation of SBL & PBL.

4.4.2 Comparison between Unreinforced Masonry and Reinforced Masonry

The purpose of this comparison is to evaluate the impact of grouted reinforcement in masonry wall during cyclic loading condition.

Based on the summary of the test results, it was demonstrated that while URM walls failed at a certain load, no cracks were observed for the reinforced masonry wall. In case of ultimate load carrying capacity, RM walls can carry 3.4 - 6.7 times more load than URM walls. At failure, RM walls exhibited 1.5 - 2.3 times more displacement and 2.5 - 3.5 times more stiffness than URM walls. For cumulative energy dissipation, RM walls dissipated 2 - 4 times more energy than URM walls.

In case of frame wall, reinforced masonry infilled wall have 38% - 70% more ultimate load carrying capacity than unreinforced infill. RIF shows 1.6 - 3 times more stiffness and dissipates 1.2% - 2.1% more energy than unreinforced infilled masonry wall.

The comparison of ultimate load carrying capacity, maximum displacement, stiffness and cumulative energy dissipation RM and URM walls are illustrated below.

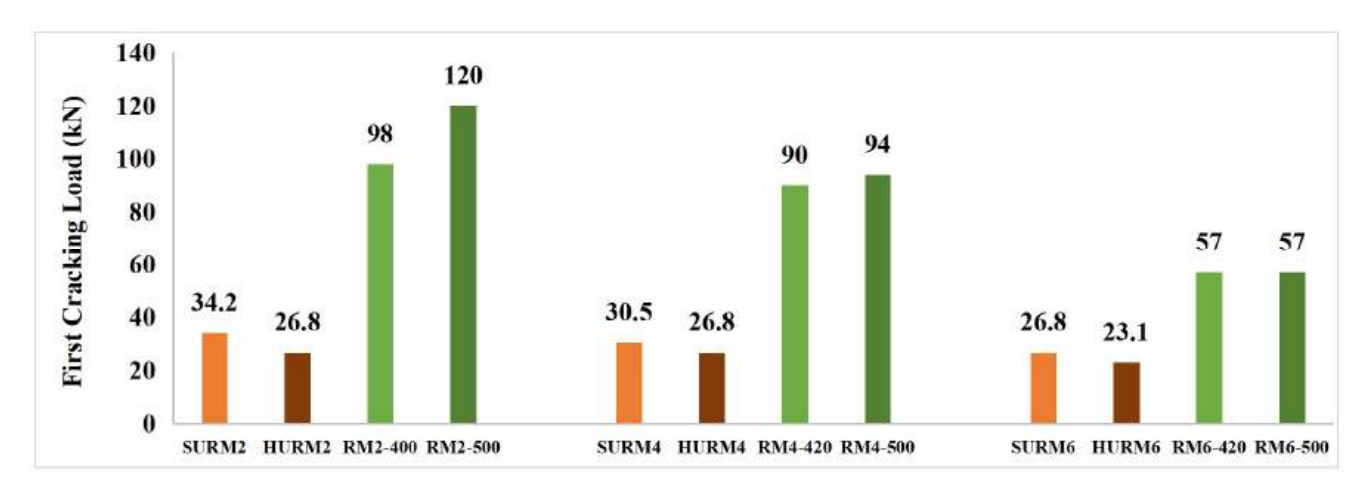


Figure 4.27- First cracking load of URM & RM walls.

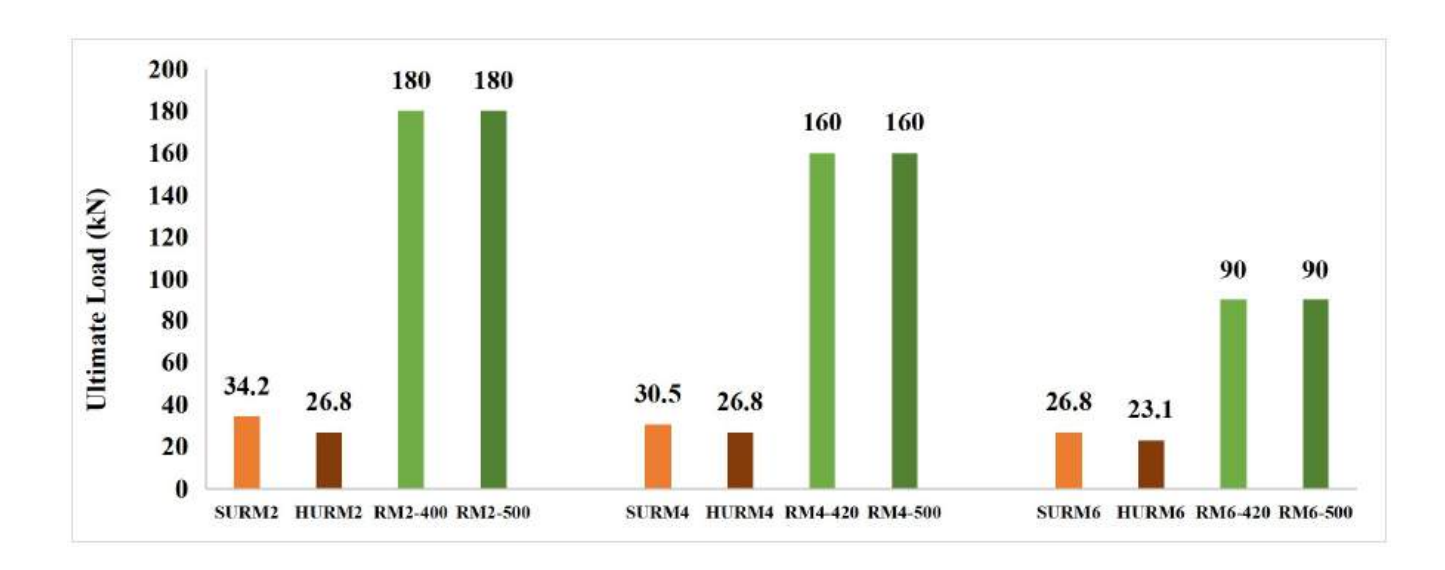


Figure 4.28- Ultimate load carrying capacity of URM & RM walls.

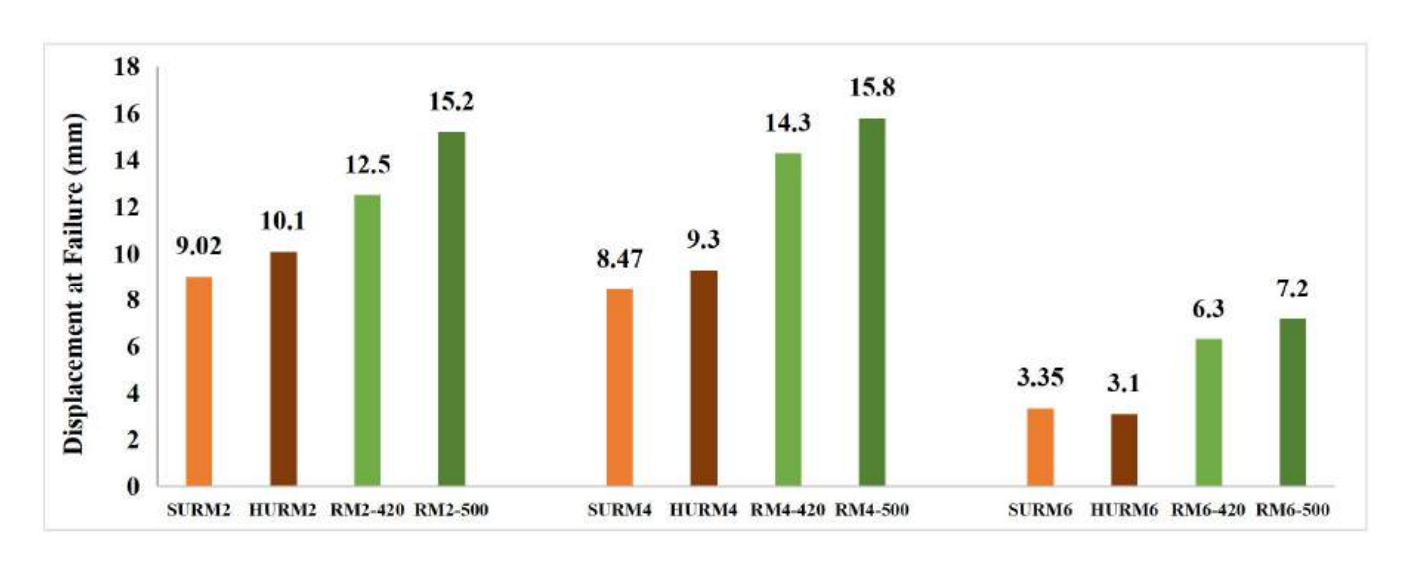


Figure 4.29- Maximum displacement of URM & RM walls.

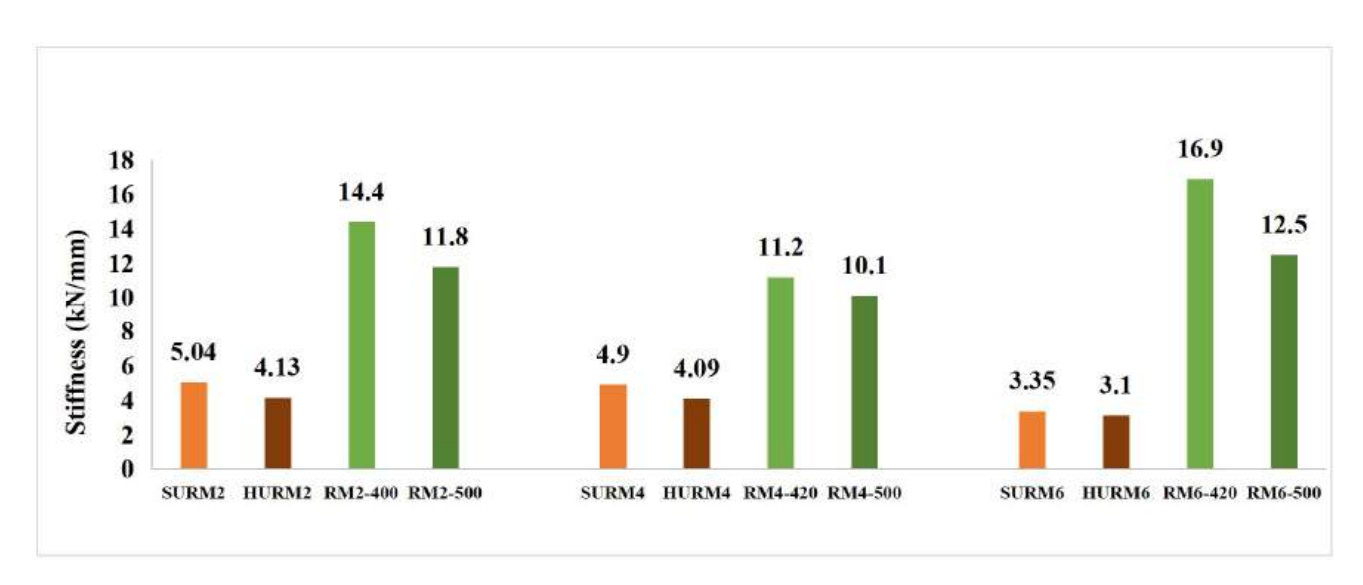


Figure 4.30- Stiffness at maximum displacement of URM & RM walls.

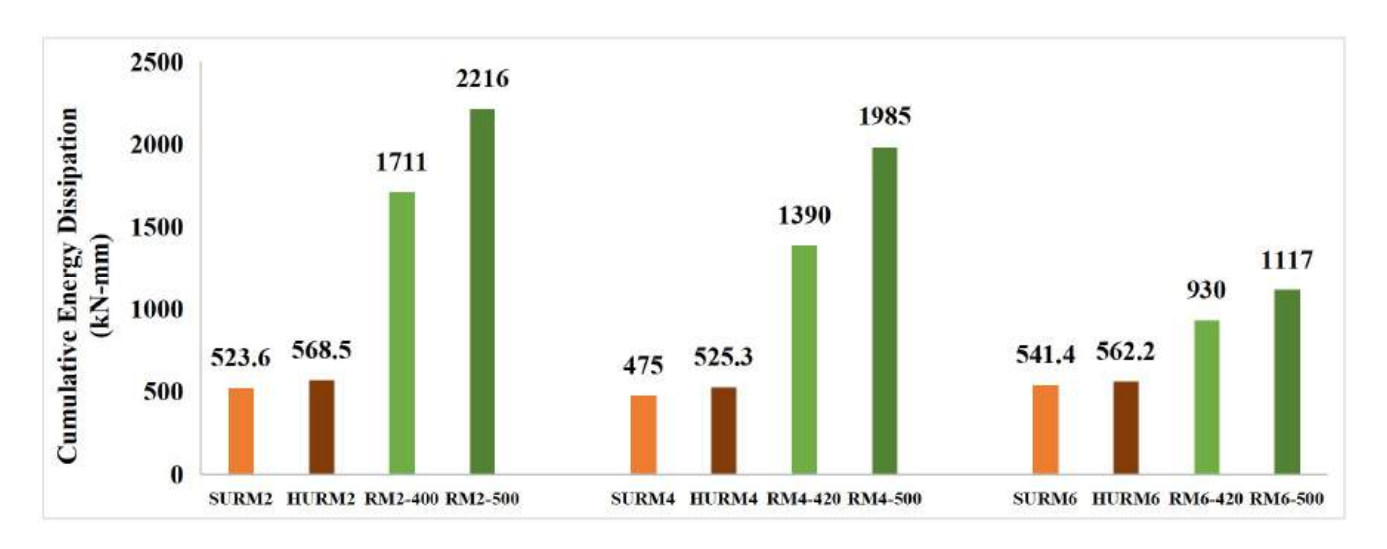


Figure 4.31- Cumulative energy dissipation of URM & RM walls.

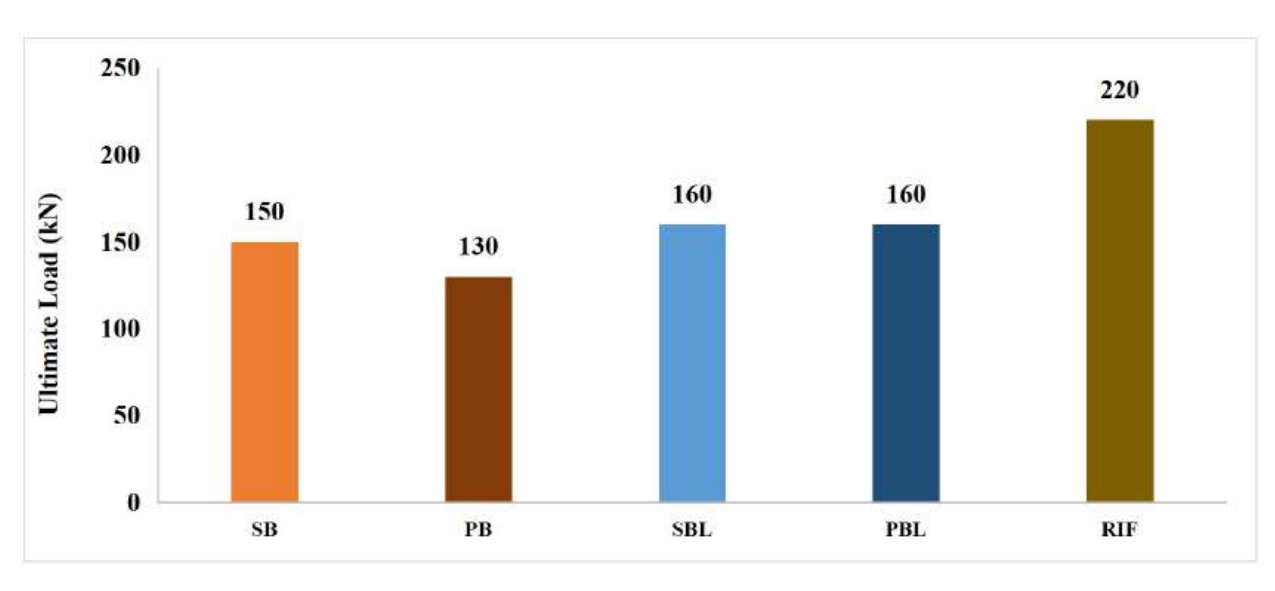


Figure 4.32- Ultimate load carrying capacity of URM & RM infilled frame walls.

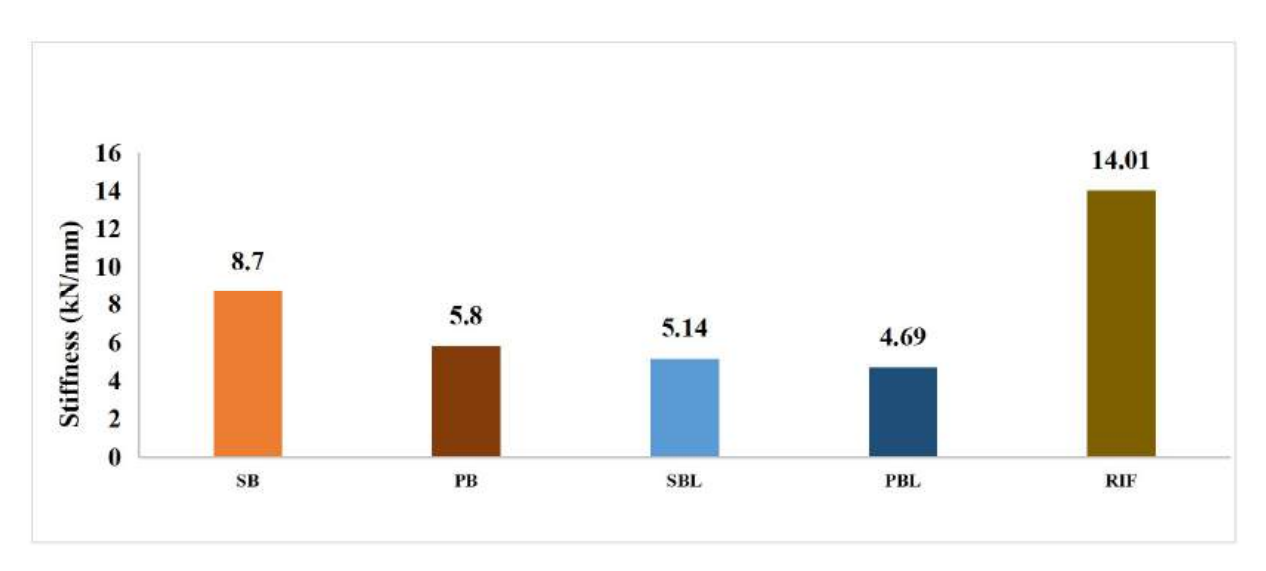


Figure 4.33- Stiffness at maximum displacement of URM & RM infilled frame walls.

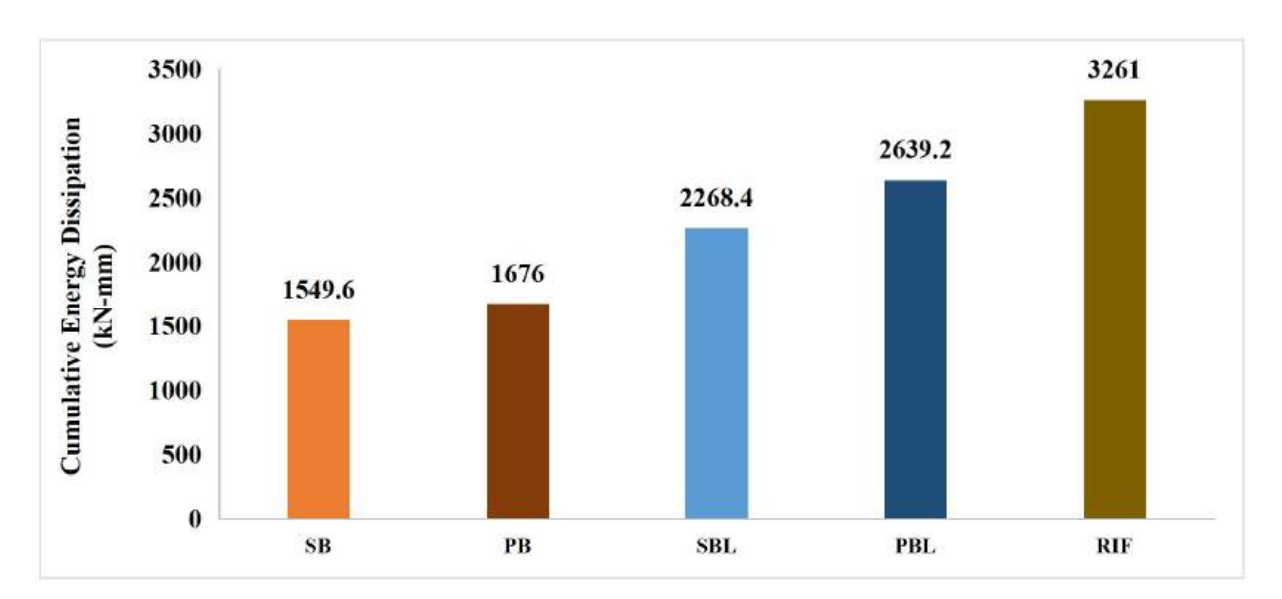


Figure 4.34- Cumulative energy dissipation of URM & RM infilled frame walls.

4.4.3 Comparison between Reinforced Masonry and Infilled Frame

The purpose of this comparison is to evaluate the performance of RM and infilled frame wall and try to understand if RM walls can perform satisfactory with respect to infilled frame wall during cyclic loading.

From the summary of the test results, it is evident that for higher mortar strength (Cement to sand ratio 1:2 & 1:4), RM walls exhibited 20% - 38% more ultimate load carrying capacity than infilled frame wall. In case of energy dissipation, RM walls dissipates 43% more energy than infilled walls.

The comparison of ultimate load carrying capacity, maximum displacement and cumulative energy dissipation RM and infilled frame walls are illustrated below.

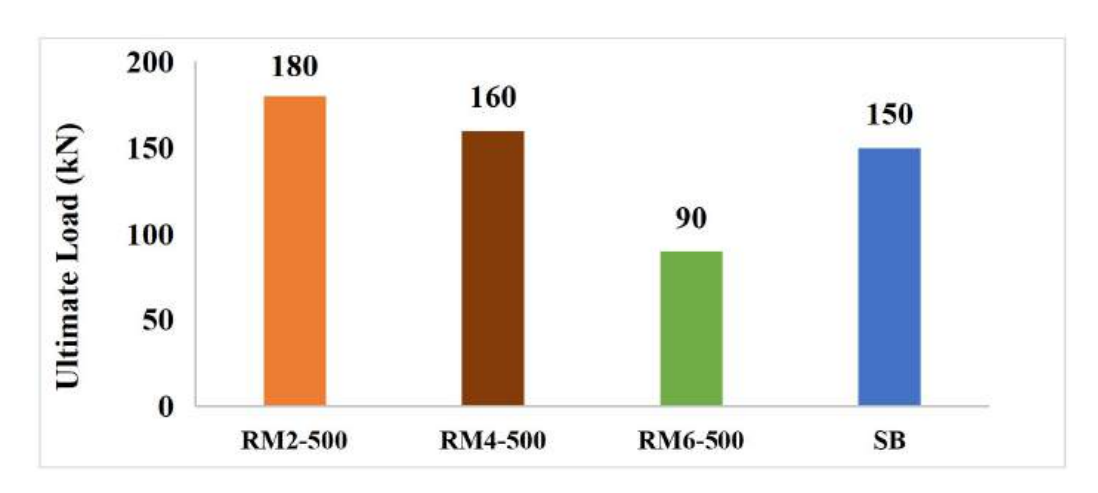


Figure 4.35- Ultimate load carrying capacity of RM walls & infilled frame walls.

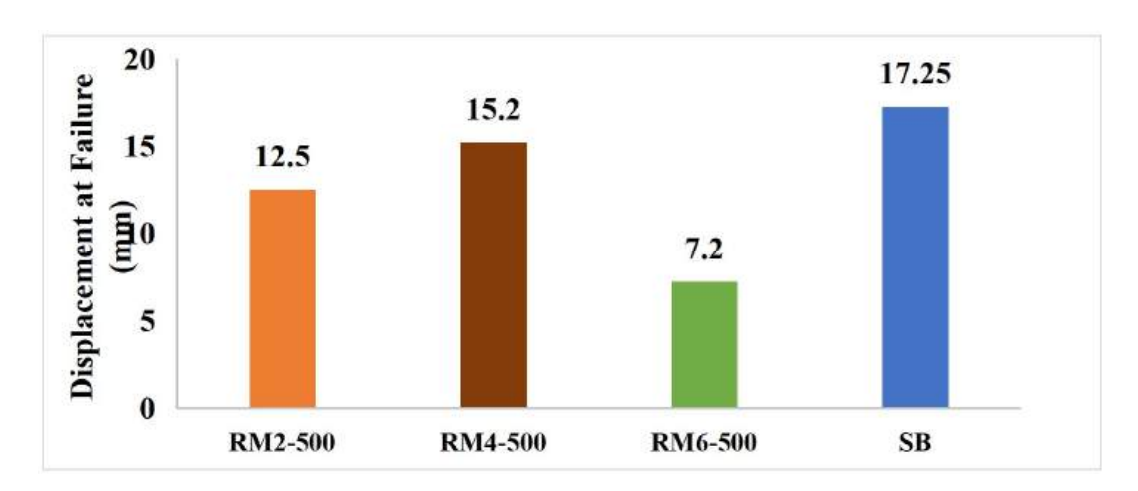


Figure 4.36- Maximum displacement of RM walls & infilled frame walls.

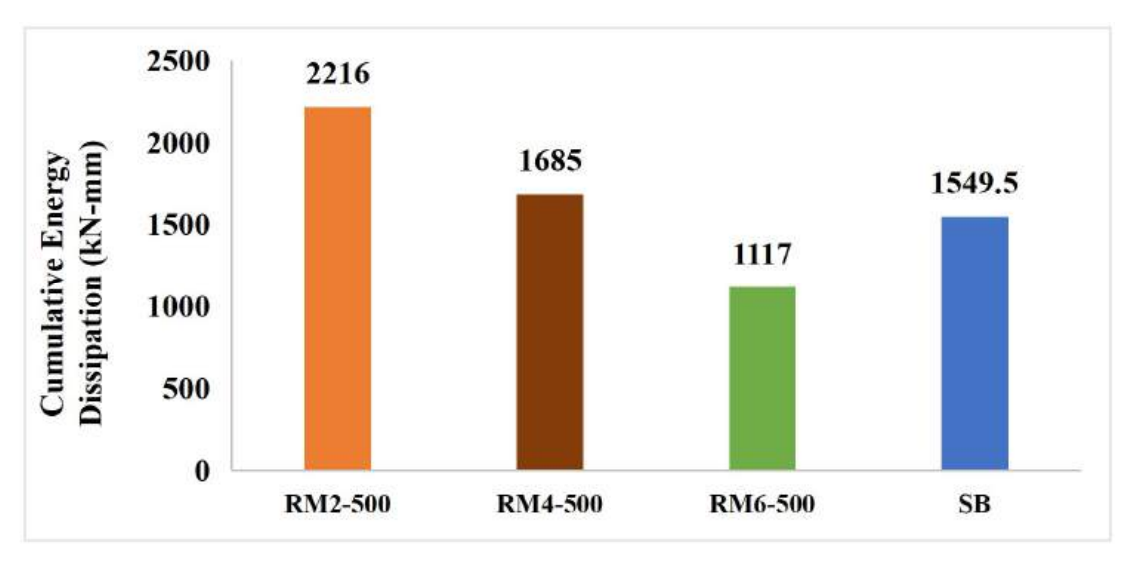


Figure 4.37- Cumulative energy dissipation of RM walls & infilled frame walls.

4.5 Cost Analysis

The cost analysis of reinforced masonry versus unreinforced masonry walls depends on various factors such as the size and height of the wall, the type of reinforcement used, the type of masonry material, and the local labor and material costs.

The cost of unreinforced masonry walls is generally lower than reinforced masonry walls, as they require fewer materials and labor for construction. However, unreinforced masonry walls may not be suitable for high-stress and cyclic load and require additional maintenance and repairs over time.

Reinforced masonry walls generally cost 15% - 20% more to construct than unreinforced masonry walls, as they require additional materials and skilled labor for the reinforcement installation but reinforced masonry walls offer significant benefits over unreinforced masonry walls, such as increased strength, durability, and resistance to seismic loads discussed in section 4.4.2.

On the other hand, reinforced masonry walls are almost 40% less expensive than concrete frame wall as masonry materials are typically less expensive than reinforced concrete. The cost of labor for concrete frame structure construction are higher than reinforced masonry, as concrete work requires skilled labor and construction process is more time-consuming than RM. Although, RM structures cost lower than concrete frame, reinforced masonry walls provide notable advantage including higher ultimate load carrying capacity and energy dissipation as well as improved ability to resist seismic loads compared to concrete frame wall as discussed in section 4.4.3.

CHAPTER 5

CONCLUSIONS

B 5.1 General

The principal purpose of this study is to assess the effect of perforated clay brick and grouted reinforcement in masonry wall by experimental investigation. Total seventeen specimens were constructed. Between these, there are six unreinforced masonry walls, six reinforced masonry walls and five infilled frame walls. URM and RM walls are having three different mortar type. After preparation, all of the specimens were subjected to cyclic loading and their structural behavior was carefully observed.

5.2 Conclusions from the Experiments

The significant findings obtained from the experiments are mentioned below.

- Perforated clay brick are effective to increase the ductility of the specimen. Perforated bricks masonry exhibited 9% 11% more displacement before failure than solid brick masonry walls. For infilled frame walls, 10% 30% more displacement were exhibited than solid infill.
- Though perforated bricks have lesser volume of material and less weight to resist external forces, the ultimate load carrying capacity of perforated brick masonry walls were only 8% 9% less than walls having solid brick.
- Perforated clay brick are also effective to enhance the energy dissipating capacity of the specimens. For masonry wall, wall having perforated bricks dissipated 3% - 10% and for infilled frame 8% - 16% more cumulative energy than wall having solid bricks.
- Reinforcement is effective to enhance the ultimate load-carrying capacity of RM walls significantly. The load-carrying capacity of RM walls is 3.4 to 6.7 times higher than that of URM walls.
- Reinforced masonry walls are stiffer than URM walls. RM walls showed 2.5 3.5 times more stiffness than URM walls.

- The ductility of masonry walls is enhanced by the addition of reinforcement, with RM walls demonstrating 1.5 to 2.3 times more displacement at failure than URM walls.
- Reinforced Masonry increase the energy absorption capacity of masonry wall as RM walls dissipates 2 4 times more energy than unreinforced masonry wall.
- For higher mortar strength, RM walls shows 20% 38% more ultimate load carrying capacity and dissipates 43% more energy than infilled walls.
- Reinforced masonry walls are considerably more cost-effective to build when compared to infilled frame walls, with potential cost savings of up to 40%.

In summary, Unreinforced masonry walls are more affordable option but not suitable for resisting cyclic load. On the other hand, Concrete frame walls provide adequate seismic resistance but are the most expensive option. While reinforced masonry walls having higher mortar strength (1:2 & 1:4) provides a balance of strength durability and cost-effectiveness compared to URM and concrete infilled frame.

REFERENCES

Alcocer, S. M., and Meli, R., (1995) "Test Program on the Seismic Behavior of Confined Masonry Structure", *The Masonry Society*, J.,13, 68-76.

American Society for Testing and Materials (ASTM) C33, (2020) "Standard Specification for Concrete Aggregates", *ASTM International*, West Conshohocken, PA, United States of America.

American Society for Testing and Materials (ASTM) C39, (2020) "Standard Test Method for Compressive Strength of Cylindrical Concrete Specimens", *ASTM International*, West Conshohocken, PA, United States of America.

American Society for Testing and Materials (ASTM) C67, (2020) "Standard Test Methods for Sampling and Testing Brick and Structural Clay Tile", *ASTM International*, West Conshohocken, PA, United States of America.

American Society for Testing and Materials (ASTM) C109, (2020) "Standard Test Method for Compressive Strength of Hydraulic Cement Mortars (Using 2-in. or [50-mm] Cube Specimens)", ASTM International, West Conshohocken, PA, United States of America.

American Society for Testing and Materials (ASTM) C476, (2020) "Standard Specification for Grout for Masonry", *ASTM International*, West Conshohocken, PA, United States of America.

American Society for Testing and Materials (ASTM) C1314, (2020) "Standard Test Method for Compressive Strength of Masonry Prisms", *ASTM International*, West Conshohocken, PA, United States of America.

Araya-Letelier, G., Calderón, S., Sandoval, C., Sanhueza, M., and Murcia-Delso, J., (2019) "Fragility functions for partially-grouted masonry shear walls with bed-joint reinforcement," *Engineering Structure*, vol. 191, doi: 10.1016/j.engstruct.2019.03.114.

BDS EN 197-1:2003. "Cement composition, specifications and conformity criteria for common cements," Bangladesh Standards and Testing Institution, Dhaka.

BNBC, Volume 2, Part 6-Structural Design, chapter 7, (2020) Masonry Structures, Housing and Building Research Institute, Bangladesh, *Bangladesh National Building Code*.

Fardis, M. N., Bousias, S. N., Franchioni, G., and Panagiotakos, T.B., (1999) "Seismic Response and Design of RC Structures with Plan-Eccentric Masonry Infills", *Journal of Earthquake Engineering and Structural Dynamics*, Vol. 28, pp. 173-191.

FEMA 306, (1998) Evaluation of Earthquake Damaged Concrete and Masonry Wall Buildings. *Basic procedures manual*, Washington D.C.: Federal Emergency Management Agency.

FEMA 307, (1998) Evaluation of Earthquake Damaged Concrete and Masonry Wall Buildings. *Technical resources*, Washington D.C.: Federal Emergency Management Agency.

Fódi, A., (2011) "Experimental and numerical investigation of reinforced and plain masonry walls," *PhD Thesis, Department of Structural Engineering, Faculty of Civil Engineering, Budapest University of Technology and Economics*, Budapest, Hungary.

Ganern, G., and Salarn, A. E., (1994) "An overview on the draft of the Egyptian code for masonry and proposed research to cover the shortcomings A1 - Alcocer, Sergio," *Masonic Society Journal*, vol. 13, no. 2, pp. 68–76.

Ghiassi, Soltani, M., and Tasnimi, A. A., (2012) "A simplified model for analysis of unreinforced masonry shear walls under combined axial, shear and flexural loading," *Engineering Structure*, vol. 42, doi: 10.1016/j.engstruct.2012.05.002.

Haider, W., (2007) "In-plane response of wide spaced reinforced masonry shear walls." *Central Queensland University,* Australia.

Kareem, K., M., and Guneyisi, E. M., (2019) "Effect of Masonry Infill Wall Configuration and Modelling Approach on the Behaviour of RC Frame Structures", *Springer, Arabian Journal for Science and Engineering*, Vol. 44, pp. 4309–4324, DOI: 10.1007/s13369-018-3389-6.

Latif, A., Shedid, M., Okail, H., and Rahman, A., (2019) "Numerical modeling of reinforced masonry walls under lateral loading at the component level response as opposed to system level response," *Ain Shams Engineering Journal*, vol. 10, no. 2, doi: 10.1016/j.asej.2018.12.003.

Maidiawati, and Sanada, Y., (2017). "R/C frame-infill interaction model and its application to Indonesian Buildings", *Earthquake Engineering & Structural Dynamics*, Vol. 46, No.2, pp. 221-241, DOI: 10.1002/eqe.2787.

Matsumura, (1987) "Shear strength of reinforced hollow unit masonry walls," 4th North American Masonry Conference, pp. 50–51.

Mehrabi, A. B., and Shing, P. B., (1997) "Finite Element Modeling of Masonry-Infilled RC Frames", *The American Society of Civil Engineers (ASCE), Journal of Structural Engineering*, Vol. 123, No. 5, pp. 604-613.

Murthy, C. V. R., and Jain, S. K., (2000) "Beneficial Influence of Masonry Infill Walls on Seismic Performance of RC Frame Buildings", *12WCEE 2000 : 12th World Conference on Earthquake Engineering*, New Zealand.

Okamoto, S., Yamazaki, Y., Kaminosono, T., Teshigawara, M., and Hirashi, H., (1987) "Seismic capacity of reinforced masonry walls and beams," *18th Joint Meeting of the US-Japan Cooperative Program in Natural Resource Panel on Wind and Seismic Effects, NBSIR*, pp. 87–3540.

Polyakov, S. V., (1960) "On the Interaction between Masonry Filler Walls and Enclosing Frame when Loaded in the Plane of the Wall", *Translation in earthquake engineering*, pp. 36-42.

Samy, S., Zaghlal, M., Elsisi, A. A., Husain, M., (2022) "A Comprehensive Review on Unreinforced and Reinforced Masonry Structures Modeling Strategies," *The Egyptian International Journal of Engineering Sciences and Technology*, vol. 39, pp 13-24.

Sandeep, M. Renukadevi, V., Manjunath, S., and Somanath, (2013) "Influence Of Reinforcement On The Behavior Of Hollow Concrete Block Masonry Prism Under Compression-An Experimental And Analytical Approach," *International Research Journal of Engineering and Technology (IRJET)*.

Sandoval, C., Caldero, S., Almaza, J. L., (2018) "Experimental cyclic response assessment of partially grouted reinforced clay brick masonry walls", *Bull Earthquake Engineering*.

Sivaraja, S. S., Thandavamoorthyb, T.S., Vijayakumarc, S., Mosesaranganathana, S., Rathnasheelad, P.T., and Dasarathy, A.K., (2012) "GFRP Strengthening and Applications of Unreinforced Masonry wall (UMW)", *The 2nd International Conference on Rehabilitation and Maintenance in Civil Engineering*.

Tomazevic, M., (1999) "Earthquake - resistant design of masonry buildings", *London: Imperial College Press*.

Wilson, B., and Varkey, D., (2019) "Experimental and Analytical Study on Masonry Panels Strengthened with Geotextile Comparison," *International Research Journal of Engineering and Technology (IRJET)*, vol. 6.

Xu, H., Gentulini, C., and Yu, Z., (2018) "A unified model for the seismic analysis of brick masonry structures," *Construction and Building Materials*, vol. 184.

Appendix-A

Yield Strength And Ultimate Strength Of Reinforcement

 Table A.1- Yield strength and ultimate strength of reinforcement

Dia (mm)	Area (mm²)	Yield Load (kN)	Yield Strength (MPa)	Average Yield Strength (MPa)	Ultimate Load (kN)	Ultimate Strength (MPa)	Average Ultimate Strength (MPa)
8	50	23.4	468		34.3	686	
8	50	23.6	472	472	34.3	686	686
8	50	23.8	476		34.3	686	
8	50	28.7	574		33.2	664	
8	50	28.5	570	566	33.0	660	660
8	50	27.7	554		32.8	656	
12	113	53.0	469		72.0	637	
12	113	52.5	465	465	72.0	637	637
12	113	52.0	460		72.0	637	



Figure A.1- Testing of rebar.

Appendix-B

Compressive Strength Of Solid And Perforated Clay Brick

Table B.1- Compressive strength of solid clay brick

Brick	Length (mm)	Width (mm)	Height (mm)	Area (mm²)	Observed load (kN)	Actual load (kN)	Compressive Strength (MPa)	Average Compressive strength (MPa)
1	100.50	55.00	31.00	5527.50	276	266.4	48.20	
2	100.50	53.50	33.00	5376.75	242	232.27	43.20	
3	99.50	55.50	31.00	5522.25	230	220.22	39.88	40.39
4	99.50	51.50	32.00	5124.25	194	184.08	35.92	
5	100.00	53.00	31.00	5300.00	194	184.08	34.73	

Table B.2- Compressive strength of perforated clay brick

Brick	Length (mm)	Width (mm)	Height (mm)	Area (mm²)	Observed load (kN)	Actual load (kN)	Compressive Strength (MPa)	Average Compressive strength (MPa)
1	102.50	58.00	30.00	5114.05	140	129.86	25.39	
2	103.00	55.50	33.00	4885.55	196	186.08	38.09	
3	102.00	56.00	32.00	4881.05	112	101.75	20.85	26.80
4	102.00	57.50	33.00	5034.05	124	113.80	22.61	
5	100.00	57.00	33.00	4869.05	142	131.87	27.08	







Figure B.1- (a) Capping of solid and parforated brick before testing,

(b) Compressive strength testing of brick.

Appendix-C

Water Absorption Capacity Of Solid And Perforated Clay Brick

Table C.1- Water absorption capacity of solid clay brick

Brick	SSD weight	Dry Weight	Absorption Capacity	Average Absorption
	(gm)	(gm)	(%)	Capacity (%)
1	396	345	14.78	
2	389	340	14.41	
3	404	352	14.77	14.67
4	399	347	14.99	
5	366	320	14.38	

Table C.2- Water absorption capacity of perforated clay brick

Brick	SSD weight	Dry Weight	Absorption Capacity	Average Absorption
	(gm)	(gm)	(%)	Capacity (%)
1	353	313	12.78	
2	351	310	13.23	
3	326	290	12.41	12.84
4	346	306	13.07	
5	346	307	12.70	

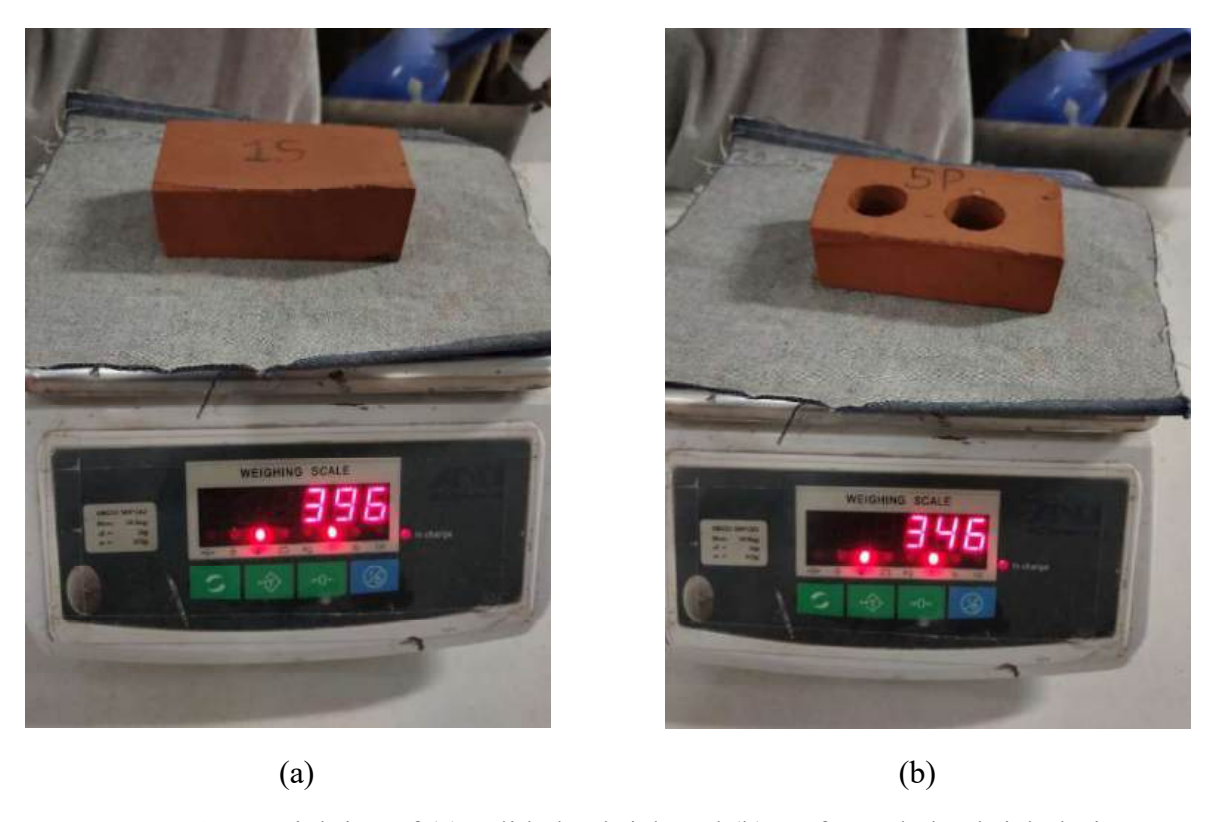


Figure C.1- Weighting of (a) solid clay brick and (b) perforated clay brick during absorption capacity testing.

Appendix-D

Compressive Strength Of Mortar Cube

 Table D.1- Compressive strength of mortar cube

Cement : Sand	Days	Cube	Area (mm²)	Observed Load (kN)	Actual Load (kN)	Stress (MPa)	Average Stress (MPa)
		1	2500	45.20	46.17	18.47	
	7	2	2500	44.30	45.27	18.11	18.30
		3	2500	44.80	45.77	18.31	
		1	2500	59.50	60.54	24.22	
1:2	14	2	2500	56.50	57.53	23.01	23.72
		3	2500	58.80	59.84	23.94	
		1	2500	81.00	82.14	32.86	
	28	2	2500	68.70	69.78	27.91	32.28
		3	2500	89.00	90.18	36.07	
		1	2500	17.00	17.84	7.14	
	7	2	2500	20.00	20.86	8.34	7.27
		3	2500	15.00	15.83	6.33	
		1	2500	28.60	29.50	11.80	
1:4	14	2	2500	30.50	31.40	12.56	12.67
		3	2500	33.20	34.12	13.65	
		1	2500	31.98	32.89	13.16	
	28	2	2500	35.80	36.73	14.69	14.45
		3	2500	37.78	38.72	15.49	
		1	2500	5.15	5.94	2.37	
1:6	7	2	2500	5.61	6.40	2.56	2.56
		3	2500	6.111	6.90	2.76	

	1	2500	9.952	10.76	4.30	
14	2	2500	9.142	9.95	3.98	4.33
	3	2500	10.919	11.73	4.69	
	1	2500	11.04	11.85	4.74	
28	2	2500	12.429	13.25	5.30	5.02
	3	2500	11.748	12.56	5.03	







Figure D.1- Prepared mortar cubes mortar testing.

Appendix-E

Compressive Strength Of Solid And Perforated Brick Prism

Table E.1- Compressive strength of solid and perforated brick prism for three mortar type.

Mix Ratio (Cement: Sand)	Brick Type	Brick No	Length (mm)	Width (mm)	Height (mm)	Area (mm²)	Applied Load (kN)	Compressive Strength (MPa)	Average Compressive Strength (MPa)
		1	117	105	193	12285	167	13.59	
	Solid	2	115	107	197	12305	131	10.65	11.56
1:2		3	118	107	195	12626	132	10.45	
1.2		1	128	105	198	12609	81	6.42	
	Perforated	2	119	101	194	11188	77	6.88	6.55
		3	120	100	194	11169	71	6.36	
		1	110	100	180	11000	139	12.64	
	Solid	2	115	100	190	11500	119	10.35	10.48
1:4		3	115	105	190	12075	102	8.45	
1.4		1	120	100	190	11169	62	5.55	
	Perforated	2	118	102	190	11205	54	4.82	4.85
		3	115	105	180	11244	47	4.18	
		1	114	103	187	11742	93	7.92	
	Solid	2	117	109	189	12753	87	6.82	6.92
1:6		3	114	105	204	11970	72	6.02	
1.0		1	116	110	183	11929	53	4.44	
	Perforated	2	118	100	190	10969	39	3.56	3.96
		3	118	103	197	11323	44	3.89	







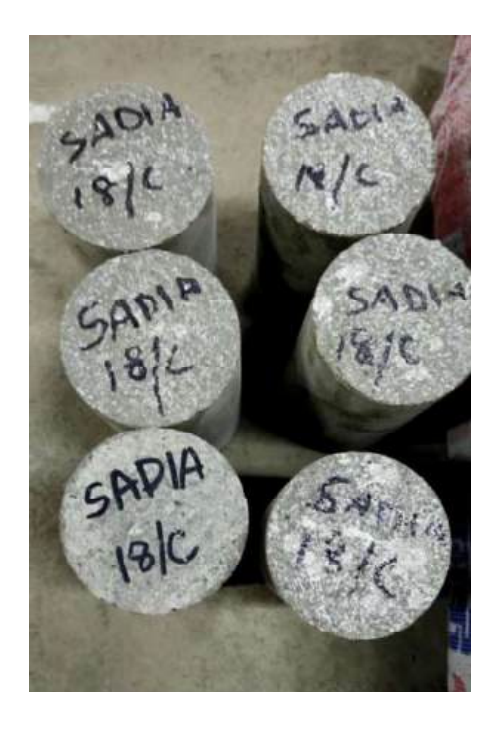
Figure E.1- Testing of prepared prisms.

Appendix-F

Compressive Strength Of Concrete Cylinder

Table F.1- Compressive strength of concrete cylinder

Days	Cylinder	Average Dia (mm)	Area (mm²)	Observed load (KN)	Actual Ioad (KN)	Compressive Strength (MPa)	Average Compressive Strength (MPa)	
	1	101.225	8047.60	150.00	147.13	18.28		
14	2	101.05	8019.80	150.00	147.13	18.35	17.90	
197917	3	101.225	8047.60	140.00	137.28	17.06		
	4	101	8011.87	185.00	183.14	22.86		
21	5	101.15	8035.68	170.00	168.12	20.92	20.72	
	6	101.3	8059.53	150.00	148.09	18.37		
28	7	101	8011.87	181.00	177.64	22.17		
	8	101.325	8063.51	178.00	174.69	21.66	21.63	
	9	101.325	8063.51	173.00	169.77	21.05		





(a) (b)

Figure F.1- (a) Prepared concrete cylinders (b) cylinder testing.

Appendix-G

Hydraulic Jacks

Hydraulic Jack 1 (Jack ID: 31431)

Piston diameter: 85 mm

Piston Perimeter: 267 mm

Ram area: 5675 mm²

Body Height: 370 mm

Operating Temperature: 24°C

Pump: Manual

Capacity: 50 Ton

Allowable Pressure Range of Pressure Gauge: 0-150 MPa

Calibration Device Used Digital (Display in Load (KN)) Load Cell: CCDHA-50t-004-000 s/n: 49625.

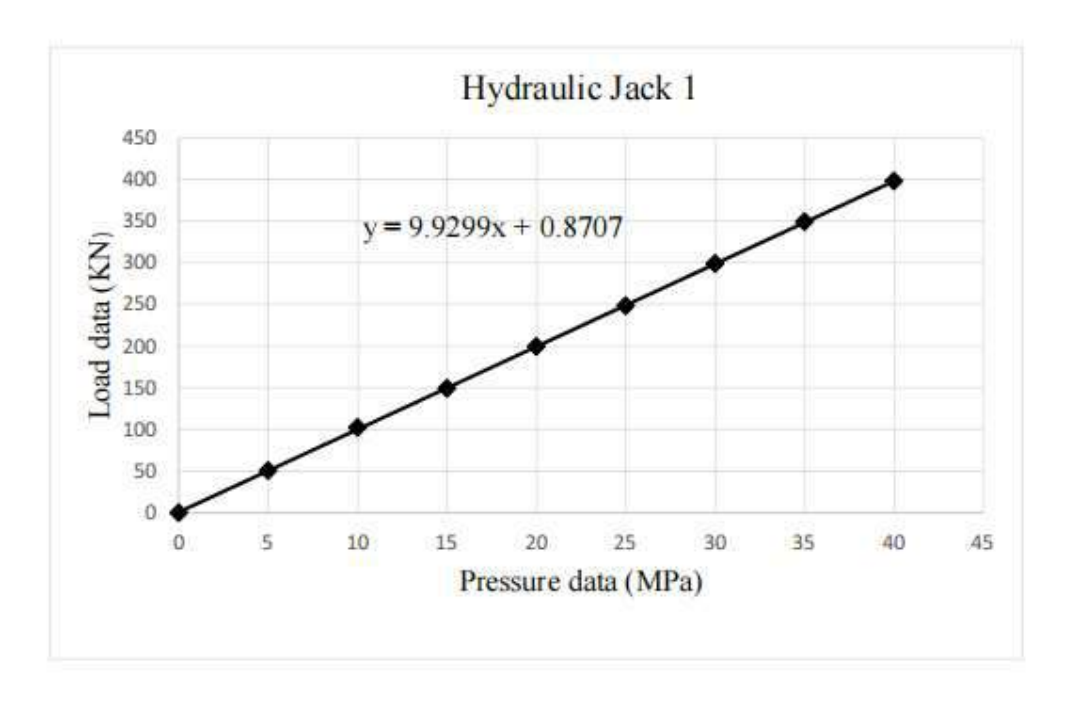


Figure G.1- Calibration curve of hydraulic jack 1.

Hydraulic Jack 2 (Jack ID: SM01)

Piston diameter: 50 mm

Piston Perimeter: 157 mm

Ram area: 1964 mm²

Body Height: 313 mm

Operating Temperature : 24°C

Pump: Manual

Capacity: 30 Ton

Allowable Pressure Range of Pressure Gauge: 0-60000 lbs

Calibration Device Used Digital (Display in Load (KN)) Load Cell: CCDHA-50t-004-000 s/n: 49625.

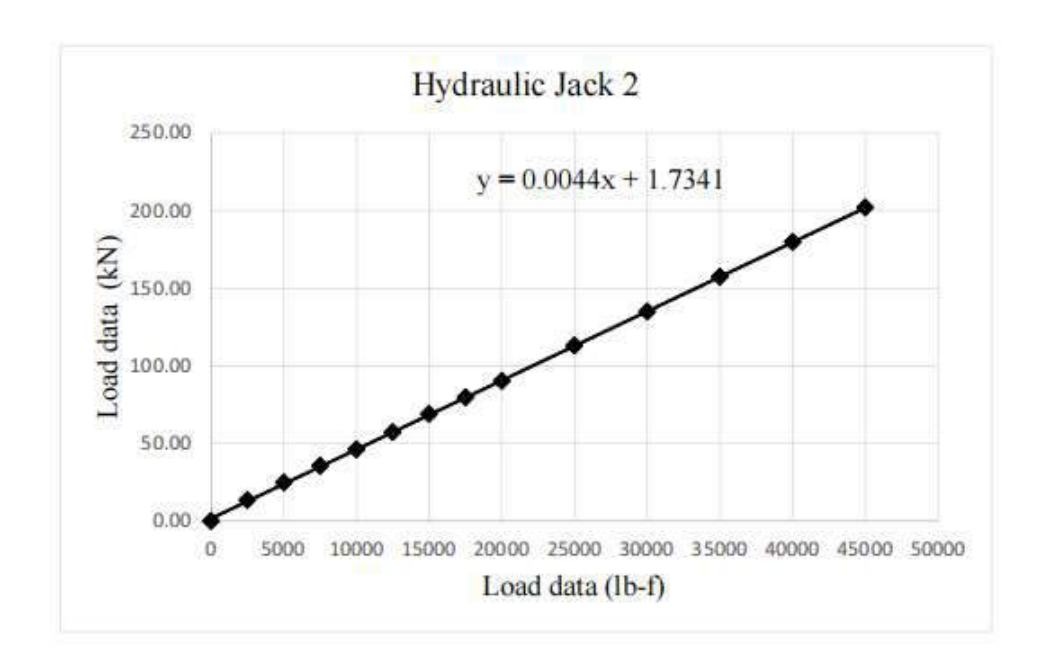


Figure G.2- Calibration curve of hydraulic jack 2.

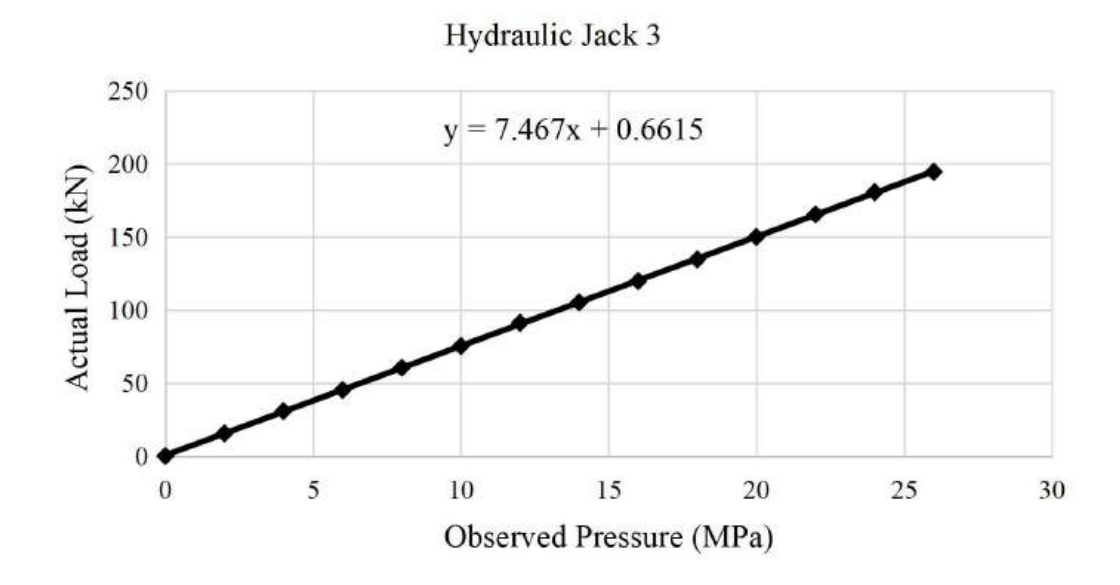


Figure G.3- Calibration curve of hydraulic jack 3.

Appendix-H

Failure pattern of the walls

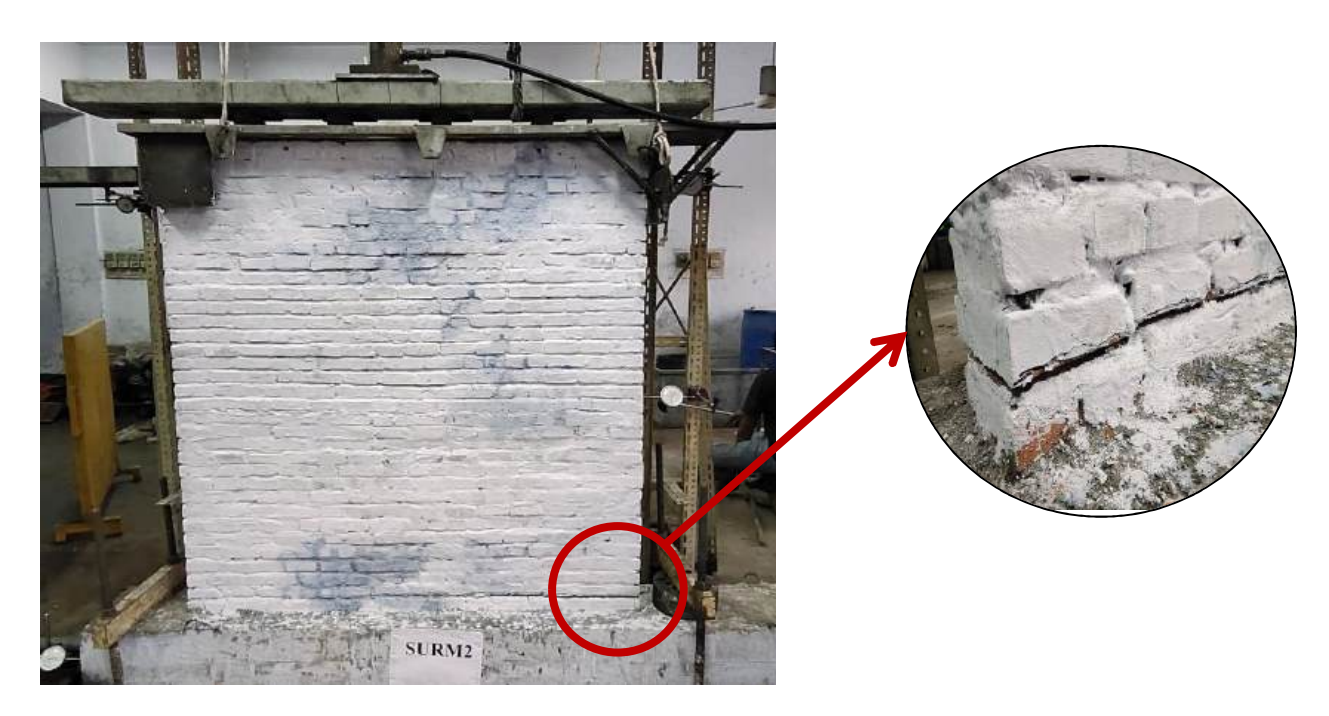


Figure H.1- SURM2 at complete failure.

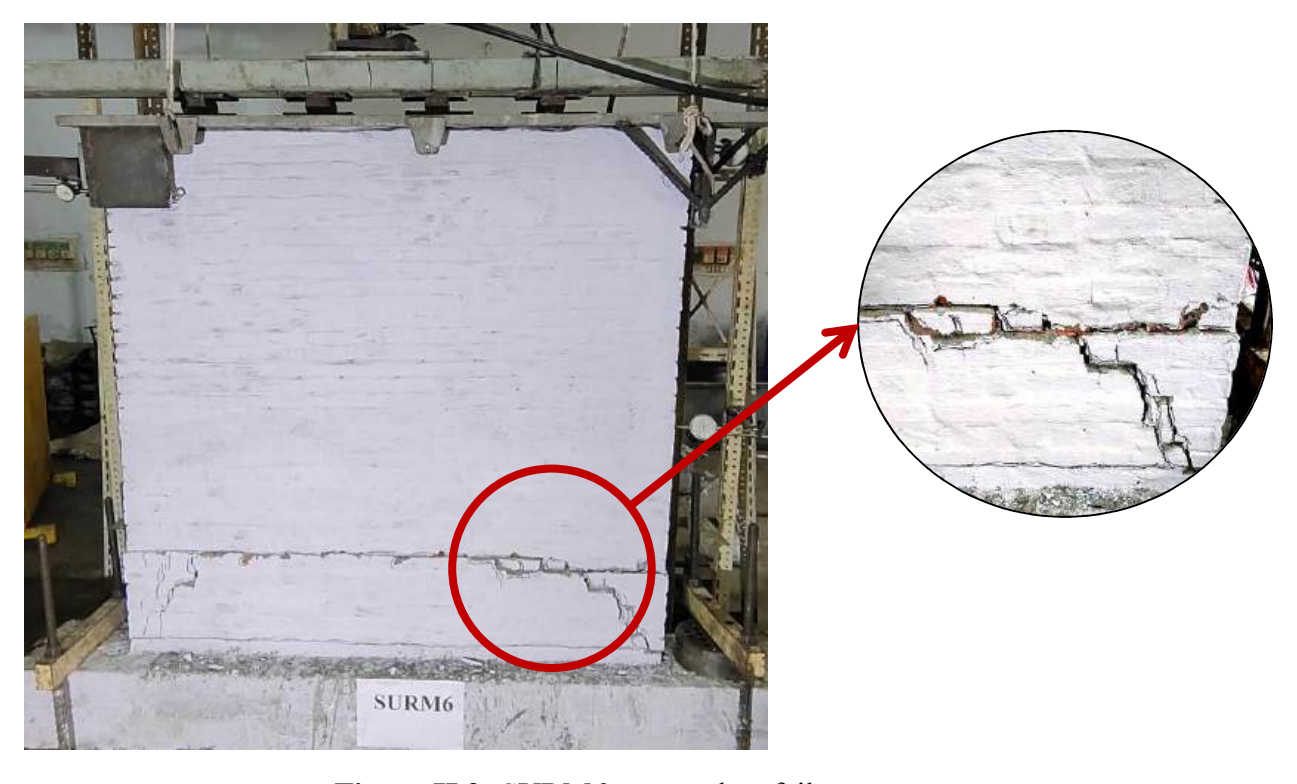


Figure H.2- SURM6 at complete failure.

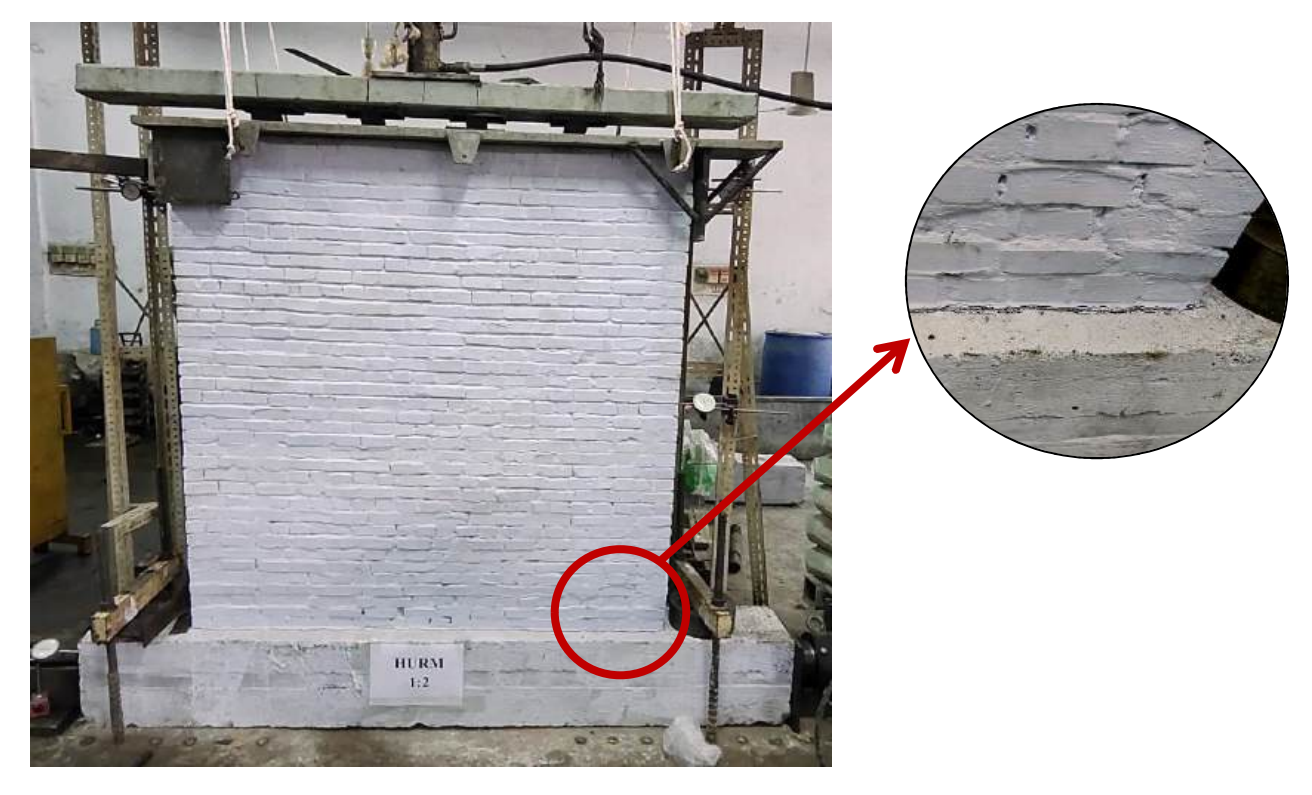


Figure H.3- HURM2 at complete failure.

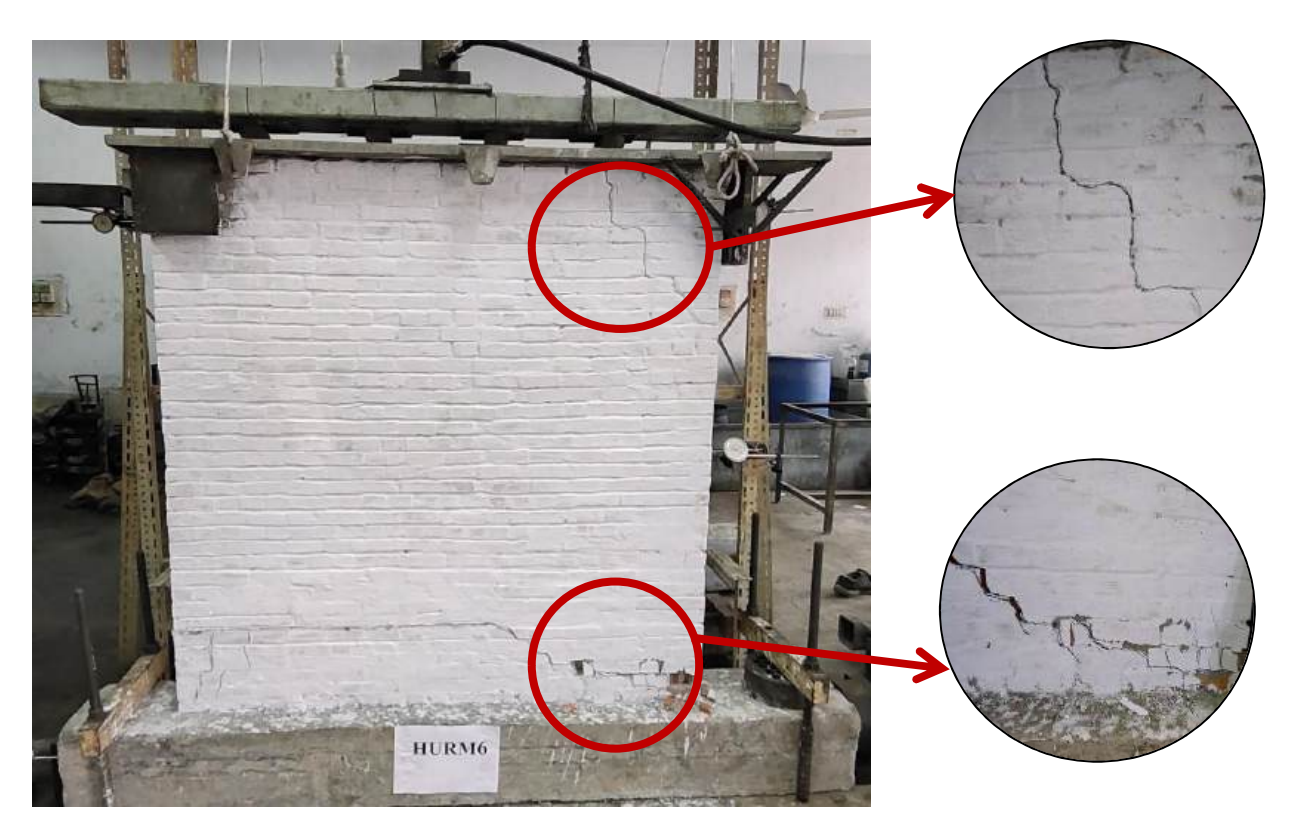


Figure H.4- HURM6 at complete failure.

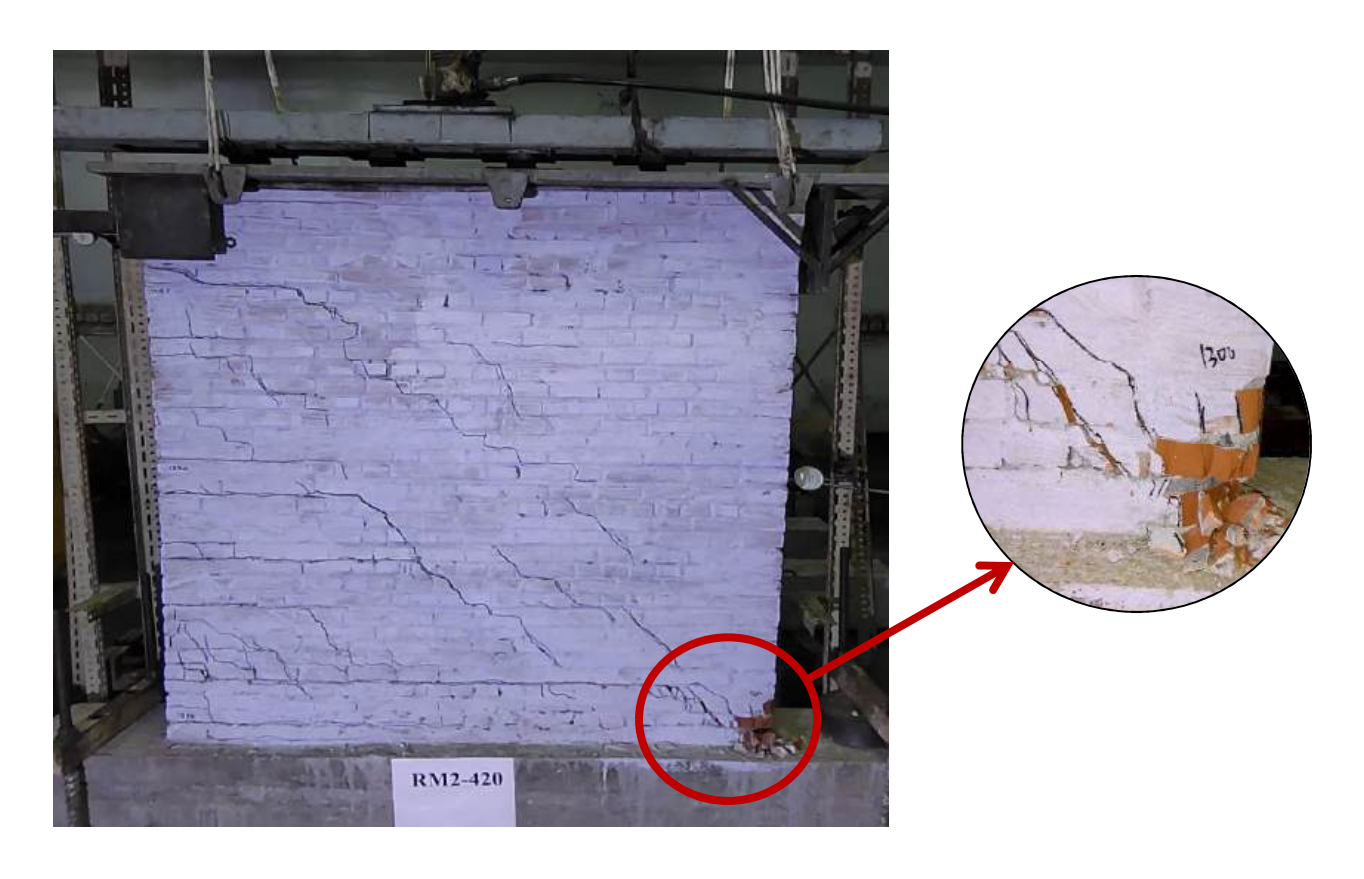


Figure H.5- RM2-420 at complete failure.

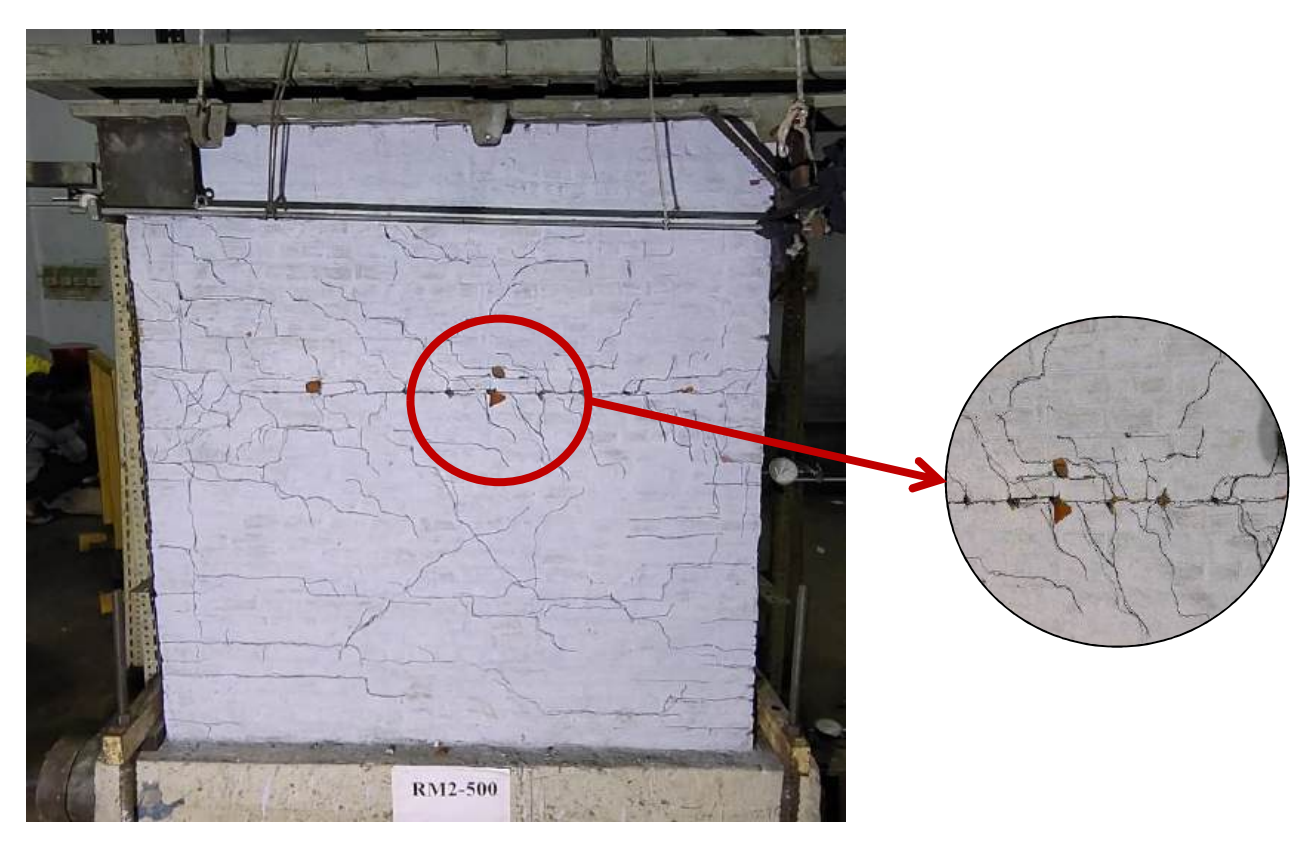


Figure H.6- RM2-500 at complete failure.

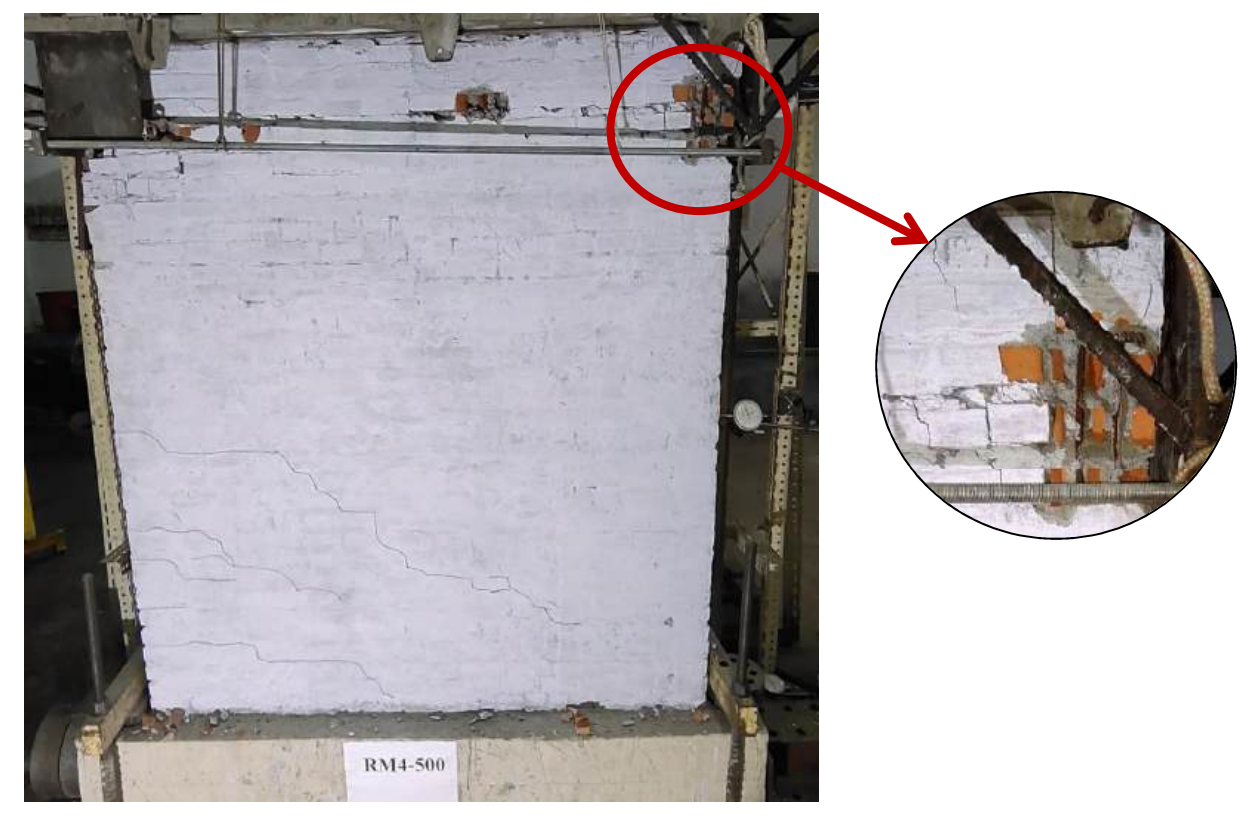


Figure H.7- RM4-500 at complete failure.

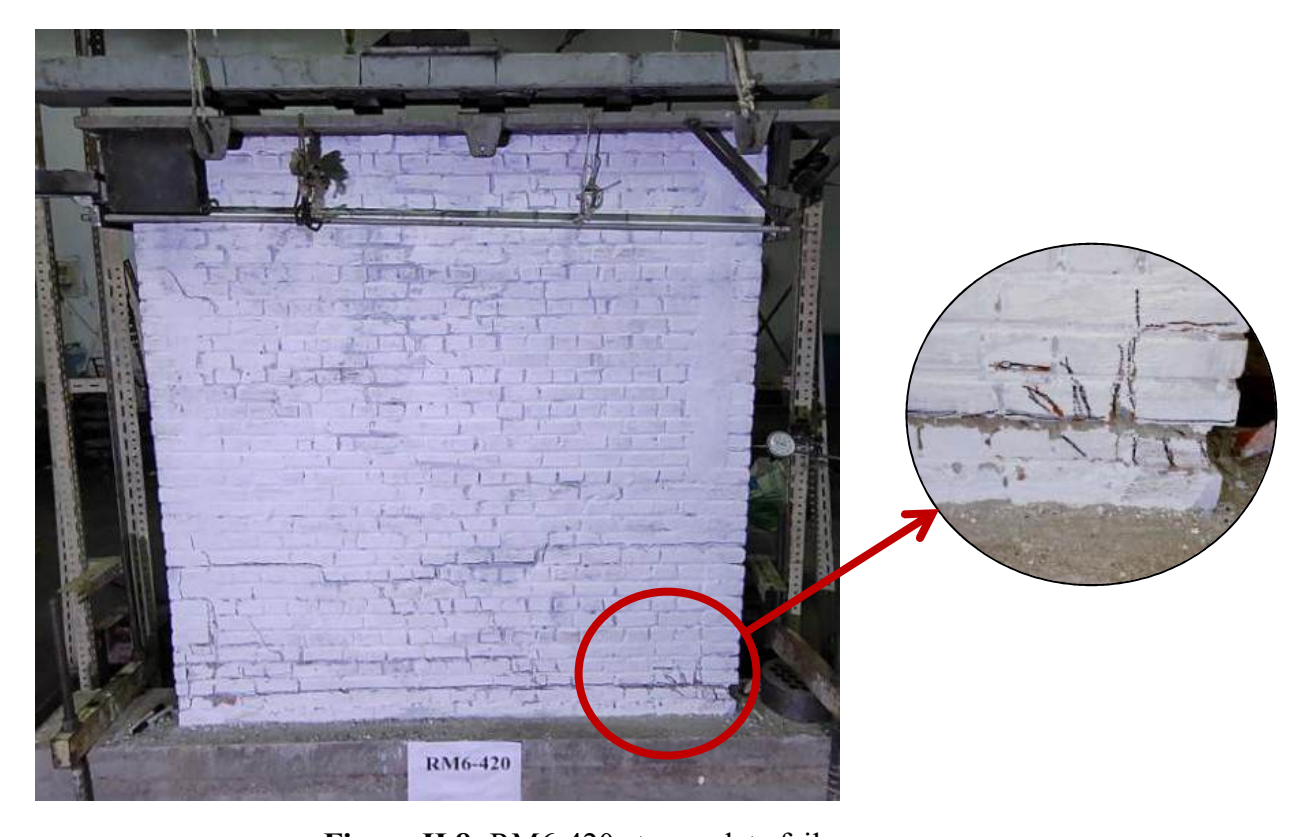


Figure H.8- RM6-420 at complete failure.

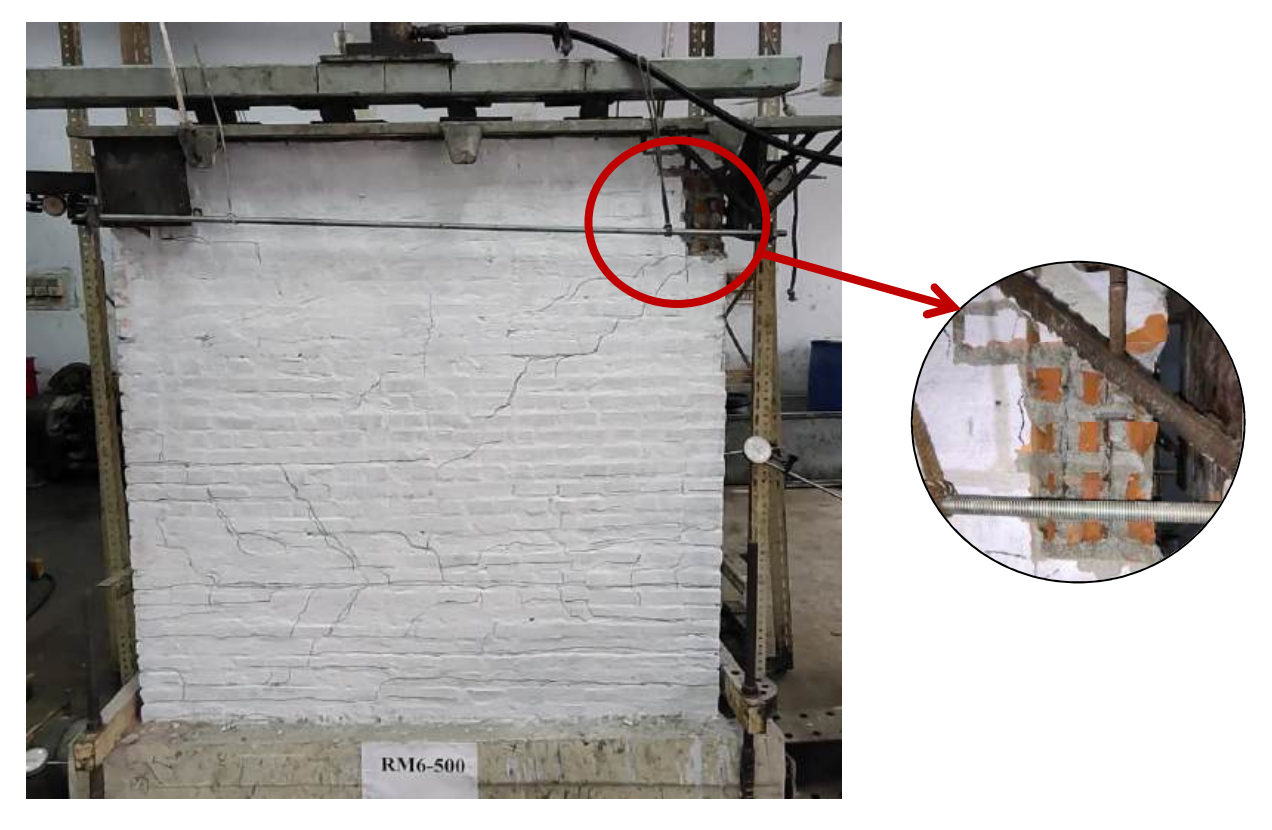


Figure H.9- RM6-500 at complete failure.

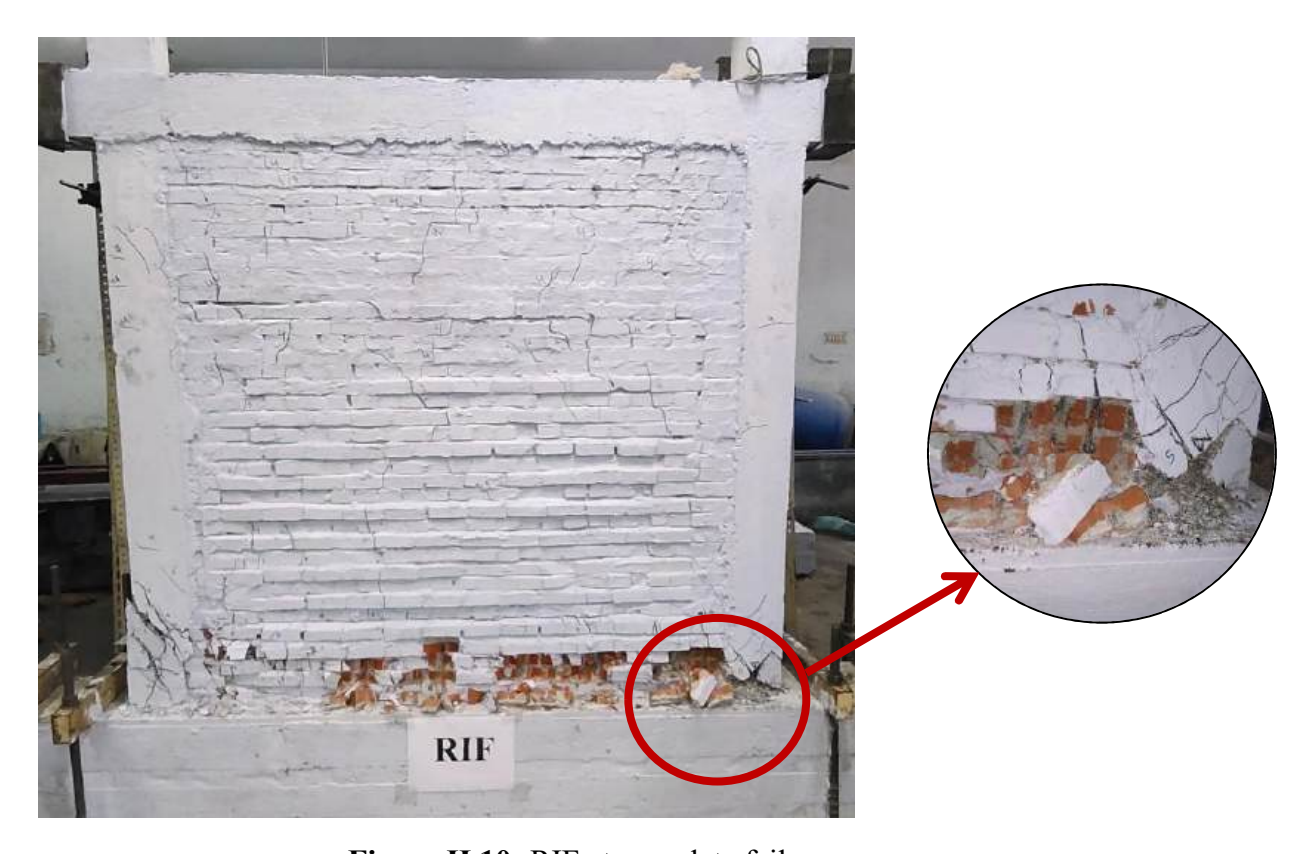


Figure H.10- RIF at complete failure.



Figure H.11- PB at complete failure.



Figure H.12- SBL at complete failure.

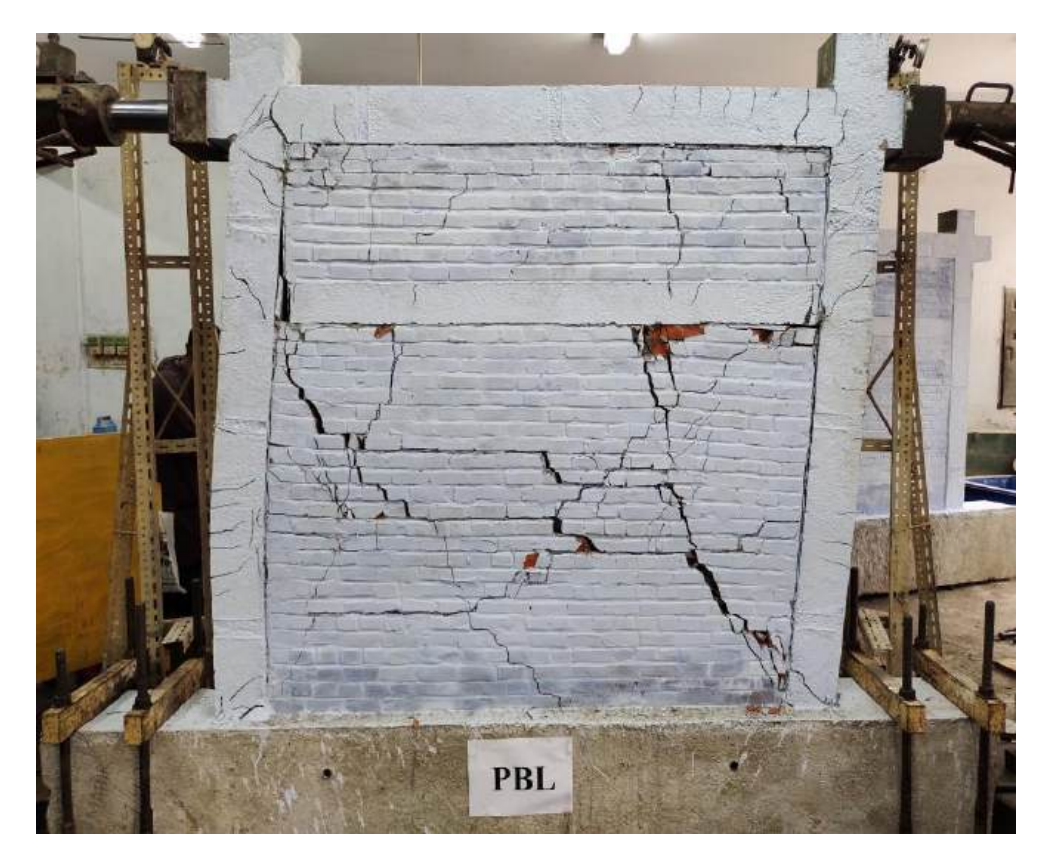


Figure H.13- PBL at complete failure.

Appendix-I

Hysteretic Load-Displacement Curve of the Specimen

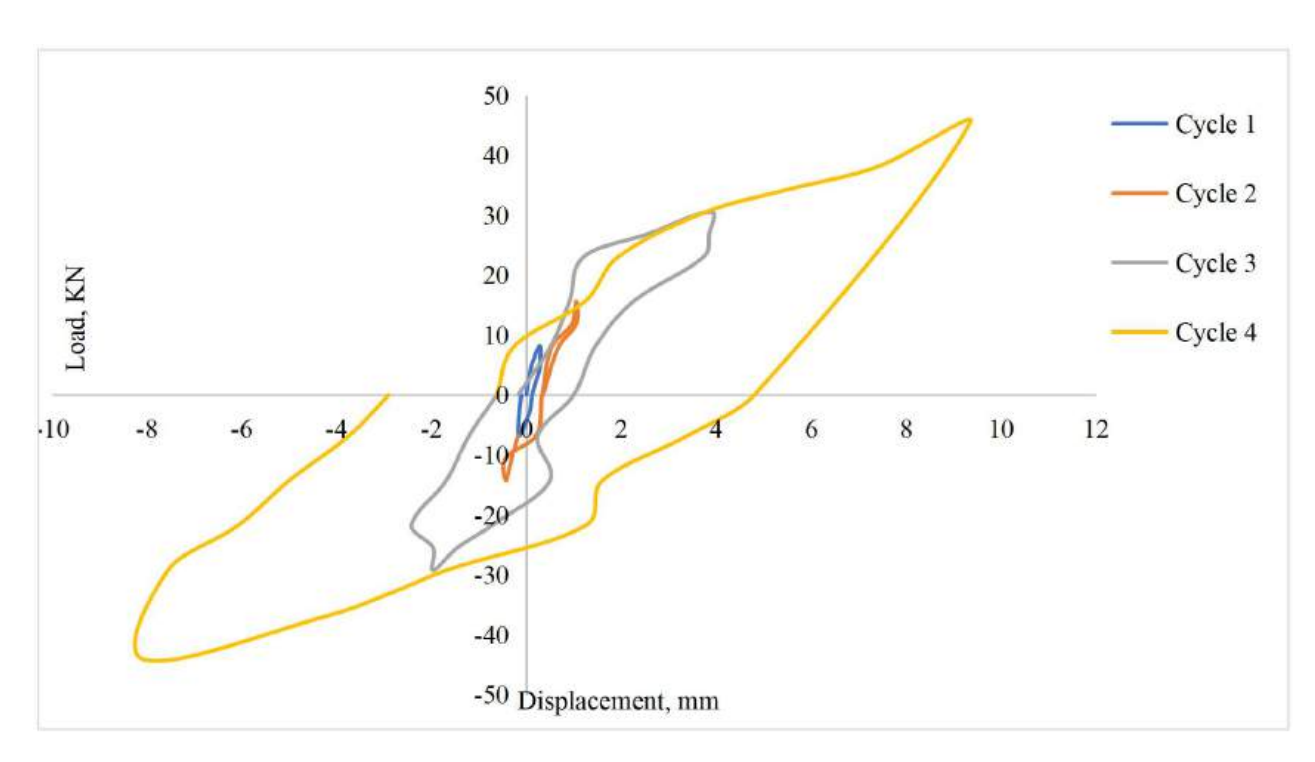


Figure I.1- Hysteretic load-displacement curve for SURM2.

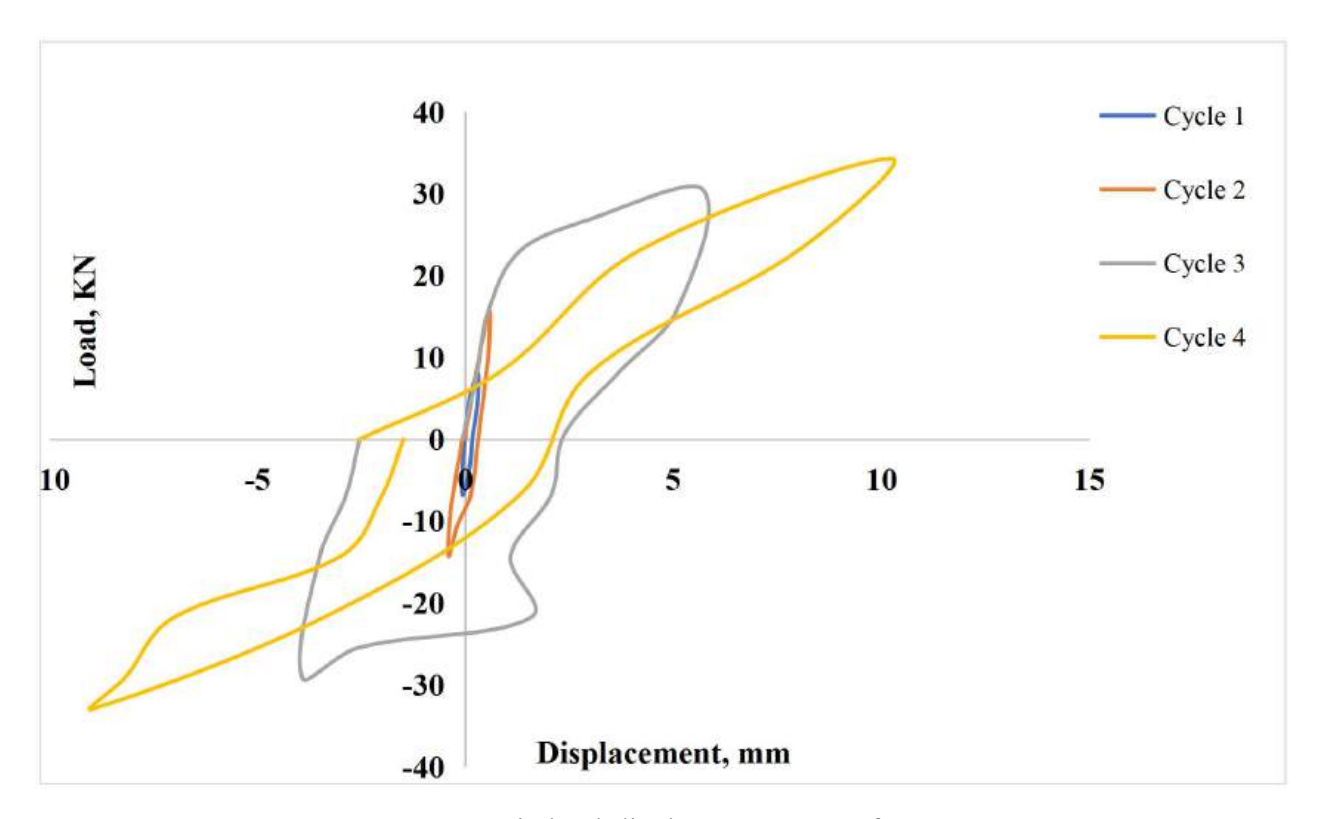


Figure I.2- Hysteretic load-displacement curve for SURM6.

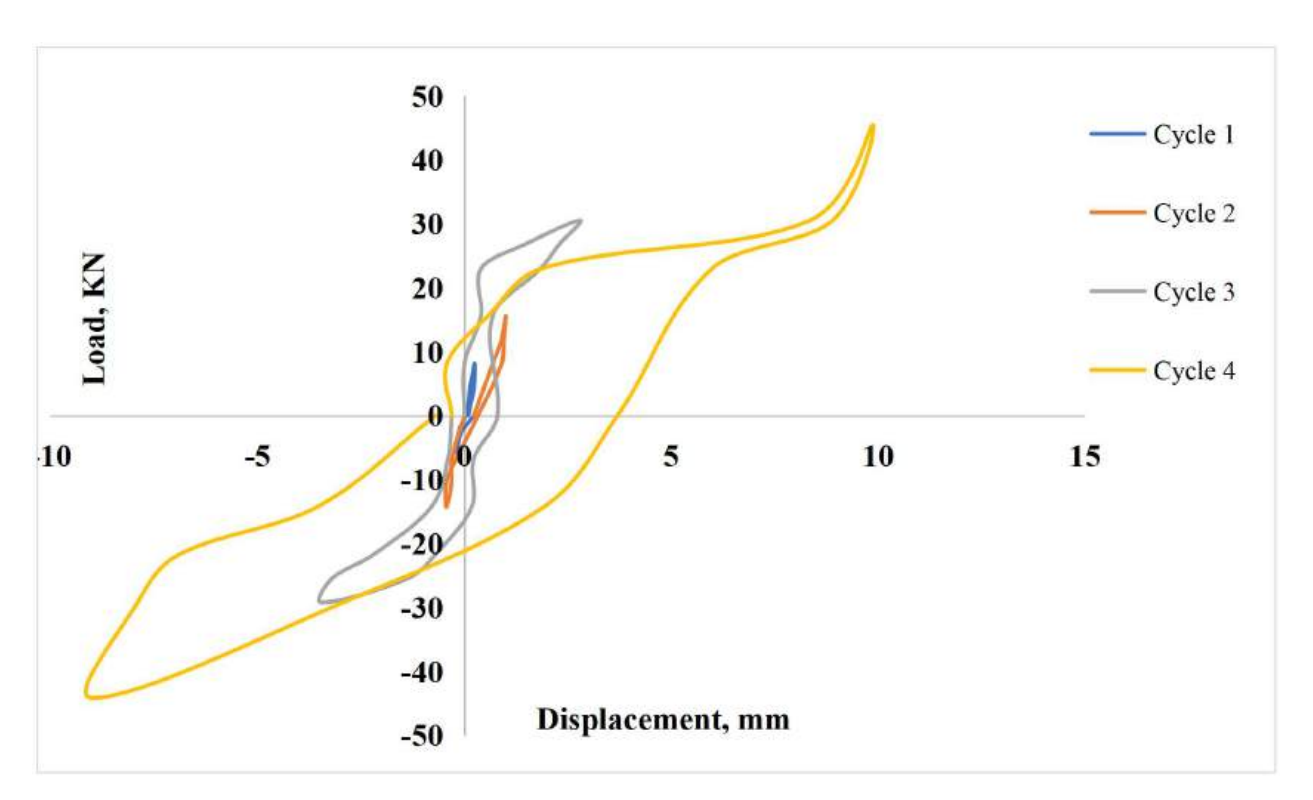


Figure I.3- Hysteretic load-displacement curve for HURM2.

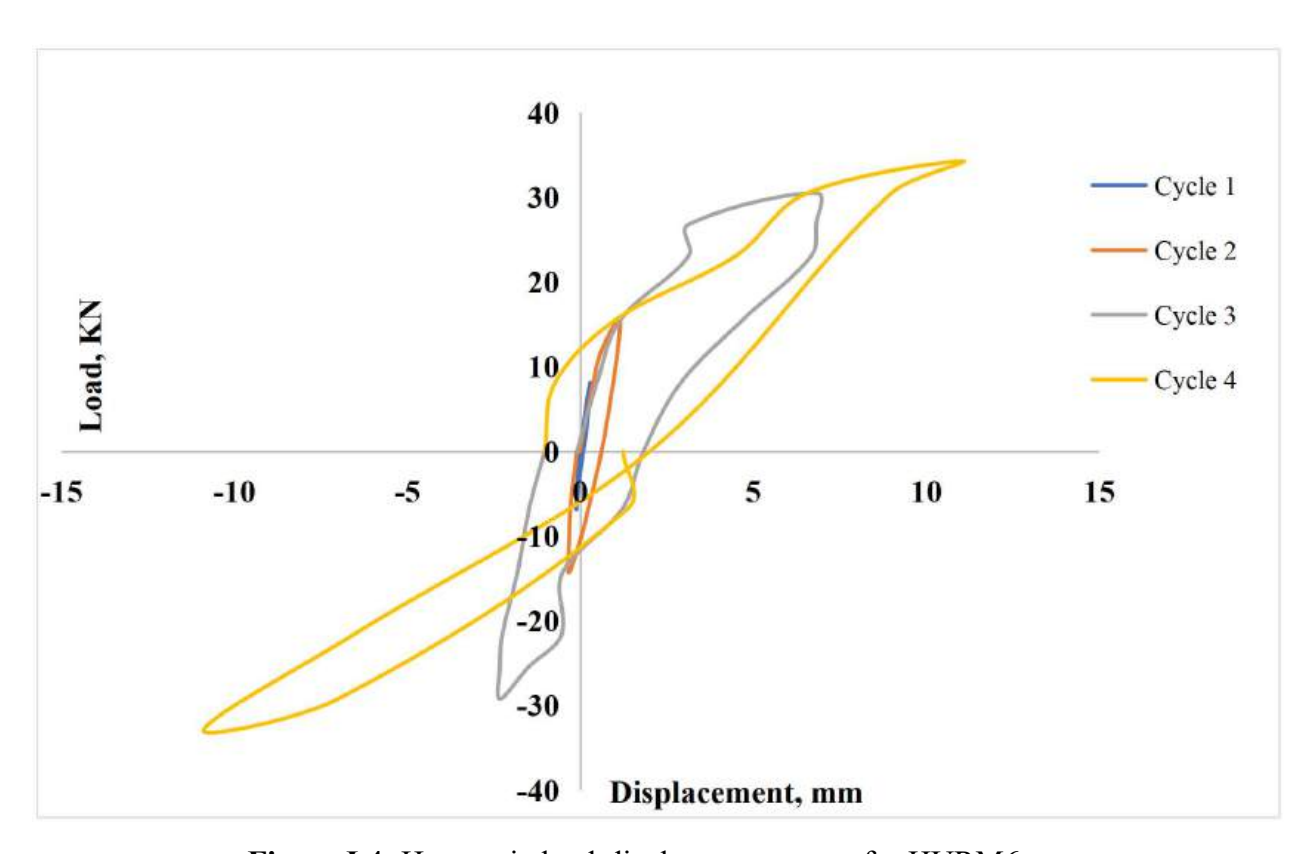


Figure I.4- Hysteretic load-displacement curve for HURM6.

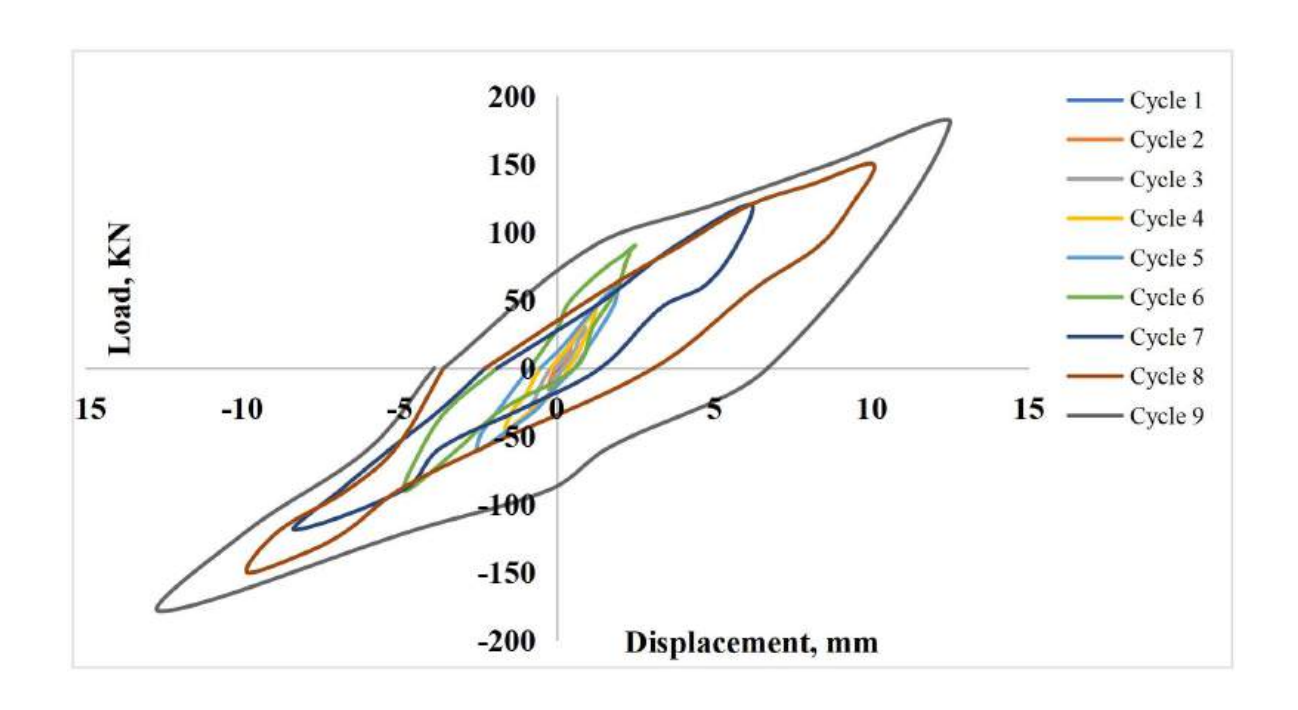


Figure I.5- Hysteretic load-displacement curve for RM2-420.

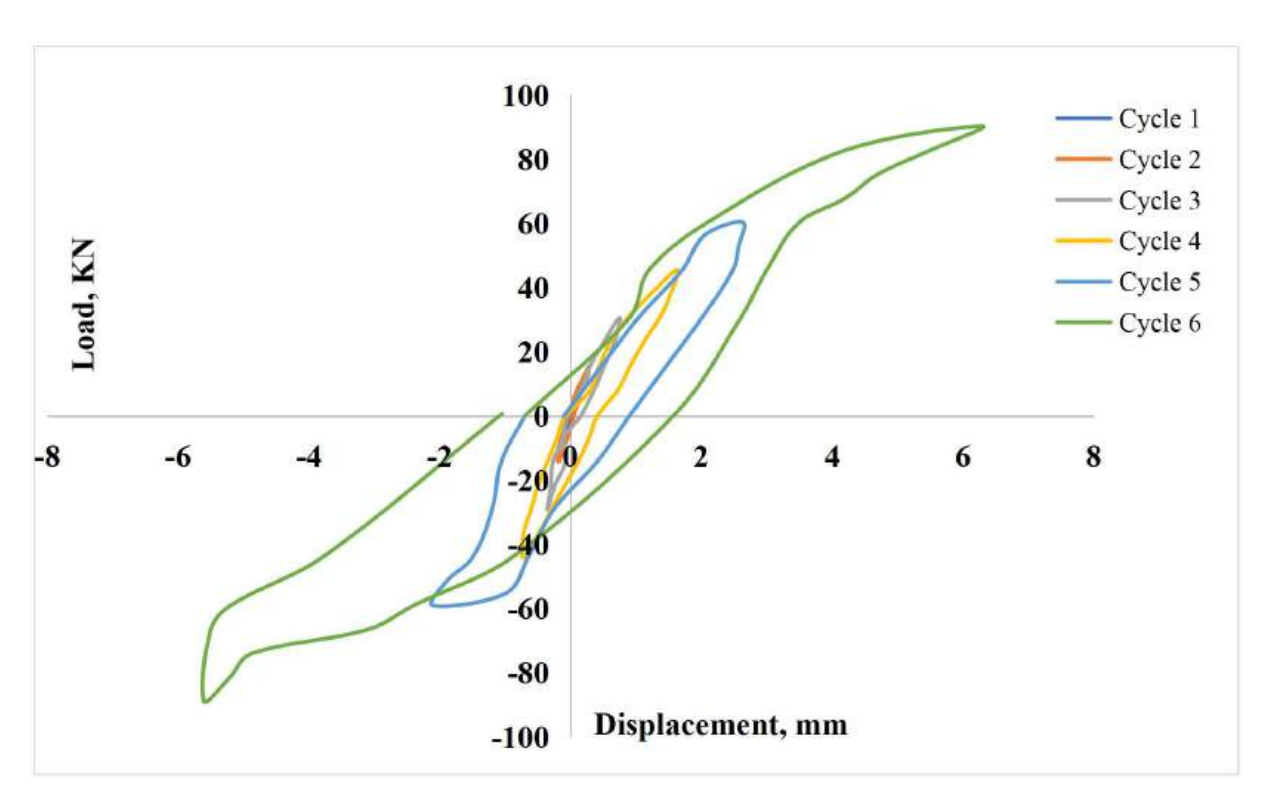


Figure I.6- Hysteretic load-displacement curve for RM6-420.

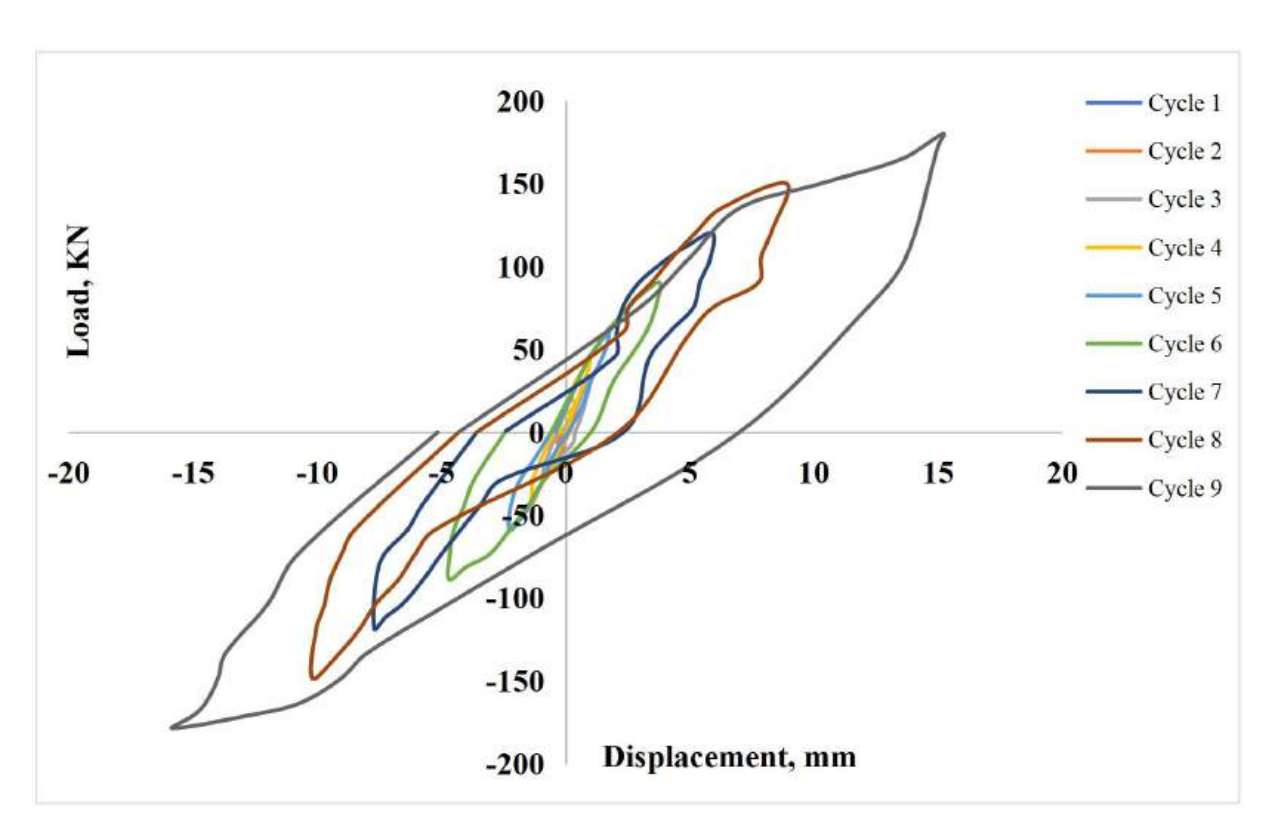


Figure I.7- Hysteretic load-displacement curve for RM2-500.

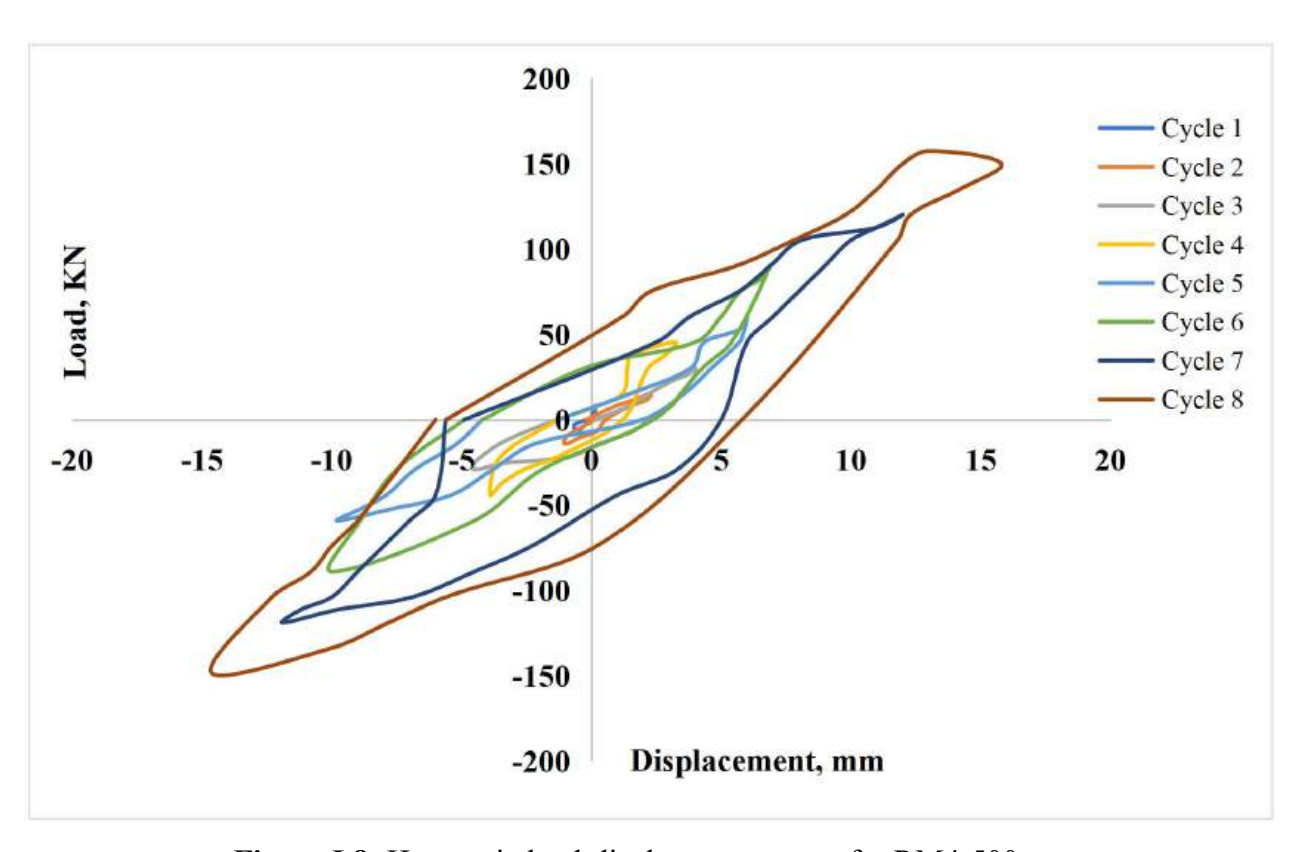


Figure I.8- Hysteretic load-displacement curve for RM4-500.

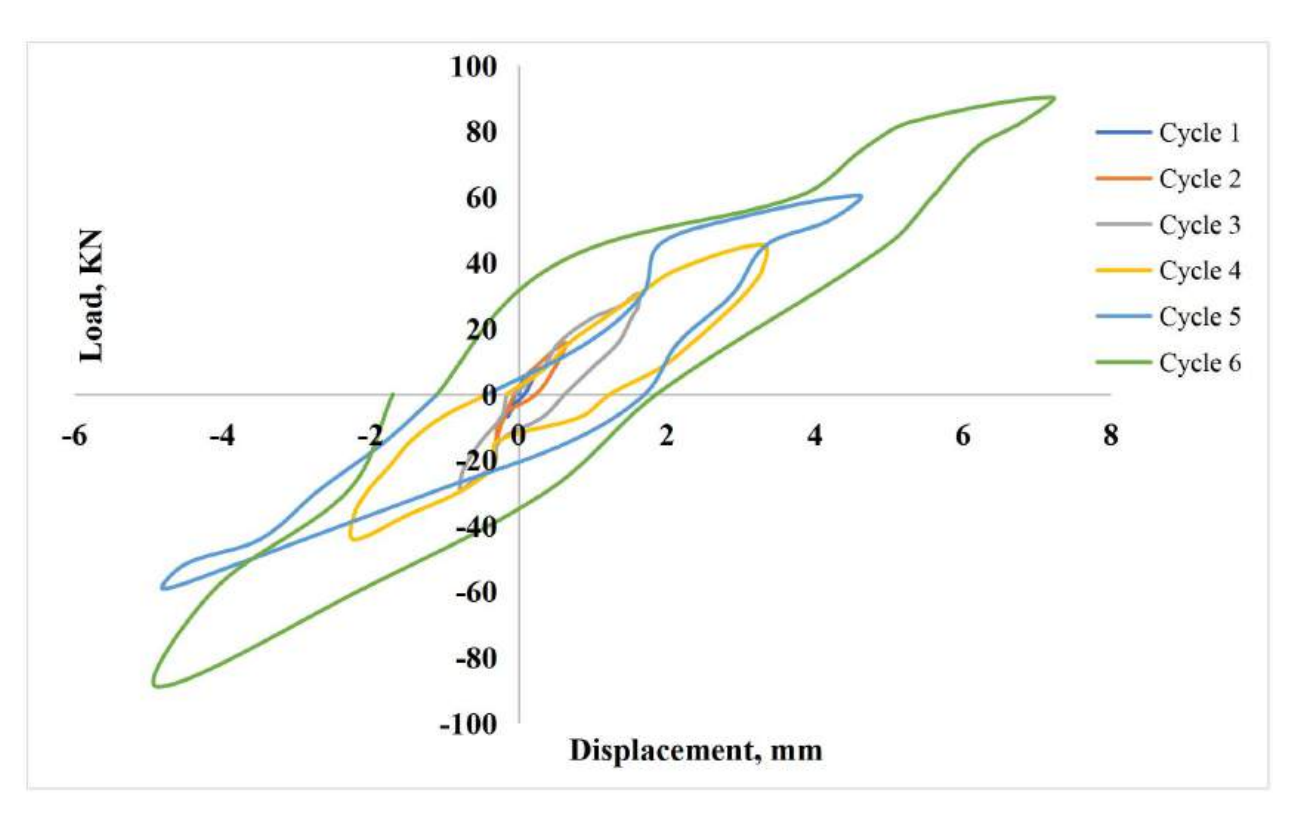


Figure I.9- Hysteretic load-displacement curve for RM6-500.

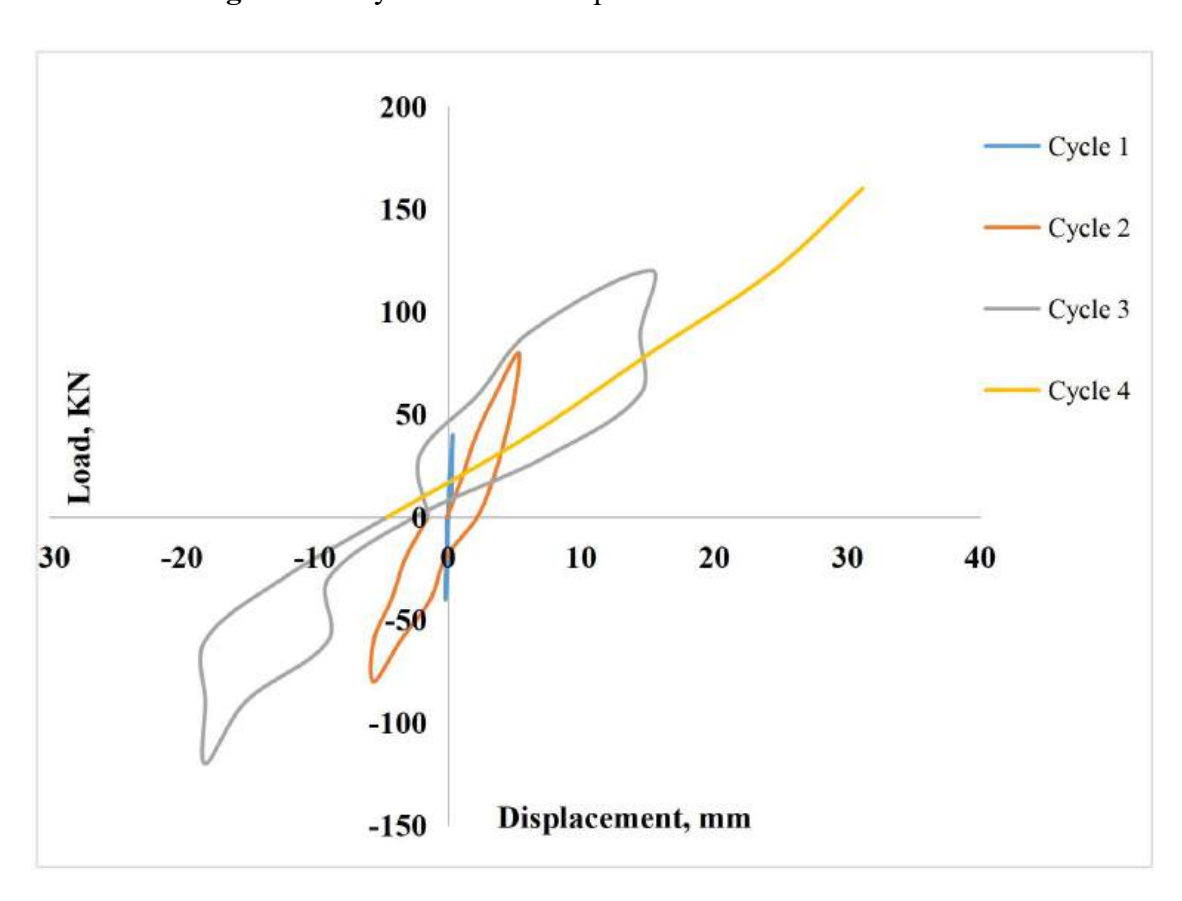


Figure I.10- Hysteretic load-displacement curve for SBL.

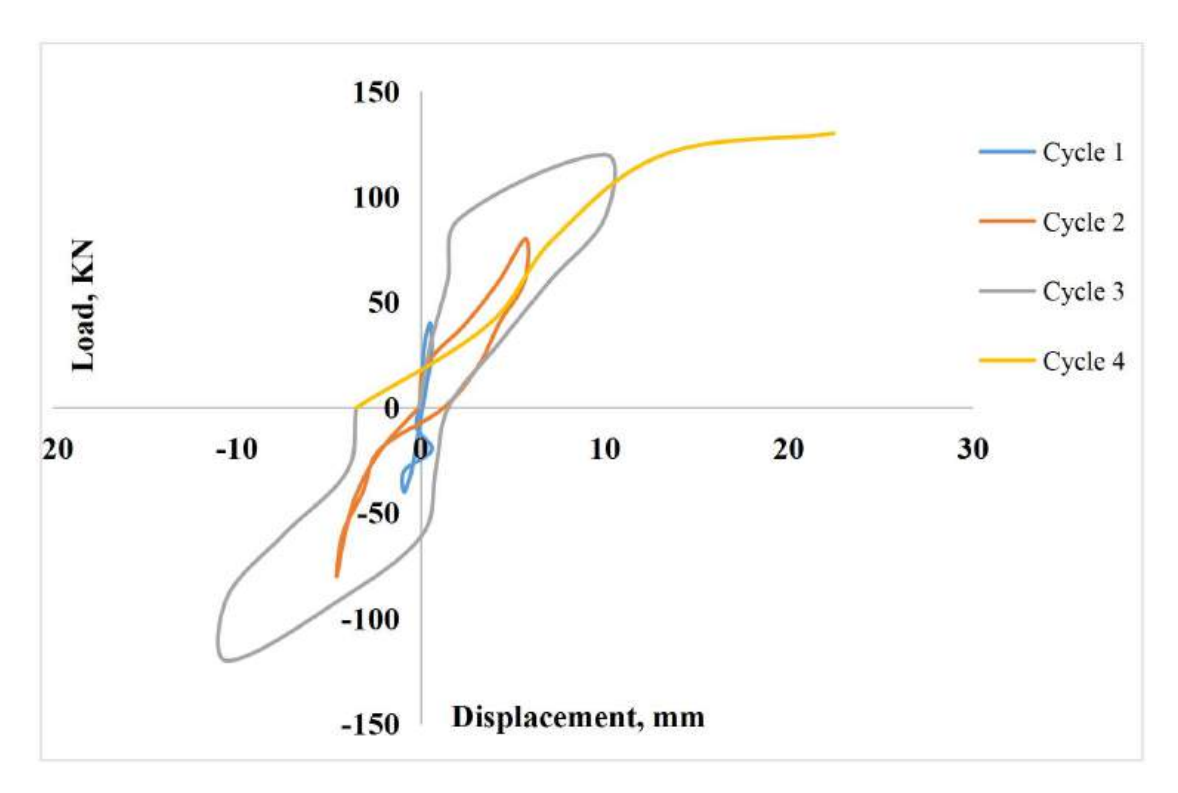


Figure I.11- Hysteretic load-displacement curve for PB.

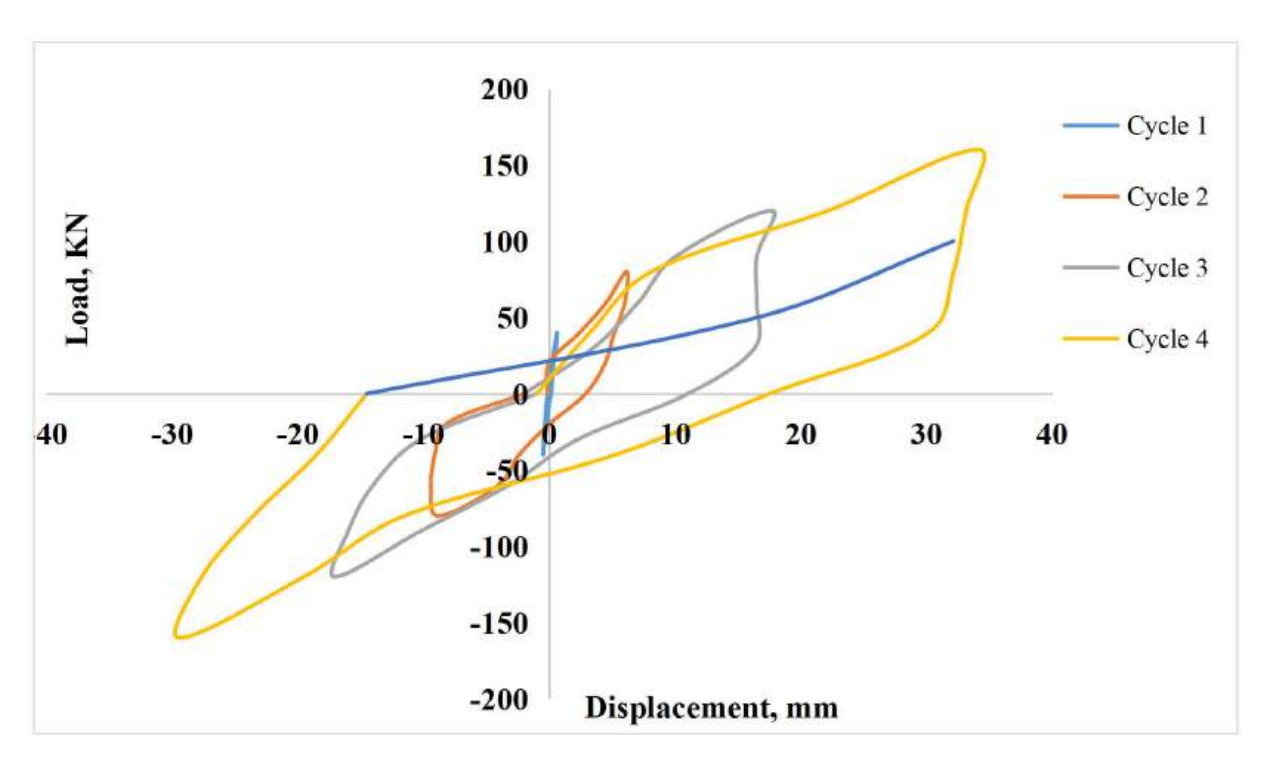


Figure I.12- Hysteretic load-displacement curve for PBL.

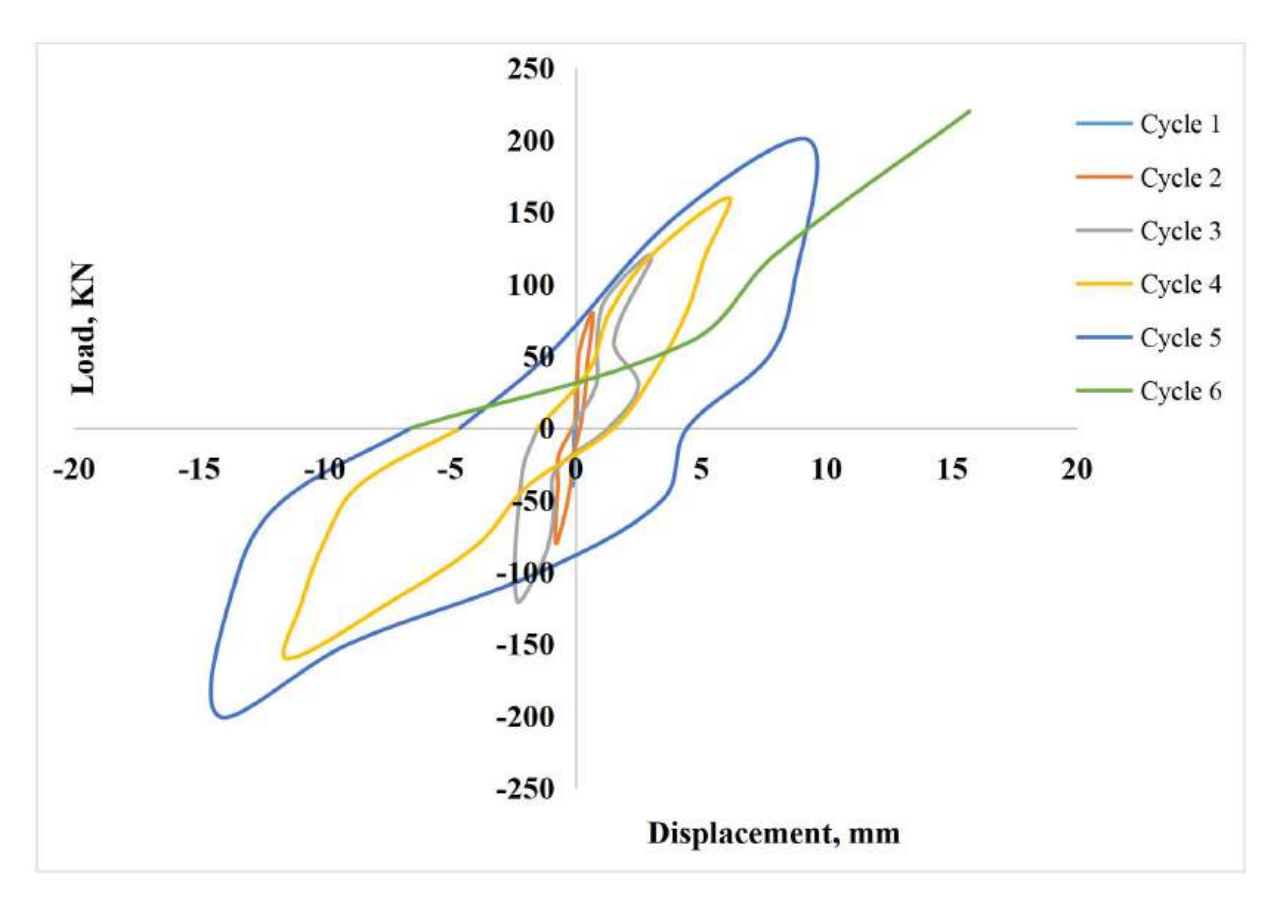


Figure I.13- Hysteretic load-displacement curve for RIF.

Appendix-J

Stiffness Degradation Curve of the Specimen

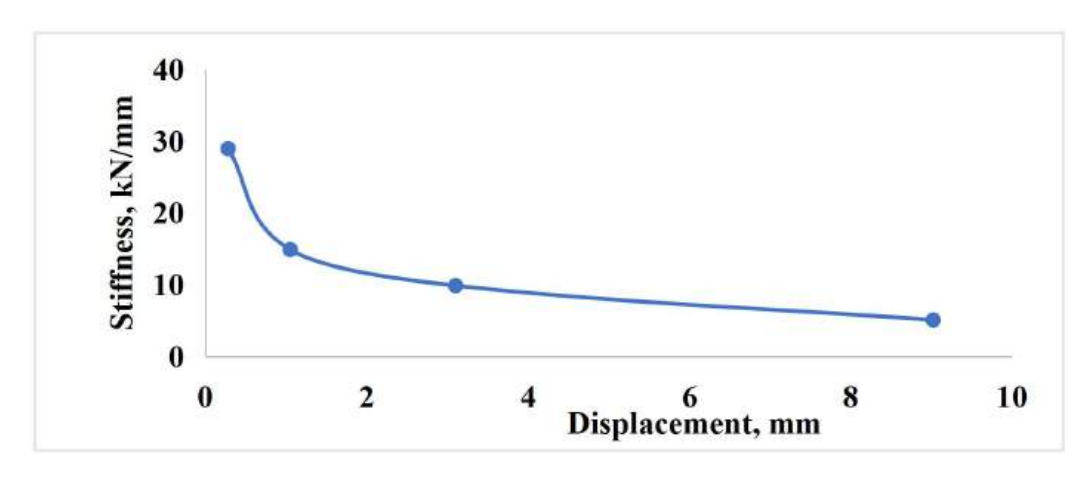


Figure J.1- Stiffness degradation curve for SURM2.

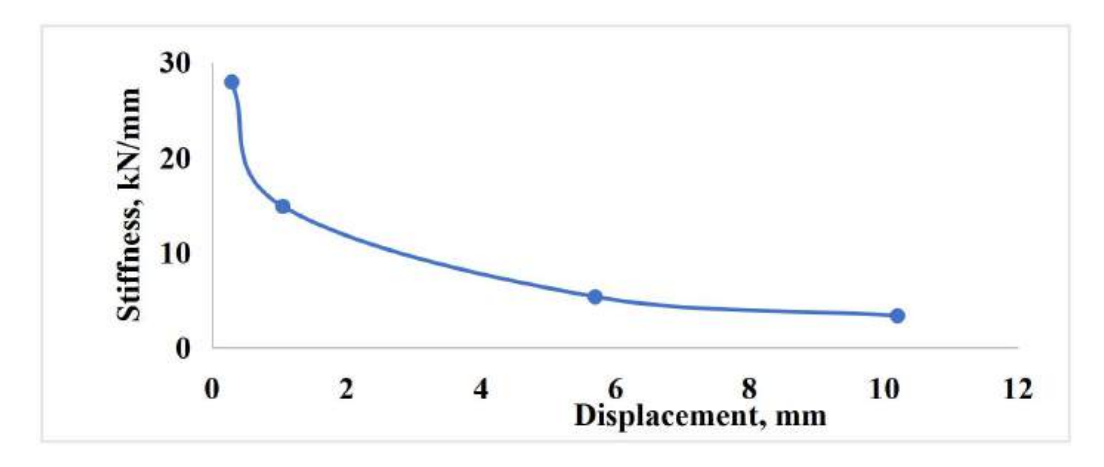


Figure J.2- Stiffness degradation curve for SURM6.

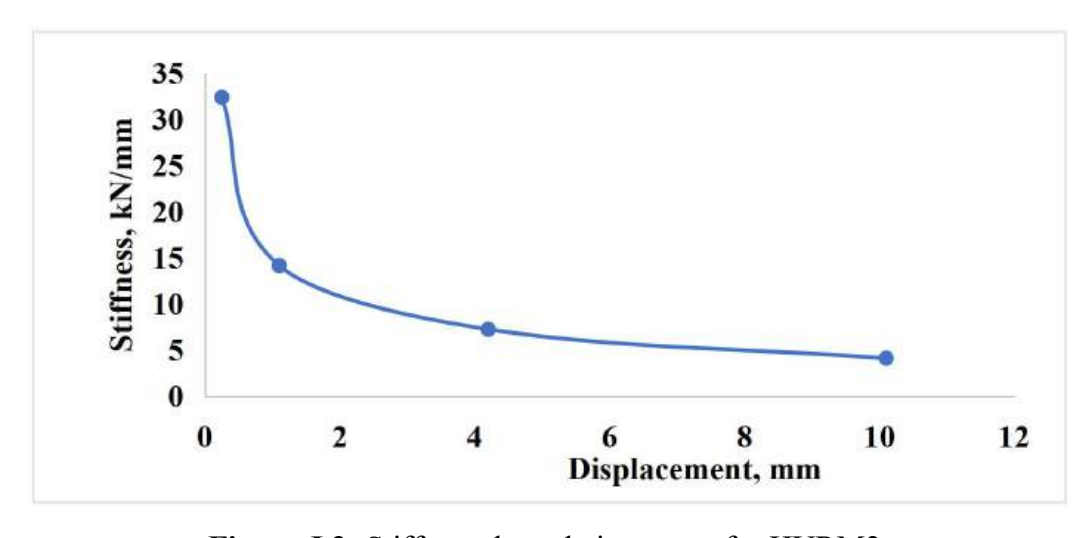


Figure J.3- Stiffness degradation curve for HURM2.

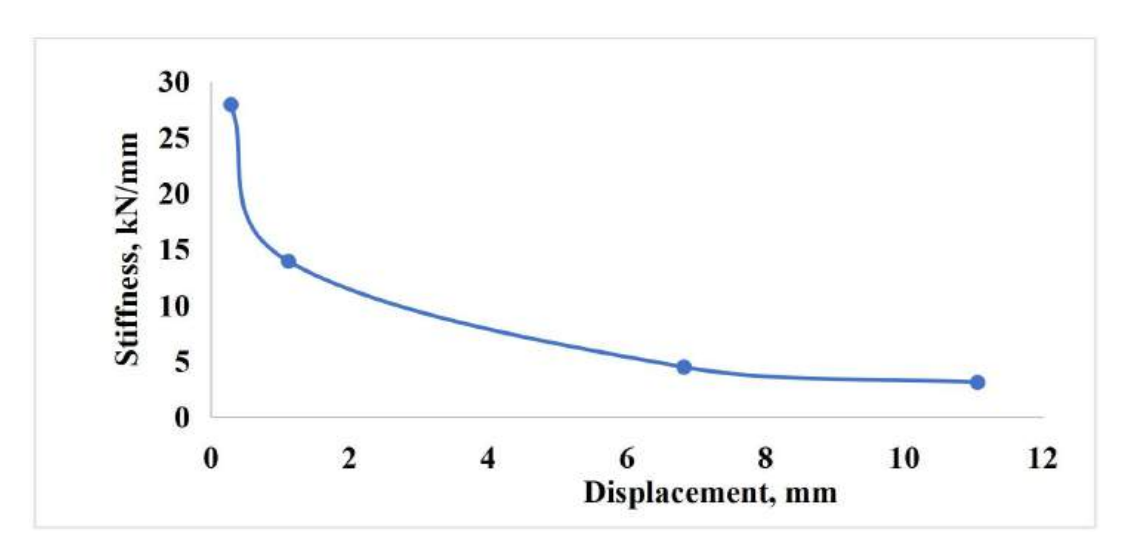


Figure J.4- Stiffness degradation curve for HURM6.

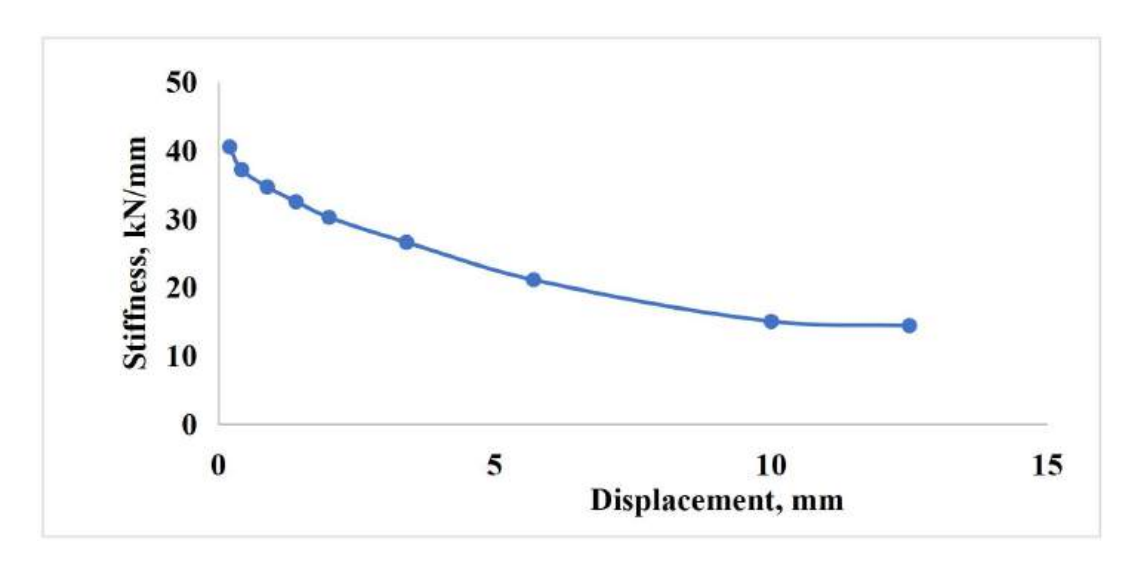


Figure J.5- Stiffness degradation curve for RM2-420.

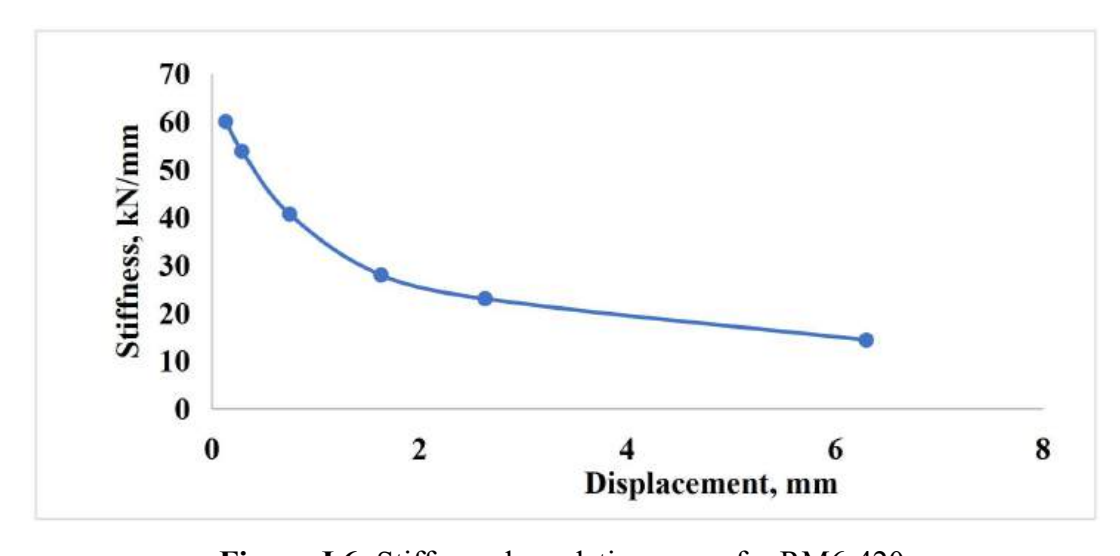


Figure J.6- Stiffness degradation curve for RM6-420.

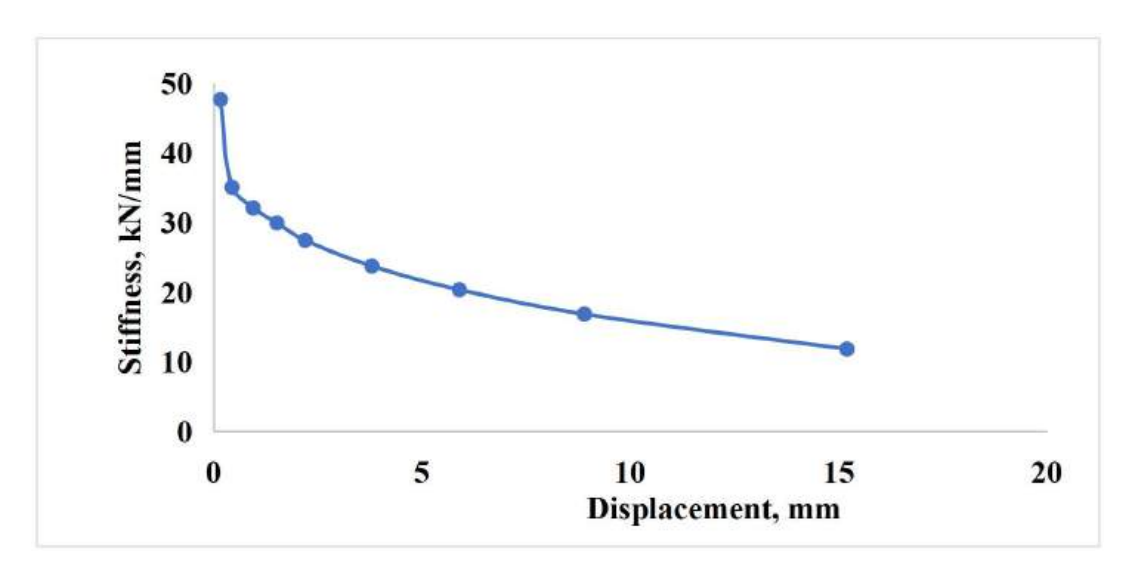


Figure J.7- Stiffness degradation curve for RM2-500.

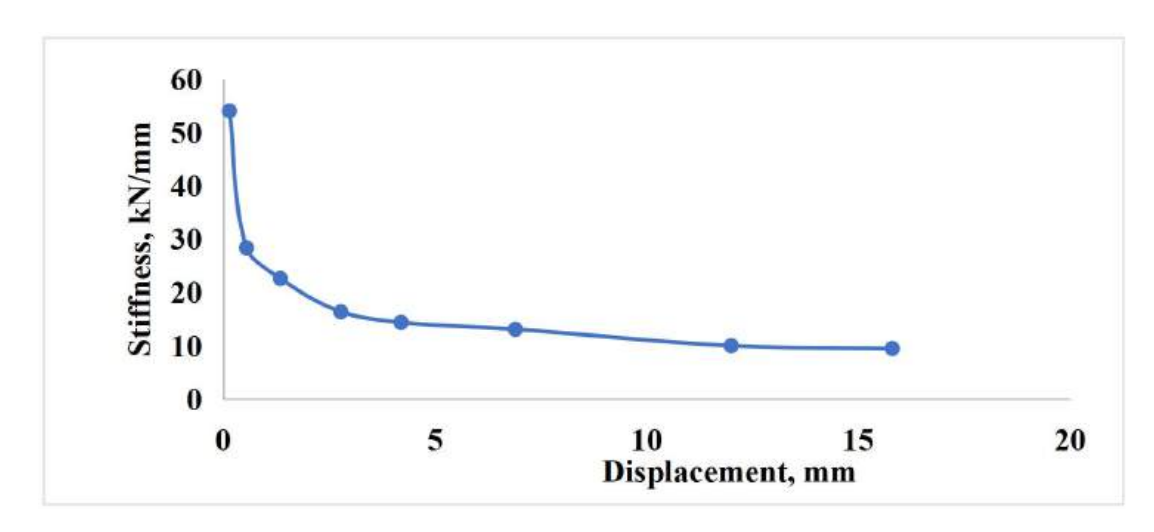


Figure J.8- Stiffness degradation curve for RM4-500.

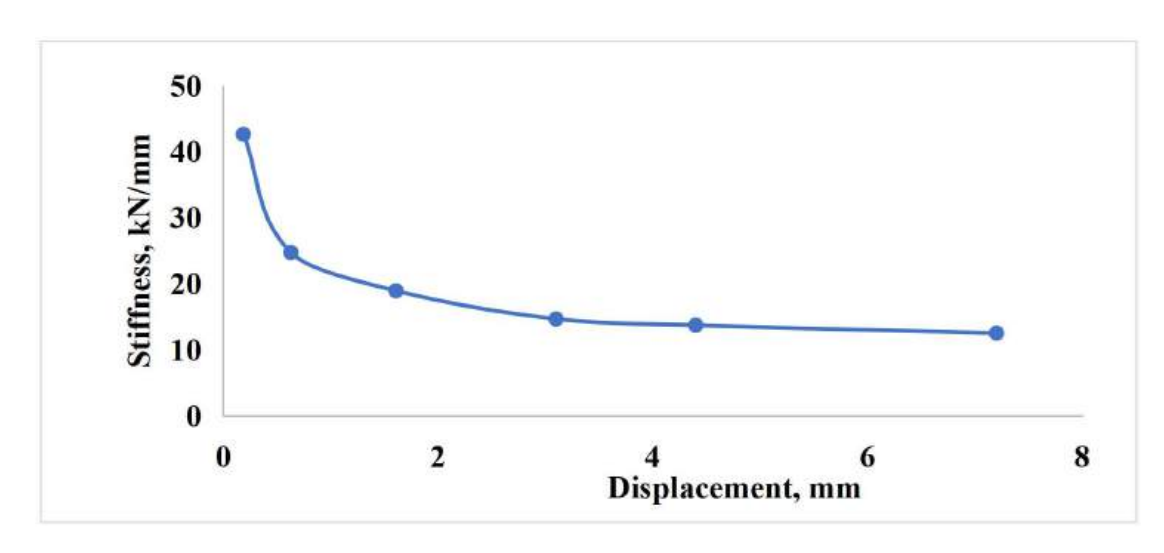


Figure J.9- Stiffness degradation curve for RM6-500.

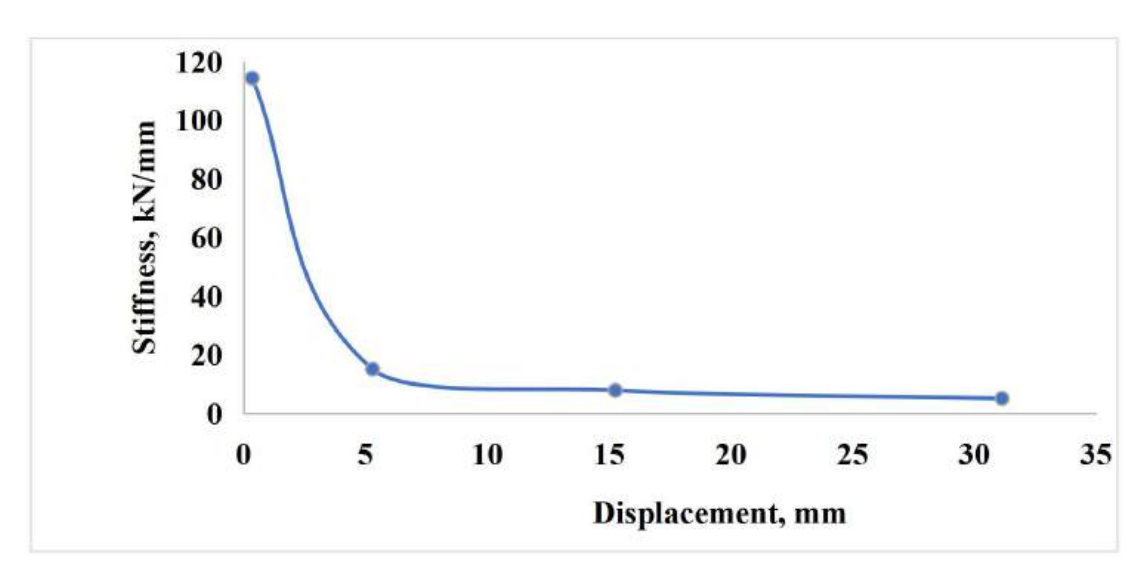


Figure J.10- Stiffness degradation curve for SBL.

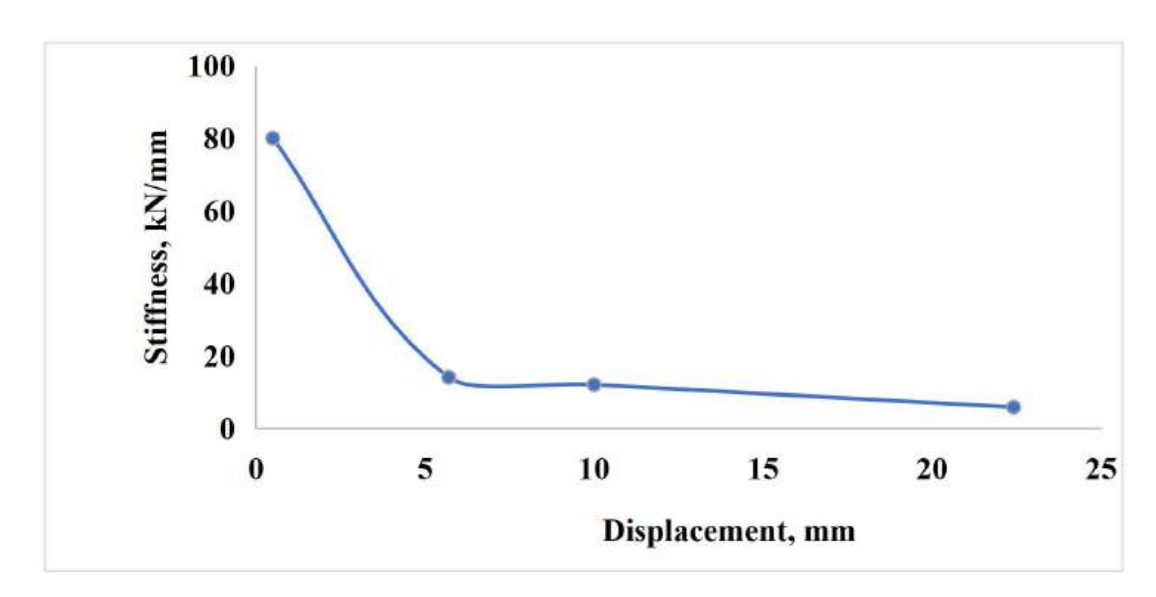


Figure J.11- Stiffness degradation curve for PB.

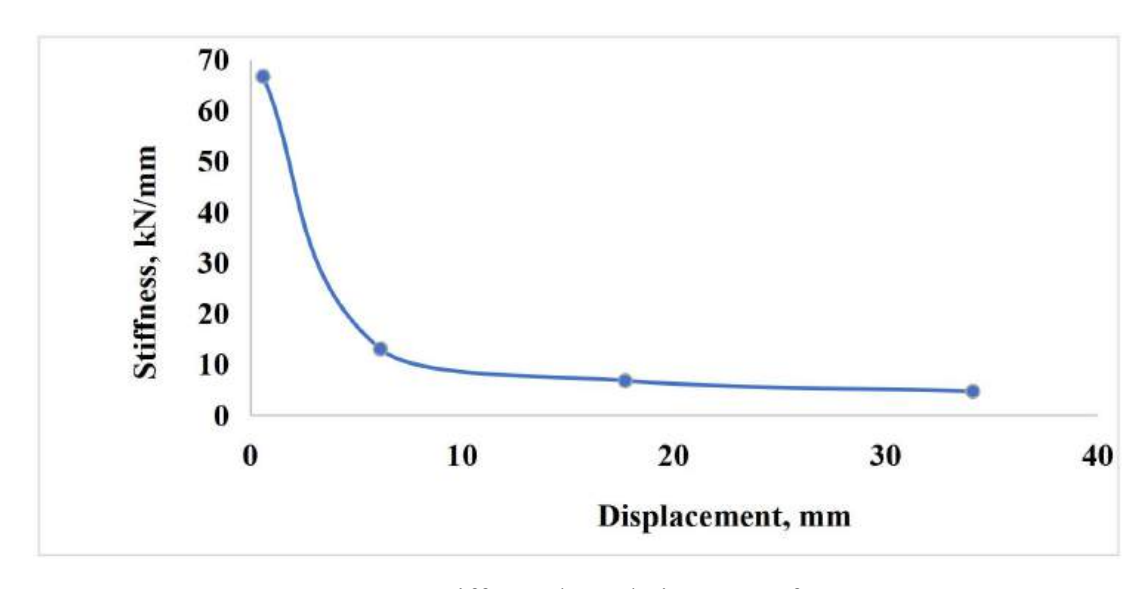


Figure J.12- Stiffness degradation curve for PBL.

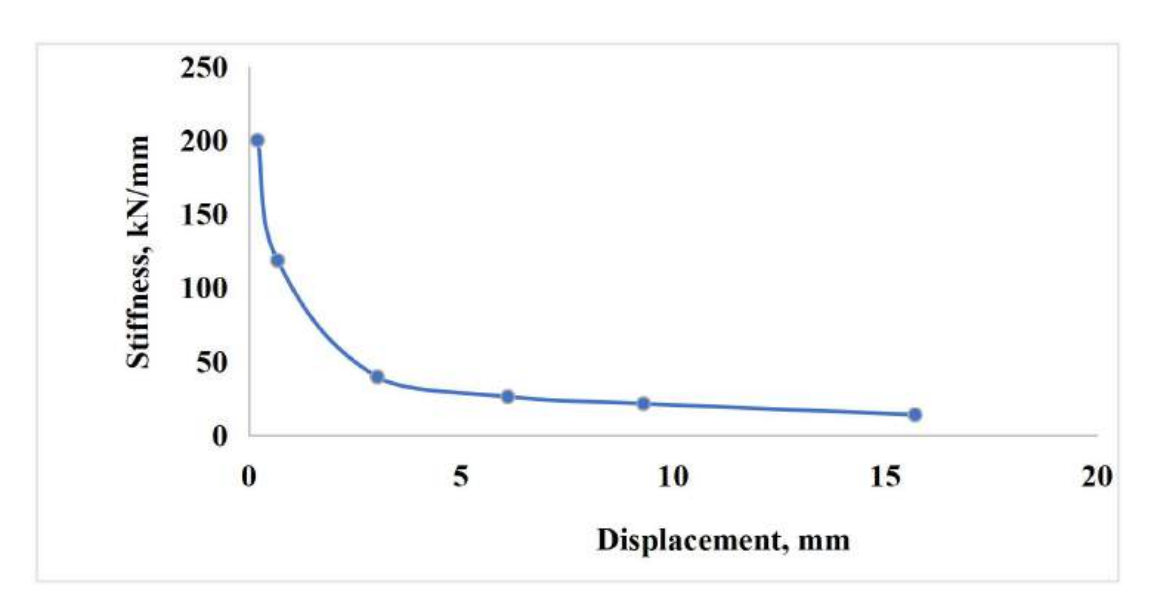


Figure J.13- Stiffness degradation curve for RIF.